

UNIVERSITÀ DEGLI STUDI DI FERRARA
FACOLTÀ DI SCIENZE MATEMATICHE, FISICHE E NATURALI
DIPARTIMENTO DI FISICA

**Precision measurements
of IVB parameters
and bounds on New Physics**

Relatore

Chiar.mo Prof. **Mikhail I. Vysotsky**

Candidato

Dott. **Michele Maltoni**

Relatore

Chiar.mo Prof. **Giovanni Fiorentini**

Contents

Introduction	1
1 General properties of the Standard Model and SUSY extensions	5
1.1 The Standard Model	5
1.1.1 The gauge and higgs sector	5
1.1.2 The fermion sector	8
1.2 Regularization and renormalization	10
1.2.1 General discussion	10
1.2.2 Renormalization of the Standard Model	12
1.3 Supersymmetry	15
1.3.1 Motivations for New Physics	15
1.3.2 The Minimal Supersymmetric Standard Model	17
2 The numerical closeness between θ and the $\overline{\text{MS}}$ parameter $\hat{\theta}$	21
2.1 The bare quantities and the tree approximation	22
2.1.1 The fine structure constant	23
2.1.2 The W and Z pole masses	24
2.1.3 The Fermi coupling constant	24
2.1.4 The g_V/g_A ratio	25
2.2 The one-loop approximation	26
2.2.1 \hat{s}^2 versus s^2	26
2.2.2 s_l^2 versus s^2	28
2.2.3 \hat{s}_l^2 versus s_l^2	30

2.3	Higher-order corrections and numerical estimates	33
2.3.1	\hat{s}^2 versus s_t^2	33
2.3.2	\hat{s}^2 versus s^2	34
2.4	Conclusions	35
3	$\hat{s}_{\text{SM}}^2, \hat{s}_{\text{ND}}^2$ and the value of $\hat{\alpha}_s(m_Z)$ from SUSY Grand Unification	37
3.1	RGE in the $\overline{\text{MS}}$ scheme and the concept of threshold	38
3.1.1	Effects of new physics on the initial values	39
3.1.2	Writing and solving the RGE	40
3.1.3	Running in the decoupling approach	42
3.2	The numerical value of $\hat{\alpha}_s(m_Z)$ from SUSY GUT	43
3.2.1	The SUSY parameters $\tan\beta$ and m_{SUSY}	44
3.2.2	The SM parameters $\hat{\alpha}$, \hat{s}^2 and \hat{m}_t	45
3.3	Conclusions	47
4	Charginos nearly degenerate with the lightest neutralino	49
4.1	Experimental bounds	50
4.2	Theoretical analysis	52
4.2.1	The higgsino-dominated case	54
4.2.2	The wino-dominated case	55
4.3	Data analysis and fits	57
4.4	Recent developments and new fits	60
4.5	Conclusions	61
5	Extra quark-lepton generations and precision measurements	63
5.1	General formulas	64
5.2	Comparison with experimental data: heavy fermions	70
5.3	Comparison with experimental data: $m_N < m_Z$	77
5.4	The case of SUSY	79
5.5	Conclusions	84

Contents	v
Conclusions	85
Acknowledgments	87
A The V_i functions	89
Bibliography	91

List of Tables

1.1	Particle contents of the fermionic sector of the Standard Model	8
1.2	Particle contents of the Minimal Supersymmetric Standard Model	18
2.1	Contributions of self-energies to $\hat{s}^2 - s^2$	27
4.1	Experimental value and theoretical prediction of precision measurements	58

List of Figures

1.1	Running of $\hat{\alpha}_i$ in the Standard Model	16
1.2	Running of $\hat{\alpha}_i$ in the Minimal Supersymmetric Standard Model	19
2.1	Plot of $\hat{s}^2 - s^2$ as a function of m_H	28
2.2	Plot of $\hat{s}^2 - s^2$ as a function of m_t	29
2.3	Plot of $s_l^2 - s^2$ as a function of m_H	30
2.4	Plot of $s_l^2 - s^2$ as a function of m_t	31
2.5	Plot of $\hat{s}^2 - s_l^2$ as a function of m_t	32
3.1	Running of $\hat{\alpha}_i$ in the <i>decoupling</i> and <i>non-decoupling</i> approaches	42
3.2	Plot of $\hat{\alpha}_s$ as a function of $\tan \beta$	45
3.3	Plot of $\hat{\alpha}_s$ as a function of m_{SUSY}	46
3.4	Plot of $\hat{\alpha}_s$ as a function of $1/\hat{\alpha}$	47
3.5	Plot of $\hat{\alpha}_s$ as a function of \hat{s}^2	48
3.6	Plot of $\hat{\alpha}_s$ as a function of \hat{m}_t	48
4.1	Exclusion plot in the plane $(m_{\tilde{\chi}}, \Delta M^\pm)$	51
4.2	Plot of $\delta^{\tilde{H}} V_i$ as a function of $m_{\tilde{\chi}}$	55
4.3	Plot of $\delta^{\tilde{W}} V_i$ as a function of $m_{\tilde{\chi}}$	57
4.4	Plot of C.L. as a function of $m_{\tilde{\chi}}$	59
4.5	Improved plot of C.L. as a function of $m_{\tilde{\chi}}$	61
4.6	Improved exclusion plot in the plane $(m_{\tilde{\chi}}, \Delta M^\pm)$	62
5.1	Plot of δV_i^l as a function of $(m_N/m_Z)^2$	67
5.2	Plot of δV_i^q as a function of $(m_U/m_Z)^2$	68

5.3	Plot of ΔV_i as a function of $(m_{N,U}/m_Z)^2$	69
5.4	Exclusion plot in the plane $(N_g, \Delta m)$ (horizontal degeneracy)	71
5.5	Exclusion plot in the plane $(N_g, \Delta m)$ (cross degeneracy)	72
5.6	Exclusion plot in the plane $(N_g, \Delta m)$ (anti-cross degeneracy)	73
5.7	Exclusion plot in the plane (N_g, m_{inf})	74
5.8	Plot of $m_{E/U} - m_{N/D}$ as a function of N_g	76
5.9	Exclusion plot in the plane (m_E, m_N)	77
5.10	Exclusion plot in the plane (N_g, m_N)	78
5.11	Exclusion plot in the plane $(N_g, m_{\text{sbottom}})$	80
5.12	Exclusion plot in the plane $(N_g, \Delta m)$ (higgsino-dominated case)	81
5.13	Exclusion plot in the plane $(N_g, m_{\tilde{\chi}})$ (higgsino-dominated case)	82
5.14	Exclusion plot in the plane $(N_g, m_{\tilde{\chi}})$ (wino-dominated case)	83

Introduction

In the last 30 years, since the formulation of the *Standard Model* (SM) as a unified theory for electromagnetic and weak interactions, particle physics has enjoyed a period of great success. All the predictions of the SM, except for the existence of the Higgs boson which still has to be observed, have so far been confirmed with very good accuracy, and recent fits including LEP I, LEP II and SLC data are characterized by the excellent value $\chi^2/\text{d.o.f} = 14.4/14$, which cannot be better.

However, despite of its success, the SM is currently not believed to be the ultimate theory of Nature. The absence of a relation between the electroweak and strong coupling constants, the need of a fine tuning to protect scalar masses, the large number of free parameters are all problems which since many years are leading theoretical physicists towards the formulation of “more fundamental” theories, of course having the SM as a low-energy limit. Among these theories, the concept of *supersymmetry* plays a central role, and despite of the fact that no evidence of superpartners has so far been found it is widely believed that supersymmetry will ultimately occur at some energy scale.

Many of the present experimental confirmations of the SM, as well as most of the present bounds on its extensions, come from accelerator physics. *Direct search* experiments have reached a very high level of accuracy, and recent results from LEP II and Tevatron allow to put stringent bounds on New Physics. However, there are special situations where direct search analysis, for some peculiar reason, fails, and in these cases experimental bounds become sensibly weaker. When this happens, the study of *radiative corrections* to electroweak observables emerges as the only way to investigate the existence of New Physics in these domains, and in the last years the analysis of *precision measurements* has proved to be a strong tool for constraining wide regions of parameter space.

The main purpose of this thesis is to discuss the impact of precision measurements of *intermediate vector boson* (IVB) parameters on the present knowledge of particle physics, both in the framework of the Standard Model and of its most straightforward extensions. The research presented in the following chapters is organized in a natural way, starting from the SM and then moving towards New Physics.

In Chapter 1, we give a general overview of the Standard Model and of its supersymmetric extension. We do not present here any original result, nor we pretend to be exhaustive, but simply provide the technical background for the next chapters and discuss the main motivations

for looking beyond the Standard Model. The structure of this chapter closely resembles that of the whole thesis, following on a smaller scale the same logical line.

The rest of this thesis is mainly oriented into three complementary subjects:

- (1) the study of the relations between the phenomenological electroweak mixing angle θ , the $\overline{\text{MS}}$ parameter $\hat{\theta}$ and the effective angle θ_l describing decay of Z boson into charged leptons;
- (2) the analysis of contributions of “charginos almost degenerate with the lightest neutralino” to oblique radiative corrections, and bounds on mass of these particles from precision data;
- (3) the possibility to have extra fermion generations without spoiling precision data description, both in the framework of the SM and of its minimal supersymmetric extension (MSSM).

Concerning point (1), in Chapter 2 we analyze the effects of radiative corrections in the electroweak sector of the SM, with particular attention to various definitions of the electroweak mixing angle θ (or equivalently of its sine squared, s^2). It happens that s^2 and \hat{s}^2 are equal with 0.1% accuracy, though they are split by radiative corrections and a natural estimate for their difference is 1%. We study the origin of this degeneracy and show that it occurs only if the top mass is close to 170 GeV, so no deep physical reason can be attributed to it. However, another puzzle of the Standard Model, the degeneracy of s_l^2 and s^2 , is not independent of the previous one since a good physical reason exists for s_l^2 and \hat{s}^2 degeneracy. We also present explicit formulas relating these three angles.

The analysis of the relations between different definitions of the electroweak mixing angle is then extended in Chapter 3 from the SM to New Physics, dealing with some aspects of the running of $\overline{\text{MS}}$ quantities from low (electroweak) to high (unification) energy scale. In particular, we emphasize how two apparently different approaches to the running of coupling constants, the one in which high-energy new physics is NOT decoupled from low-energy scale quantities, and the one in which these contributions are decoupled but thresholds are introduced, are essentially equivalent. As an application of the techniques described here, we conclude discussing what is the value of $\hat{\alpha}_s$ which can be predicted from the demand of SUSY Grand Unification.

Concerning point (2), in Chapter 4 we study the case of a chargino almost degenerate with the lightest neutralino in the framework of the MSSM. In the general case, gaugino contributions to oblique radiative corrections cannot be written analytically, but for the special case considered here this is possible and the corresponding expressions are reported. Then we analyze effects on precision measurements, giving lower bounds for nearly degenerate chargino/neutralino. It is important to note that for the considered case experimental bounds from direct search are rather weak, just half of the Z boson mass, and the study of oblique corrections allows a concrete improvements of these bounds.

Finally, in Chapter 5 we deal with point (3), investigating the effects of new fermion generations on precision measurements. We show that even one extra generation with all particles heavier than Z boson is strongly disfavored by experimental data. However, for the specific case of a heavy neutrino (around 50 GeV in mass), the situation changes and the quality of the fit is

not worse than the SM. Moreover, as a direct application of the results of the previous chapter, effects of almost degenerate chargino/neutralino on a new generation are discussed, showing that also in this case experimental bounds are relaxed.

The results discussed in this thesis are presented in the published papers [1, 2, 3] and in Ref. [4], currently submitted for publication on PLB. Also, results quoted in Chapters 4 and 5 were presented at the conference PASCOS99, and will appear in the proceedings [5, 6]. Other results, not contained here, are in Refs. [7, 8, 9].

Chapter 1

General properties of the Standard Model and SUSY extensions

The purpose of this chapter is to provide a general overview on some concepts which will be widely used in the following chapters. Its structure closely resembles that of the present thesis: we start from the general properties of the tree-level Lagrangean of the electroweak interactions in Sec. 1.1, then we extend our analysis to include effects of radiative corrections in Sec. 1.2, and finally we outline the main problems of the Standard Model and introduce supersymmetry in Sec. 1.3. We do not intend to be exhaustive, and we will only consider topics which are relevant in the framework of the present dissertation.

1.1 The Standard Model

The present theory of the electroweak interactions, known as “Standard Model”, is the Glashow-Salam-Weinberg theory [10] of leptons, extended to quarks [11] and made anomaly free through the introduction of the concept of color. Intermediate vector bosons get mass through the *Higgs mechanism*, and Fermi model arises as a low energy effective theory; *spontaneous symmetry breaking* is also used to generate leptons and quark masses. All the predictions of the SM are actually in perfect agreement with all the experimental data.

1.1.1 The gauge and higgs sector

The core of the Standard Model is a renormalizable Yang-Mills theory [12] based on the non-Abelian gauge group $SU(2)_L \times U(1)_Y$ [13, 14]. The generators of the corresponding Lie algebra are the three isospin operators I_1, I_2, I_3 and the hypercharge Y . Each of these operators is associated with a vector field, so the model includes the isotriplet W_μ^a and the isosinglet B_μ . The corresponding field strengths are:

$$W_{\mu\nu}^a = \partial_\mu W_\nu^a - \partial_\nu W_\mu^a - g\epsilon^{abc}W_\mu^b W_\nu^c, \quad (1.1)$$

$$B_{\mu\nu} = \partial_\mu B_\nu - \partial_\nu B_\mu. \quad (1.2)$$

The Lagrangean for the pure gauge fields can be written in the usual way:

$$\mathcal{L}_G = -\frac{1}{4}W_{\mu\nu}^a W_a^{\mu\nu} - \frac{1}{4}B_{\mu\nu}B^{\mu\nu}. \quad (1.3)$$

In addition to these vector particles, the model also includes an $SU(2)_L$ doublet Φ of complex scalar fields with hypercharge $Y = 1$. This field is known as *Higgs* field and the corresponding Lagrangean is:

$$\mathcal{L}_H = (D_\mu\Phi)^\dagger (D_\mu\Phi) - V(\Phi^\dagger\Phi), \quad (1.4)$$

$$V(\Phi^\dagger\Phi) = \frac{\lambda}{4} \left(\Phi^\dagger\Phi - \frac{\eta^2}{2} \right)^2, \quad (1.5)$$

with the covariant derivative:

$$D_\mu\Phi = \left(\partial_\mu + igW_\mu^a I_a + \frac{1}{2}ig'B_\mu \right) \Phi. \quad (1.6)$$

The whole Lagrangean $\mathcal{L}_G + \mathcal{L}_H$ is invariant under $SU(2)_L \times U(1)_Y$ gauge transformations:

$$B_\mu \rightarrow B'_\mu = B_\mu - \frac{1}{g'}\partial_\mu\alpha, \quad (1.7)$$

$$W_\mu \equiv W_\mu^a I_a \rightarrow W'_\mu = e^{i\beta_a I_a} \left(W_\mu - \frac{i}{g}\partial_\mu \right) e^{-i\beta_a I_a}, \quad (1.8)$$

$$\Phi \rightarrow \Phi' = e^{i\alpha Y/2 + i\beta_a I_a} \Phi. \quad (1.9)$$

The presence of a gauge symmetry is responsible for the renormalizability of the model. However, the scalar potential V , which describes the Higgs self-interaction, is constructed in such a way that its minima occur for a non-vanishing value of Φ :

$$V(\Phi^\dagger\Phi) = 0 \quad \Leftrightarrow \quad \Phi^\dagger\Phi = \frac{\eta^2}{2} \quad \Rightarrow \quad \langle\Phi\rangle \neq 0. \quad (1.10)$$

It is convenient to rewrite Φ in the following way:

$$\Phi = \frac{1}{\sqrt{2}} e^{-i\theta_a I_a} \begin{pmatrix} 0 \\ \eta + H \end{pmatrix}, \quad (1.11)$$

where θ_a and H are real scalar fields. Comparing Eq. (1.11) with (1.10), it is straightforward to see that any field configuration $\bar{\Phi}$ satisfying the condition (1.10) is characterized by a specific choice of the three fields $\bar{\theta}_a$ and has $\bar{H} \equiv 0$. Now, looking at Eq. (1.9) it is clear that such a ground state $\bar{\Phi}$ is *not* invariant under a generic gauge transformation. Therefore, the gauge symmetry obeyed by the *Lagrangean* is not respected by the *vacuum* of the theory; this mechanism is called *spontaneous symmetry breaking*, and within the framework of the SM it is responsible for all the gauge bosons (as well as leptons and quarks) to acquire a non-zero mass. To understand how it happens, let us substitute Eq. (1.11) into (1.4), so to rewrite \mathcal{L}_H in terms of the new fields θ_a and H . It is easy to see that all the θ_a can be reabsorbed into W_μ^a by means of a gauge transformation (1.7-1.9) having $\beta_a = \theta_a$ and $\alpha = 0$:

$$B'_\mu = B_\mu, \quad (1.12)$$

$$W'_\mu = e^{i\theta_a I_a} \left(W_\mu - \frac{i}{g} \partial_\mu \right) e^{-i\theta_a I_a}, \quad (1.13)$$

$$\Phi' = \frac{1}{\sqrt{2}} \begin{pmatrix} 0 \\ \eta + H \end{pmatrix}. \quad (1.14)$$

Since both \mathcal{L}_G and \mathcal{L}_H are invariant under transformations (1.7-1.9), their new expressions in terms of B'_μ , W'^a_μ and Φ' are identical to the old ones in terms of B_μ , W_μ^a and Φ , so the only visible effect of (1.12-1.14) is to make the fields θ_a to disappear from the Lagrangean. However, to achieve this result we have to pay the price of *fixing* three of the four gauge parameters in a proper way, and as a consequence the symmetry of the model decreases. The only gauge transformation which is still allowed is the one preserving the form (1.14) of Φ' , i.e. the $U(1)_{\text{em}}$ subgroup of transformations (1.7-1.9) having $\beta_1 = \beta_2 = 0$ and $\beta_3 = -\alpha$. In this way, the original $SU(2)_L \times U(1)_Y$ symmetry has been broken to $U(1)_{\text{em}}$.

For simplicity, let us drop the prime in Eqs. (1.12-1.14) and denote the new fields B'_μ , W'^a_μ and Φ' by B_μ , W_μ^a and Φ . The scalar potential V given in Eq. (1.5) can be written as:

$$V(H) = \frac{\lambda^2 \eta^2}{4} H^2 + \frac{\lambda^2 \eta}{4} H^3 + \frac{\lambda^2}{16} H^4, \quad (1.15)$$

while from Eq. (1.6) and (1.14) we have:

$$\begin{aligned} (D_\mu \Phi)^\dagger (D_\mu \Phi) &= \frac{1}{2} \partial_\mu H \partial^\mu H + \frac{g^2}{8} (W_\mu^1 W_1^\mu + W_\mu^2 W_2^\mu) (\eta + H)^2 \\ &\quad + \frac{1}{8} (g W_\mu^3 - g' B_\mu)^2 (\eta + H)^2. \end{aligned} \quad (1.16)$$

Looking at this expression we see that the real field H (called the *physical* Higgs field) describes a particle with mass $m_H = \eta \sqrt{\lambda/2}$. Also, Eq. (1.16) provides the mass terms for the W_μ^a and B_μ fields, which therefore are no longer massless fields. The mass Lagrangean is:

$$\mathcal{L}_m = \frac{g^2 \eta^2}{8} (W_\mu^1 W_1^\mu + W_\mu^2 W_2^\mu) + \frac{\eta^2}{8} (W_\mu \quad B_\mu) \begin{pmatrix} gg & -g'g \\ -g'g & g'g' \end{pmatrix} \begin{pmatrix} W^\mu \\ B^\mu \end{pmatrix}. \quad (1.17)$$

To diagonalize the mass matrix in the second term of Eq. (1.17), let's introduce an angle θ (known as the *electroweak angle*) and let's denote by $c \equiv \cos \theta$ and $s \equiv \sin \theta$ its sine and cosine. It is convenient to define the following fields:

$$W_\mu^\pm = \frac{W_\mu^1 \mp i W_\mu^2}{\sqrt{2}}, \quad (1.18)$$

$$\begin{pmatrix} Z_\mu \\ A_\mu \end{pmatrix} = \begin{pmatrix} c & -s \\ s & c \end{pmatrix} \begin{pmatrix} W_\mu^3 \\ B_\mu \end{pmatrix}. \quad (1.19)$$

Substituting Eq. (1.19) into (1.17) we see that (A_μ, Z_μ) are mass eigenstates *if* θ is related to g and g' by the expression:

$$c = \frac{g}{\sqrt{g^2 + g'^2}}, \quad s = \frac{g'}{\sqrt{g^2 + g'^2}}, \quad (1.20)$$

I	II	III	$SU(3)_c$	$SU(2)_L$	$U(1)_Y$	Q
$\begin{pmatrix} \nu_e \\ e_L \end{pmatrix}$	$\begin{pmatrix} \nu_\mu \\ \mu_L \end{pmatrix}$	$\begin{pmatrix} \nu_\tau \\ \tau_L \end{pmatrix}$	1	2	-1	$\begin{pmatrix} 0 \\ -1 \end{pmatrix}$
e_R	μ_R	τ_R	1	1	-2	-1
$\begin{pmatrix} u_L \\ d_L \end{pmatrix}$	$\begin{pmatrix} c_L \\ s_L \end{pmatrix}$	$\begin{pmatrix} t_L \\ b_L \end{pmatrix}$	3	2	1/3	$\begin{pmatrix} 2/3 \\ -1/3 \end{pmatrix}$
u_R	c_R	t_R	3	1	4/3	2/3
d_R	s_R	b_R	3	1	-2/3	-1/3

Table 1.1: The particle contents of the fermionic sector of the Standard Model. If the mixing among quarks is neglected, the three generations are identical to one another (apart from particle masses) and independent. *Leptons* are $SU(3)_c$ singlets, and *quarks* are $SU(3)_c$ triplets. Note that no right-handed neutral lepton is present in the minimal model.

It is easy to see that the field A_μ is massless, and that the residual $U(1)_{\text{em}}$ gauge symmetry corresponds to transformations $A_\mu \rightarrow A_\mu - \partial_\mu \chi$; therefore, we can identify A_μ with the electromagnetic field. The masses of the W^\pm and Z bosons are:

$$\left. \begin{aligned} m_W &= \frac{1}{2}g\eta \\ m_Z &= \frac{1}{2}f\eta \end{aligned} \right\} \Rightarrow m_W = m_Z c, \quad (1.21)$$

where $f \equiv \sqrt{g^2 + g'^2}$.

Interactions among W^\pm , Z , A , H are described by the cubic and quartic terms in the Lagrangeans \mathcal{L}_G and \mathcal{L}_H . In particular, one finds that Z and H do not couple to A (i.e. they are *neutral*), while W^\pm is *charged* and its coupling constant to the photon field is gs .

1.1.2 The fermion sector

Fermions observed in Nature can be divided into two classes, depending on whether or not they participate to *strong* (color) interactions: *leptons*, which are color singlets and only have electromagnetic and weak interactions, and *quarks*, which are color triplets. Both of them can be further divided into three *families*, or generations, all carrying the same $SU(3)_c \times SU(2)_L \times U(1)_Y$ quantum numbers and differing from one another only in masses. The general structure of the fermionic sector of the SM is shown in Table 1.1.

In the present discussion, we will neglect mixing among quarks, since in this thesis we will never make use of this concept. With this simplifying assumption, all the three families are independent from one another, and the Lagrangean describing interactions of leptons and quarks with W^\pm , Z , A , H bosons is naturally split into three identical parts. Therefore, to describe fermions in a simple way we will introduce a generation index $f = 1, 2, 3$, and denote by l_L^f , q_L^f each lepton and quark left $SU(2)_L$ doublet and by E_R^f , U_R^f , D_R^f each down-lepton, up-quark and down-quark right $SU(2)_L$ singlet, respectively. With this notation, the fermionic part of the SM Lagrangean

is:

$$\mathcal{L}_l = i \sum_f \left[l_L^{f\dagger} \bar{\sigma}^\mu D_\mu l_L^f + E_R^{f\dagger} \sigma^\mu D_\mu E_R^f \right] - \sum_f \lambda_E^f \left[l_L^{f\dagger} \Phi E_R^f + \text{h.c.} \right], \quad (1.22)$$

$$\begin{aligned} \mathcal{L}_q = i \sum_f & \left[q_L^{f\dagger} \bar{\sigma}^\mu D_\mu q_L^f + U_R^{f\dagger} \sigma^\mu D_\mu U_R^f + D_R^{f\dagger} \sigma^\mu D_\mu D_R^f \right] \\ & - \sum_f \lambda_U^f \left[q_L^{f\dagger} \tilde{\Phi} U_R^f + \text{h.c.} \right] - \sum_f \lambda_D^f \left[q_L^{f\dagger} \Phi D_R^f + \text{h.c.} \right], \end{aligned} \quad (1.23)$$

where σ^i are the Pauli matrices:

$$\sigma^0 = \begin{pmatrix} 1 & 0 \\ 0 & 1 \end{pmatrix}, \quad \sigma^1 = \begin{pmatrix} 0 & 1 \\ 1 & 0 \end{pmatrix}, \quad \sigma^2 = \begin{pmatrix} 0 & -i \\ i & 0 \end{pmatrix}, \quad \sigma^3 = \begin{pmatrix} 1 & 0 \\ 0 & -1 \end{pmatrix}, \quad (1.24)$$

$$\bar{\sigma}^0 = \sigma^0, \quad \bar{\sigma}^i = -\sigma^i, \quad (1.25)$$

and the covariant derivatives are:

$$D_\mu X_L^f = \left(\partial_\mu + ig W_\mu^a I_a + ig' \frac{Y_X}{2} B_\mu \right) X_L^f \quad X = l, q; \quad (1.26)$$

$$D_\mu X_R^f = \left(\partial_\mu + ig' \frac{Y_X}{2} B_\mu \right) X_R^f \quad X = E, U, D. \quad (1.27)$$

The field $\tilde{\Phi}$ is used to give mass to the up-quarks, and is defined as:

$$\tilde{\Phi} = i\sigma^2 \Phi^*. \quad (1.28)$$

After spontaneous symmetry breaking, Φ acquire a non-zero vacuum expectation value and it is convenient to rewrite it as in Eq. (1.11); again, the unphysical fields θ_a can be gauged away and we have:

$$\Phi = \frac{1}{\sqrt{2}} \begin{pmatrix} 0 \\ \eta + H \end{pmatrix}, \quad \tilde{\Phi} = \frac{1}{\sqrt{2}} \begin{pmatrix} \eta + H \\ 0 \end{pmatrix}. \quad (1.29)$$

Replacing Eq. (1.29) into \mathcal{L}_l and \mathcal{L}_q we obtain both fermion masses and fermion-higgs interaction terms:

$$\mathcal{L}_H^{f\bar{f}} = -\frac{\eta + H}{\sqrt{2}} \sum_f \left[\lambda_E^f \left(E_L^{f\dagger} E_R^f + \text{h.c.} \right) + \lambda_U^f \left(U_L^{f\dagger} U_R^f + \text{h.c.} \right) + \lambda_D^f \left(D_L^{f\dagger} D_R^f + \text{h.c.} \right) \right]. \quad (1.30)$$

Looking at this expression, we see first of all that all the lepton and quark masses are proportional to the vacuum expectation value η of the higgs field, just as for the gauge bosons W and Z :

$$m_X^f = \frac{1}{\sqrt{2}} \lambda_X^f \eta \quad \Rightarrow \quad \lambda_X^f = \sqrt{2} \frac{m_X^f}{\eta}, \quad X = E, U, D; \quad (1.31)$$

also, comparing Eq. (1.31) with (1.30) it is clear that the coupling of the physical higgs and with fermions is proportional to the fermion mass.

To derive an expression for the interaction between fermions and A , W^\pm , Z gauge bosons, we must insert Eqs. (1.18-1.20) and (1.26, 1.27) into (1.22) and (1.23). After some calculation, in 4-component notation the interaction Lagrangean can be written as:

$$\mathcal{L}_G^{f\bar{f}} = -gsA^\mu J_\mu^{\text{em}} - g [W^{-\mu} J_\mu^+ + \text{h.c.}] - fZ^\mu J_\mu^0, \quad (1.32)$$

where J_μ^{em} is the *electromagnetic* current and J_μ^+ , J_μ^0 are the *charged* and *neutral* weak currents:

$$J_\mu^{\text{em}} = \sum_f \left[-\bar{E}^f \gamma_\mu E^f + \frac{2}{3} \bar{U}^f \gamma_\mu U^f - \frac{1}{3} \bar{D}^f \gamma_\mu D^f \right], \quad (1.33)$$

$$J_\mu^+ = \frac{1}{2\sqrt{2}} \sum_f \left[\bar{E}^f \gamma_\mu (1 - \gamma_5) N^f + \bar{D}^f \gamma_\mu (1 - \gamma_5) U^f \right], \quad (1.34)$$

$$J_\mu^0 = \frac{1}{2} \sum_f \sum_X \bar{X}^f \gamma_\mu (g_V^X - g_A^X \gamma_5) X \quad \text{for } X = N, E, U, D, \quad (1.35)$$

and the *vector* and *axial* neutral current coupling constant g_V and g_A are:

$$g_V = I_3 - 2Qs^2, \quad (1.36)$$

$$g_A = I_3. \quad (1.37)$$

Looking at Eqs. (1.32) and (1.33), we see that the coupling constant between the electron and A is $-gs$. But A_μ is the photon field, and we know from QED that the electric charge of the electron is $-e$. Therefore:

$$e = gs = g'c. \quad (1.38)$$

In the low-energy limit, the electroweak sector of the SM must produce as an effective theory the Fermi model of weak interactions. It is easy to see that this requirement is satisfied only if the following relation between the Fermi coupling constant G_F and the vacuum expectation value of the higgs field η holds:

$$G_F = \frac{1}{\sqrt{2}\eta^2} \quad \Rightarrow \quad \eta = \frac{1}{\sqrt{\sqrt{2}G_F}}, \quad (1.39)$$

and from the numerical value $G_F \approx 1.16639 \cdot 10^{-5} \text{ GeV}^{-2}$ we get $\eta \approx 246 \text{ GeV}$.

1.2 Regularization and renormalization

1.2.1 General discussion

Any field theory, both classical and quantum, is characterized by a Lagrangean function from which the equations of motion can be derived. This tree-level Lagrangean involves a certain number of free parameters, a_i , which are not fixed by the theory. To determine them, the common strategy consists in choosing a suitable set of experimental results e_j , deriving a theoretical

prediction e_j^{th} (which is a function of the free parameters: $e_j^{\text{th}} = e_j^{\text{th}}(a_i)$ for them, and then inverting the relations thus obtaining the expressions of the free parameters a_i in terms of the measured quantities e_j . After that has been done, the bare quantities a_i , being now functions of experimental results, can be viewed as experimental quantities themselves and acquire a precise and well-defined physical meaning. If the relation between the a_i and e_j is simple enough, it may be convenient to replace a_i with e_j directly into the Lagrangean, so that now the model is formulated from the very beginning in terms of the results of some fundamental experiments. This approach is the default one in classical physics.

In quantum field theory, the situation is different. In higher order perturbation theory, the relations between formal parameters and measurable quantities get contributions not only from tree graphs but also from loop diagrams (the so-called *radiative corrections*), so in general they are different from tree level relations. The first problem one has to deal with arises when performing loop integrals: many of them turn out to be divergent, so the whole theory seems to be mathematically inconsistent. To overcome this problem, it is necessary to introduce a *regularization procedure*, i.e. a consistent way to properly parameterize the divergencies and to keep them under control by introducing in the model a new (unphysical) parameter, known as *cutoff*. The simplest way to do this is to perform integrations in the euclidian momentum space only in the finite region $p^2 \leq \Lambda^2$, rather than up to $p^2 = +\infty$; as a consequence, all the integrals are now convergent, but the relations between physical quantities and bare parameters depend also on the cutoff Λ . A more sophisticated technique, which is preferred for gauge theories since it preserves Lorentz and gauge invariance from the very beginning, is *dimensional regularization*, which consists in replacing the dimension 4 of the space-time by a lower dimension $D = 4 - 2\epsilon$ where the integrals are convergent:

$$\int \frac{d^4k}{(2\pi)^4} \quad \rightarrow \quad \mu^{4-D} \int \frac{d^Dk}{(2\pi)^D}, \quad (1.40)$$

where the mass parameter μ has been introduced in order to keep the dimensions of the coupling constants in front of the integral independent on D . Now all the integrals are mathematically well-defined objects, so we can safely derive the expressions for the bare parameters a_i in terms of the measurable quantities e_j , as in the classical case. However, if in these relations we try to perform the limits $\Lambda \rightarrow \infty$ or $\epsilon \rightarrow 0$, so to eliminate the cutoff and recover the original theory, the divergencies which were removed by the regularization procedure rises again and we find that the a_i parameters have infinite value. Therefore, it is not possible to write the Lagrangean directly through experimental quantities, and it is not clear how the model can be predictive.

The solution is straightforward. Leaving the Lagrangean written in terms of bare quantities, it is still possible to derive theoretical predictions for any experiment e'_k expressing it as a function of the a_i , and then using the previously found relations to eliminate a_i in favor of the measured quantities e_j . In this way, we can use our model to derive (cutoff dependent) relations among the different sets of experimental quantities e_j and e'_k . Now we eliminate the cutoff by performing the limit $\Lambda \rightarrow \infty$ or $\epsilon \rightarrow 0$: if for *any* choice of the measurable quantities e_j and e'_k our relations remain finite, i.e. the divergent pieces automatically cancel among one another, then our theory is told to be *renormalizable*. In this case, the predictivity of the model is preserved, although it is no longer possible to give a physical meaning to the bare parameters.

In general, writing the Lagrangean in terms of experimental quantities is a convenient and desirable fact, and to make it possible some interesting techniques have been developed. The most common take advantage of the concept of *counterterms*, which are extra (divergent) terms inserted into the tree Lagrangean to compensate the divergencies coming from loop integrals. Although this method is very useful for proving renormalizability theorems and deriving relations at two or more loops, when working at the one-loop level it is simpler to keep the Lagrangean expressed through the bare quantities and to use the approach described above.

Since in the present thesis we will rarely deal with expressions beyond one-loop, we won't discuss further details of alternative methods. However, let us conclude introducing a few ideas that will be widely used in Chapters 2 and 3. In the dimensional regularization approach, all the divergent terms are proportional to some power of $1/\epsilon$. If the model under construction has been proved to be renormalizable, we know by sure that all these terms will cancel from the final relations among physical observables. So there is no reason to keep them while performing calculations: we can simply drop all divergent terms from the very beginning. In particular, we can remove them directly in the expressions of the bare parameters a_i through the experimental quantities e_j , thus defining a new set of parameters \hat{a}_i which are completely equivalent to a_i but have a finite and cutoff-independent value. This way of eliminating divergencies is called *Minimal Subtraction* (MS) scheme, and is very useful since it allows to write the Renormalization Group equations (RGE) in a very simple form (see Chapter 3). A variant of this scheme called *modified MS* (or $\overline{\text{MS}}$) scheme, is obtained by reparameterizing the divergent pieces in terms of $\Delta = 1/\epsilon - \gamma + \ln 4\pi$ and then dropping Δ from all formulas. It is worth noting that MS or $\overline{\text{MS}}$ quantities, despite of their finite numerical value, are purely mathematical objects without any obvious physical meaning.

1.2.2 Renormalization of the Standard Model

Having discussed the general properties of renormalization, let us turn our attention to the Standard Model. The tree level Lagrangean was introduced in Sec. 1.1, and it is now intended that all the free parameters (masses, coupling constants, etc.) appearing into it have to be regarded to as *bare quantities*. From now on, we will denote them by a subscript “0” (m_{W0} , m_{Z0} , α_0 , etc.), so to distinguish them from physical observables (m_W , m_Z , α , etc.); all the tree-level expressions derived in Sec. 1.1 are valid at any order in perturbation theory, provided that they are intended as relations among bare quantities.

The electroweak sector of the Standard Model can be fully described in terms of the three experimental quantities e , m_W and m_Z , to which we must add the fermion masses m_f and the (still unknown) higgs mass m_H . As usual, the free/dressed propagators are defined as the inverse of the differential operator entering the quadratic part of the free/effective Lagrangean. It is convenient to factor out the Lorentz metrics and to write:

$$D_W^{\mu\nu} = -i g^{\mu\nu} D_W, \quad \Rightarrow \quad (D_W^{\mu\nu})^{-1} = i g^{\mu\nu} (D_W)^{-1}, \quad (1.41)$$

$$\mathbf{D}_{\gamma Z}^{\mu\nu} = -i g^{\mu\nu} \mathbf{D}_{\gamma Z}, \quad \Rightarrow \quad (\mathbf{D}_{\gamma Z}^{\mu\nu})^{-1} = i g^{\mu\nu} (\mathbf{D}_{\gamma Z})^{-1}, \quad (1.42)$$

where $\mathbf{D}_{\gamma Z}$ is a (2×2) matrix, which is non-diagonal due to the mixing between γ and Z induced by radiative corrections:

$$\mathbf{D}_{\gamma Z} = \begin{pmatrix} D_G & D_{\gamma Z} \\ D_{\gamma Z} & D_Z \end{pmatrix}. \quad (1.43)$$

The relation between the dressed propagators and the gauge boson *self-energies* are:

$$(D_W)^{-1}(k^2) = k^2 - m_{W0}^2 + \Sigma_W(k^2), \quad (1.44)$$

$$(\mathbf{D}_{\gamma Z})^{-1}(k^2) = \begin{pmatrix} k^2 + \Sigma_\gamma(k^2) & -\Sigma_{\gamma Z}(k^2) \\ -\Sigma_{\gamma Z}(k^2) & k^2 - m_{Z0}^2 + \Sigma_Z(k^2) \end{pmatrix}, \quad (1.45)$$

from which we can derive the expression for the propagators (at the one-loop level):

$$D_W(k^2) = \frac{1}{k^2 - m_{W0}^2 + \Sigma_W(k^2)}, \quad \Sigma_W(k^2) = m_W^2 \Pi_W(k^2), \quad (1.46)$$

$$D_\gamma(k^2) = \frac{1}{k^2 + \Sigma_\gamma(k^2)}, \quad \Sigma_\gamma(k^2) = m_Z^2 \Pi_\gamma(k^2), \quad (1.47)$$

$$D_Z(k^2) = \frac{1}{k^2 - m_{Z0}^2 + \Sigma_Z(k^2)}, \quad \Sigma_Z(k^2) = m_Z^2 \Pi_Z(k^2), \quad (1.48)$$

$$D_{\gamma Z}(k^2) = \frac{\Sigma_{\gamma Z}(k^2)}{k^2 [k^2 - m_{Z0}^2]}, \quad \Sigma_{\gamma Z}(k^2) = m_Z^2 \Pi_{\gamma Z}(k^2). \quad (1.49)$$

Note that the $\Sigma_i(k^2)$ self-energies have dimensions of a mass squared, while the $\Pi_i(k^2)$ quantities are adimensional.

Now, let us consider the photon propagator $D_\gamma(k^2)$ shown in Eq. (1.47). For any given Feynman diagram, each internal photon line carrying momentum squared k^2 contributes to the total amplitude with a factor $\alpha_0 D_\gamma(k^2)$, where α_0 accounts for the (bare) electric charges at the two vertices to which the photon propagator $D_\gamma(k^2)$ is attached. We can reabsorb the effects of vacuum polarization (described by $\Sigma_\gamma(k^2)$) into the fine structure constant by defining a “*running*” coupling constant $\alpha(k^2)$:

$$\frac{\alpha(k^2)}{k^2} \equiv \frac{\alpha_0}{k^2 + \Sigma_\gamma(k^2)}. \quad (1.50)$$

This relation defines $\alpha(k^2)$ for any values of k^2 . Since the bare parameter α_0 does not depend on k^2 , we can write:

$$\alpha_0 = \alpha(k^2) \left[1 + \frac{\Sigma_\gamma(k^2)}{k^2} \right] = \alpha(q^2) \left[1 + \frac{\Sigma_\gamma(q^2)}{q^2} \right] \quad \forall k, q. \quad (1.51)$$

Setting $q^2 \rightarrow 0$, and requiring that $\alpha(0)$ coincides with the fine structure constant α so to have the correct low-energy limit, we get (at one-loop):

$$\alpha(k^2) = \frac{\alpha}{1 - [\Sigma'_\gamma(0) - (m_Z^2/k^2) \Pi_\gamma(k^2)]}. \quad (1.52)$$

In this thesis, we will deal mainly with quantities which are defined at the electroweak scale. Since α is essentially a low-energy parameter, it is more convenient for our purposes to expand the perturbation series in powers of $\alpha(m_Z^2)$ rather than α . However, $\alpha(m_Z^2)$ is not a purely electromagnetic parameter (it also gains contributions from charged gauge bosons), and in principle it is sensitive to radiative effects due to New Physics. To overcome these problems, let's define:

$$\bar{\alpha} = \frac{\alpha}{1 - \delta\alpha}, \quad \delta\alpha = [\Sigma'_\gamma(0) - \Pi_\gamma(m_Z^2)]_{\text{light fermions}}, \quad (1.53)$$

where $\delta\alpha$ takes into account only the contributions of light fermions (here “light” means “lighter than Z-boson”), i.e. the 3 charged leptons (e, μ, τ) and the 5 quarks (u, d, c, s, b): top quark (t) and charged bosons (W boson and Higgs ghosts) are excluded. Defined in this way, $\bar{\alpha}$ is a purely electromagnetic gauge-invariant parameter, but conversely radiative corrections from top and gauge bosons to $\bar{\alpha}$ -related quantities are *not* automatically included, and must be added by hand [15]. For later convenience, we also define:

$$\delta\alpha_{t,W} = [\Sigma'_\gamma(0) - \Pi_\gamma(m_Z^2)]_{t,W} \quad \Rightarrow \quad \delta\alpha + \delta\alpha_{t,W} = \Sigma'_\gamma(0) - \Pi_\gamma(m_Z^2). \quad (1.54)$$

Numerically, we have $1/\alpha = 137.0359895(61)$ and $1/\bar{\alpha} = 128.878(90)$.

As already stated, the gauge sector of the Standard Model can be fully described in terms of three experimental quantities. The best measured electroweak observables are presently the Fermi coupling constant G_F , the Z boson mass m_Z , and of course the fine structure constant α ; for the above mentioned reasons, it is better to replace the last one with $\bar{\alpha}$. Using Eqs. (1.21), (1.38) and (1.39), we define the electroweak angle in the following way:

$$s^2 c^2 = \frac{\pi \bar{\alpha}}{\sqrt{2} G_F m_Z^2}, \quad (1.55)$$

and substituting the numerical values we get $s^2 = 0.23116(22)$.

When considering the effects of radiative corrections to the relations among physical observables, a number of different classes of Feynman diagrams must be taken into account. Although in principle all of them participate to the final result, in practice for most of the cases the largest contributions comes from vector boson self-energies, and vertex and box diagrams may safely be neglected. Since all the Σ_i defined in Eqs.(1.46-1.49) contain divergent terms, only some special combinations of them can enter relations among measurable quantities, and it can be proved that the total number of divergency-free independent combinations is 3. To parameterize them, let us consider the W and Z boson mass ratio m_W/m_Z , the Zee axial coupling $g_a \equiv g_a^E$, and the ratio of vector to axial coupling g_v/g_a in the Zee vertex. From the previous section, we know that the tree level value for these quantities are c , $-1/2$, and $1 - 4s^2$, respectively, so a convenient parameterization for the higher order effects is:

$$\frac{m_W}{m_Z} = c + \frac{3c\bar{\alpha}}{32\pi s^2 (c^2 - s^2)} V_m, \quad (1.56)$$

$$g_A = -\frac{1}{2} - \frac{3\bar{\alpha}}{64\pi c^2 s^2} V_A, \quad (1.57)$$

$$R \equiv \frac{g_V}{g_A} = 1 - 4s^2 + \frac{3\bar{\alpha}}{4\pi (c^2 - s^2)} V_R. \quad (1.58)$$

The expressions for the V_i functions in terms of gauge bosons self-energies, vertex and box diagrams are given in Appendix A. However, let us mention that the largest contributions are due to the big mass splitting (which breaks $SU(2)_L$ symmetry) between top and bottom quarks, and are proportional to m_t^2 ; the numerical coefficients in front of V_i in Eqs. (1.56-1.58) were chosen in such a way that the leading top contribution into V_i is simply $(m_t/m_Z)^2$ [16].

1.3 Supersymmetry

1.3.1 Motivations for New Physics

Despite of its success in explaining all the present experimental data, the Standard Model is not believed to be the ultimate theory of Nature; this is due mainly to three “problems”, or at least “unpleasantnesses”, which occur within its framework [17]. The first one is the large number of arbitrary assumptions and parameters it exhibits: besides the 3 charged lepton and 6 quark masses, we have the higgs boson mass, the higgs vacuum expectation value, the 3 gauge coupling constants, and the 4 parameters of the CKM quark mixing matrix (which we didn’t discuss in Sec. 1.1). The recently found evidence for neutrino oscillations adds to this set also neutrino masses and mixing angles. Moreover, many features of the model - for example the number of fermion generations, see Chapter 5 - have no theoretical explanation, and must be accepted as a matter of fact. This is not a “problem” in a proper sense, but it is generally believed that a fundamental theory should make as little unexplained assumptions as possible (the best being no assumptions at all), and from this point of view the SM is clearly unsatisfactory.

The second problem is that the Standard Model, due to the invariant $U(1)_Y$ subgroup of hypercharge, is not asymptotically free, so ultimately, at some energy scale, its interactions will become strong [17]. This suggests that the SM is the low-energy limit of a more fundamental theory, eventually unifying all the three gauge coupling constants into one and accommodating all known particles into a few representations of its gauge group. This idea has led to the concept of *Grand Unified Theory*, or GUT, whose prototype is $SU(5)$. In this model, the 12 generators of the Standard Model $SU(3)_c \times SU(2)_L \times U(1)_Y$ group are embedded into the 24-dimensional algebra of $SU(5)$, and the 15 Weyl spinors which form *each* SM family (N_L, E_L, E_R and $3_c \times (U_L, U_R, D_L, D_R)$) perfectly fit into a **5** and **10** representation of $SU(5)$ - in particular, no right-handed neutrino is required. When the model was first suggested [18], the poor-quality experimental data were in agreement with the hypothesis of unification of the three SM coupling constants α_i into a single one α_5 at a mass scale $m_{\text{GUT}} \sim 10^{14} \div 10^{15}$ GeV. Unfortunately, more accurate measurements proved that within the SM the coupling constants never get unified (or equivalently forcing their match at a single point lead to a wrong prediction for s^2 or α_s), as we show in Fig. 1.1; however, the basic idea of GUT is still alive and widely accepted, provided that some New Physics exists at a scale *lower* than m_{GUT} and yields unification.

The third problem, known as *the hierarchy problem*, is related to the protection of the higgs mass from effects of radiative corrections due to superheavy particles. It is well known that when the higgs mass is of the order of a few TeV, then the higgs self-coupling gets too strong, and we should not be observing the apparently successful perturbation theory at low energies. Any

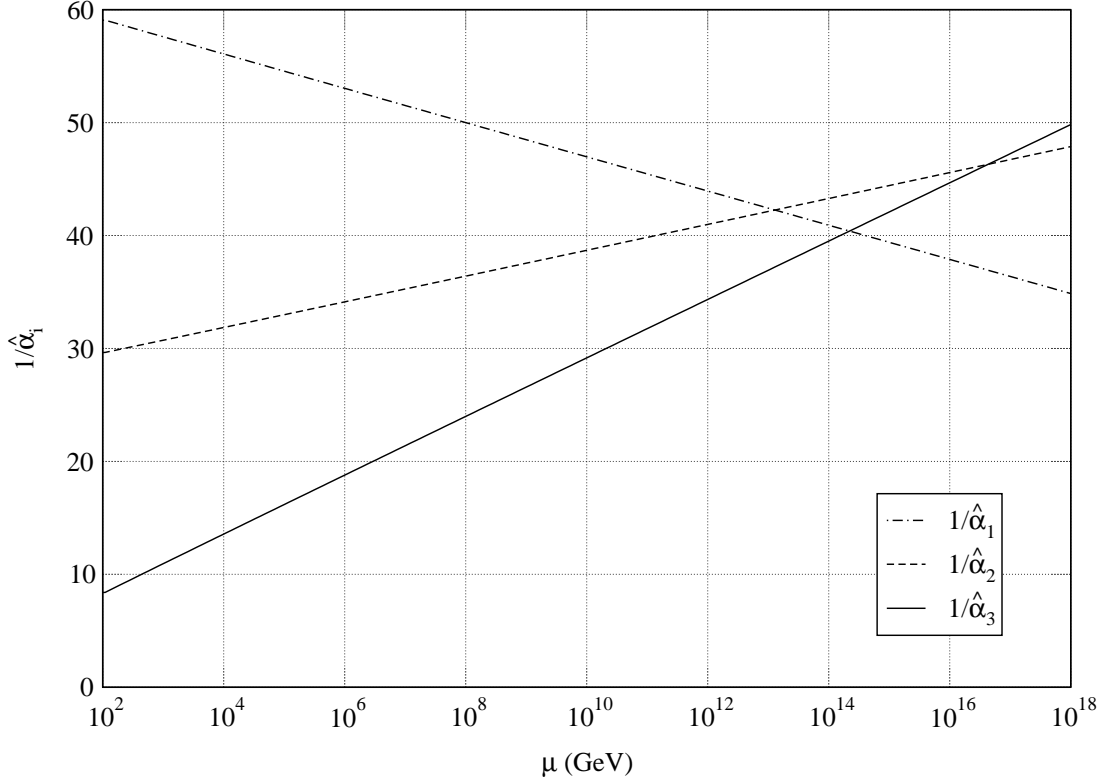


Figure 1.1: Running of the $\hat{\alpha}_1$, $\hat{\alpha}_2$ and $\hat{\alpha}_3$ coupling constants in the framework of the Standard Model, as a function of the mass scale parameter μ . The starting point is $m_Z = 91.1867$ GeV, $\hat{\alpha}(m_Z) = 1/128.1$, $s^2 = 0.23147$, $\hat{\alpha}_3(m_Z) = 0.119$, $\hat{m}_t(m_Z) = 175$ GeV.

GUT model predicts the existence of heavy gauge bosons and Higgs scalars, whose mass is of the same order of the scale at which the GUT symmetry is broken (i.e. $\sim m_{\text{GUT}}$); the reason why such a GUT scale ($\sim 10^{16}$ GeV for SUSY $SU(5)$) and the electroweak scale ($\sim 10^2$ GeV) are so different should be explained by the model. However, even if we choose the hierarchy in such a way, the radiative corrections will destroy it. To see this, let us consider the contribution to the SM higgs self-energy due to a superheavy boson of mass M [19]: it is given by the following Feynman diagram, and it is proportional to the mass squared of the heavy particle:

$$\text{---} \text{---} \text{---} \text{---} \Rightarrow \delta m^2 = \lambda^2 M^2. \quad (1.59)$$

This correction, if not canceled by some mechanism, obviously spoils the hierarchy, unless a completely unnatural fine tuning of the order of 10^{-14} for the coupling constant λ^2 is introduced.

The solution to the last problem is the main motivation to introduce supersymmetry (SUSY). The most elegant way to prevent a physical quantity to acquire an uncontrolled value due to radiative corrections is to introduce a symmetry which protects it. In (unbroken) supersymmetric models, each boson has a fermionic partner of equal mass, whose contribution should be accounted for when evaluating radiative corrections. For the case of the SM higgs in the framework of

GUT, the joint contributions of superheavy bosons and their fermionic superpartners are free of quadratic divergencies:

$$\text{---} \bullet \text{---} \text{ (loop) } + \text{---} \bullet \text{---} \text{ (loop) } \Rightarrow \delta m^2 = 0. \quad (1.60)$$

This mechanism for cancellation of quadratic divergencies is peculiar to SUSY models, and it can be proved that it occurs at any order in perturbation theory.

1.3.2 The Minimal Supersymmetric Standard Model

From a mathematical point of view, the basic idea of supersymmetry consists in the extension of the Poincaré group of space-time transformations through the introduction of new *anticommuting* generators $Q_\alpha^i, \bar{Q}_{\dot{\alpha}}^i$ (here $\alpha, \dot{\alpha} = 1, 2$ and $i = 1, \dots, N$) [20]. These extra generators have the remarkable property of transforming a boson into a fermion and vice versa, thus any supermultiplet corresponding to an irreducible representation of the SUSY algebra contains both bosonic and fermionic degrees of freedom (in equal number). For the simplest case $N = 1$ we have only 4 new generators, and in addition to the usual commutation relations among Poincaré generators we have [19]:

$$\{Q_\alpha, \bar{Q}_{\dot{\beta}}\} = 2(\sigma^\mu)_{\alpha\dot{\beta}} P_\mu, \quad (1.61)$$

$$\{Q_\alpha, Q_\beta\} = \{\bar{Q}_{\dot{\alpha}}, \bar{Q}_{\dot{\beta}}\} = 0, \quad (1.62)$$

$$[Q_\alpha, P_\mu] = [\bar{Q}_{\dot{\alpha}}, P_\mu] = 0, \quad (1.63)$$

$$[Q_\alpha, M_{\mu\nu}] = \frac{1}{2}(\sigma_{\mu\nu})_\alpha^\beta Q_\beta, \quad (1.64)$$

$$[\bar{Q}_{\dot{\alpha}}, M_{\mu\nu}] = -\frac{1}{2}\bar{Q}_{\dot{\beta}}(\bar{\sigma}_{\mu\nu})_{\dot{\alpha}}^{\dot{\beta}}, \quad (1.65)$$

$$\alpha, \dot{\alpha}, \beta, \dot{\beta} = 1, 2, \quad (1.66)$$

where P_μ and $M_{\mu\nu}$ are four-momentum and angular momentum operators, respectively. From these relations we see that Q_α and $\bar{Q}_{\dot{\alpha}}$ are spinors under rotations and invariant under spatial translations; in particular, from Eq. (1.63) we observe that even under the SUSY group P^2 is a Casimir operator, thus all particles within the same irreducible supermultiplet share the same mass.

The simplest supersymmetric model including the SM is called Minimal Supersymmetric Standard Model (MSSM). Since in the $N = 1$ case the SUSY generators commute with the generators of internal symmetries, all superpartners have the same quantum numbers as the corresponding SM particles. Within the SM, the only couple of particles with different spin but the same gauge quantum numbers is neutrino/higgs boson; however, assuming that the higgs is the superpartner of a neutral lepton would imply that it also carries a lepton number, and this is phenomenologically unacceptable. Therefore, in the MSSM *all* the superpartners are introduced as *new* particles.

Bosons		Fermions		$SU(3)_c$	$SU(2)_L$	$U(1)_Y$
gluon	g^k	gluino	\tilde{g}^k	8	1	0
weak	W^a	wino	\tilde{W}^a	1	3	0
hypercharge	B	bino	\tilde{B}	1	1	0
sleptons	$\begin{pmatrix} \tilde{N}_L \\ \tilde{E}_L \end{pmatrix}$	leptons	$\begin{pmatrix} N_L \\ E_L \end{pmatrix}$	1	2	-1
	\tilde{E}_R		E_R	1	1	-2
	$\begin{pmatrix} \tilde{U}_L \\ \tilde{D}_L \end{pmatrix}$		quarks	$\begin{pmatrix} U_L \\ D_L \end{pmatrix}$	3	2
\tilde{U}_R	U_R	3		1	4/3	
\tilde{D}_R	D_R	3		1	-2/3	
higgs	H_1	higgsino	\tilde{H}_1	1	2	1
	H_2		\tilde{H}_2	1	2	-1

Table 1.2: The particle contents of the MSSM. Supersymmetric particles are denoted adding a tilde to the letter identifying the corresponding SM partner. Note that *two* higgs doublets (rather than *one*) are included in the model.

The particle contents of the MSSM is shown in Table 1.2. Unlike the SM, *two* higgs doublets rather than *one* are introduced, each having of course a fermionic counterpart. This is due to the fact that the mechanism used in the SM to give mass to the up-quarks, i.e. the construction of the $\tilde{\Phi}$ field by means of Φ alone, cannot be applied within the MSSM since it would require the introduction of explicitly SUSY-breaking terms into the Lagrangean. As a consequence, the Higgs sector of the MSSM is richer than the SM one: we start with 8 bosonic degrees of freedom, and after incorporating 3 of them into W^\pm and Z (which gain their mass in the usual way) we are left with 3 neutral scalar particles (2 CP-even, h and H , and 1 CP-odd, A) and 1 charged one (H^\pm). Without entering the details of calculations, let us mention that the low-energy ground state of the MSSM is characterized by two different vacuum expectation values, η_1 and η_2 , and that the breaking of the $SU(2)_L$ symmetry produces at tree level the following relations:

$$\eta^2 = \eta_1^2 + \eta_2^2, \quad \tan \beta \equiv \frac{\eta_2}{\eta_1}; \quad (1.67)$$

$$\left. \begin{aligned} m_W &= \frac{1}{2}g\eta \\ m_Z &= \frac{1}{2}f\eta \end{aligned} \right\} \Rightarrow \eta \approx 246 \text{ GeV}, \quad (1.68)$$

where we see that the parameter η plays the same role as in the SM. Also, the masses of the higgs bosons are not independent from one another:

$$m_{H^\pm} = m_A^2 + m_W^2, \quad (1.69)$$

$$m_{h,H}^2 = \frac{1}{2} \left[m_A^2 + m_Z^2 \pm \sqrt{(m_A^2 + m_Z^2)^2 - 4m_A^2 m_Z^2 \cos^2 2\beta} \right]. \quad (1.70)$$

Now, looking at Eq. (1.70) it is easy to see that the lightest higgs boson, whatever the values of m_A and $\tan \beta$ are, is always lighter than m_Z . This result is only valid at tree level, and radiative corrections affect it by increasing the upper limit; however, precise calculations show that m_h

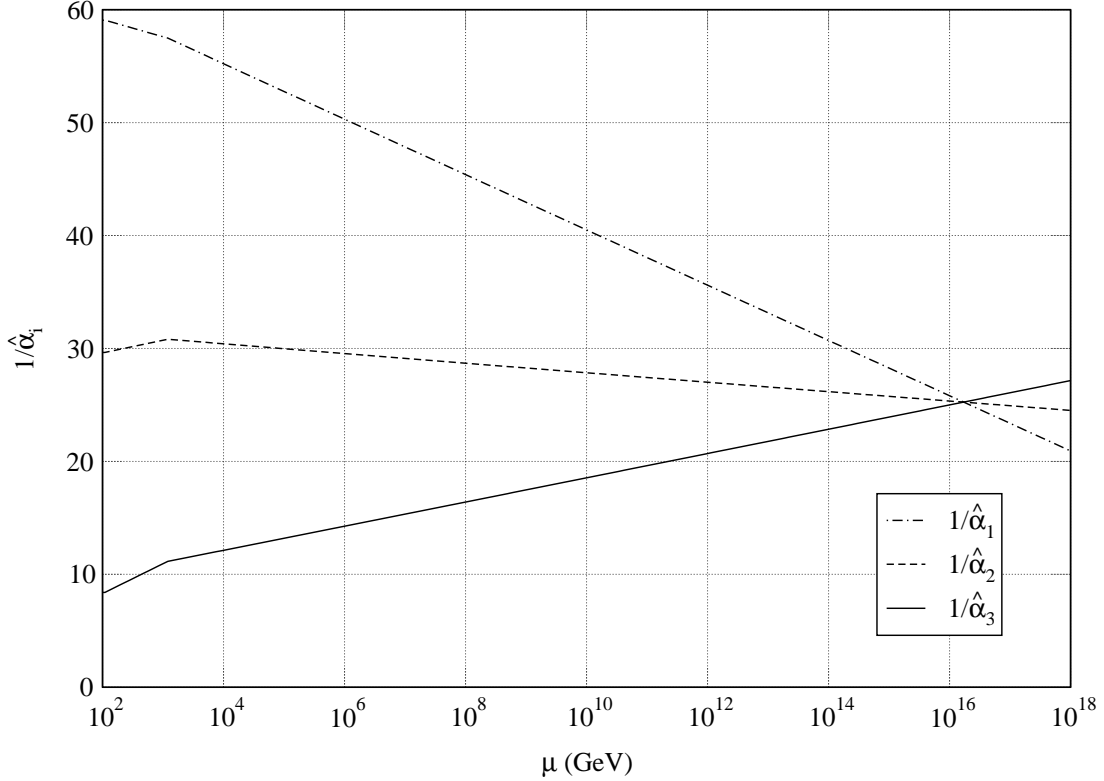


Figure 1.2: Running of the $\hat{\alpha}_1$, $\hat{\alpha}_2$ and $\hat{\alpha}_3$ coupling constants in the framework of the Minimal Supersymmetric Standard Model, as a function of the mass scale parameter μ . The starting point is $m_Z = 91.1867$ GeV, $\hat{\alpha}(m_Z) = 1/128.1$, $\hat{s}^2 = 0.23147$, $\hat{\alpha}_3(m_Z) = 0.119$, $\hat{m}_t(m_Z) = 175$ GeV.

cannot in general exceed $120 \div 130$ GeV, and this unique signature of SUSY models is probably the best test of low-energy supersymmetry which will be achieved by the next generation of accelerator experiments.

When building the most general SUSY-invariant Lagrangean extending in a minimal way the particle contents of the Standard Model, one quickly realizes that due to the many new particles present in the model the conservation of baryon and lepton numbers no longer occurs automatically. Since phenomenologically no evidence of B or L violation has been found, it is necessary to find a mechanism to suppress B and L violating terms, and in the MSSM this is achieved by introducing a new discrete symmetry called R -parity. Formally, one can define the R -parity of any particle of spin J , baryon number B and lepton number L to be $R = (-1)^{2J+3B+L}$, and it is immediate to see that all SM particles have $R = +1$, while all their superpartners have $R = -1$. The conservation of this quantities has two straightforward consequences: first, in laboratory experiments supersymmetric particles are produced in pairs; second, the lightest supersymmetric particle (LSP) *is stable*. The prediction of SUSY models with unbroken R -parity of a new stable particle is very interesting in an astrophysical contest, since it offers a chance to solve the problem of Dark Matter.

We already noted that in unbroken supersymmetric models all the particles within the same supermultiplet have the same mass. Since this is not observed to be the case in nature, we

conclude that SUSY must be broken at some scale. The mechanism adopted in the MSSM consists in an *explicit* breaking through the inclusion into the Lagrangean of the so-called “soft” terms, whose defining property is that they do not spoil the cancellation of quadratic divergencies produced by supersymmetry. The origin of these terms is usually ascribed to the spontaneous breaking of some larger symmetry, for example *supergravity* (i.e. *local* supersymmetry), at the GUT scale. In this framework, the MSSM is not a fundamental theory, but like the SM it is only a step towards it; however, the hypothesis of gauge coupling unification at a common mass scale, which is unrealizable in the Standard Model, is instead in excellent agreement with experimental data in the MSSM (see Fig. 1.2 and Chapter 3), and this represents nowadays a strong indirect hint in favor of supersymmetry.

Chapter 2

The numerical closeness between θ and the $\overline{\text{MS}}$ parameter $\hat{\theta}$

As we have seen in the previous chapter, the phenomenological angle θ plays a central role in the description of the electroweak sector of the Standard Model. This angle is defined in Eq. (1.55) through the best measured quantities G_F , m_Z and $\bar{\alpha}$, and is therefore very simple to deal with and is suitable for describing the electroweak precision measurements in a natural way. According to the last data from Ref. [21], we have:

$$s^2 = 0.23116(22). \quad (2.1)$$

However, as everybody knows, it is the value of $\hat{s}^2 \equiv \sin^2 \hat{\theta}$ which is used to study gauge couplings unification in the framework of GUT models. The corresponding angle is calculated in the modified minimal subtraction scheme ($\overline{\text{MS}}$), with $\mu = m_Z$. From Ref. [21] one can see that this quantity appears to be numerically very close to the phenomenological parameter s^2 :

$$\hat{s}^2 = 0.23144(24). \quad (2.2)$$

It can be seen immediately that s^2 and \hat{s}^2 are equal with an accuracy better than 0.1%. However, the splitting between them is generated by one-loop radiative corrections, and a natural estimate for their difference is about 1%. As an example, let us consider another possible definition of the electroweak angle, s_W^2 , which is related to the ratio between the W and Z boson masses:

$$s_W^2 = 0.22346(107). \quad (2.3)$$

The splitting between Eq. (2.3) and Eqs. (2.1), (2.2) is more than 3%, which is what can be expected for one-loop radiative corrections; therefore, the numerical closeness of s^2 and \hat{s}^2 is completely unnatural, and represents a puzzle of the Standard Model.

At this point it is useful to remind that there is one more coincidence in the Standard Model: the parameter $s_l^2 \equiv \sin^2 \theta_l$, which describes asymmetries in Z boson decays, also happens to be very close to s^2 . Numerically we have: [16]

$$s_l^2 = 0.23157(19). \quad (2.4)$$

This coincidence is known to be accidental, since it occurs only for the top quark mass m_t close to 170 GeV.

The aim of the present chapter is to present an explicit formula which provides the relation between s^2 and \hat{s}^2 . Such a relation is relevant since it provides a simple connection between *theoretical GUT models* (which are usually described in terms of \hat{s}^2) and *experimental results* (from which s^2 is defined), and will be widely used in Chapter 3. Analyzing this formula, we will see that the numerical closeness between s^2 and \hat{s}^2 occurs only for m_t close to 170 GeV, as for the case of s_l^2 , so it is really a coincidence without any physical reason. However, writing the expression for \hat{s}^2 through s_l^2 it will become clear that these two angles are naturally close, and their coincidence does not depend on the top mass and has a straightforward physical explanation. In this way we will see that, instead of two accidental coincidences between three mixing angles, we have only one.

In Sec. 2.1, we will quickly introduce the fundamental relations between bare quantities and physical observables. The rest of this chapter is based on the two published papers [1] and [2].

2.1 The bare quantities and the tree approximation

Let us start our discussion analyzing some relations among *bare quantities*. As was shown in Chapter 1, the electroweak mixing angle θ_0 (or, equivalently, its sine s_0 or cosine c_0) is defined from the ratio between the W and Z boson coupling constants g_0 and f_0 :

$$c_0 = \frac{g_0}{f_0}. \quad (2.5)$$

However, using formulas from the previous chapter it is possible to rewrite this expression in many different ways, so to relate θ_0 to other parameters of the model. In particular, from Eq. (1.21) we can express it through the ratio between the W and Z boson masses:

$$c_0 = \frac{m_{W0}}{m_{Z0}}. \quad (2.6)$$

Another interesting relation can be obtained by means of Eqs. (1.21), (1.38) and (1.39):

$$c_0^2 s_0^2 = \frac{\pi \alpha_0}{\sqrt{2} G_{F0} m_{Z0}^2}. \quad (2.7)$$

Finally, for the present discussion it will be useful to rewrite θ_0 in terms of the vector and axial neutral current coupling constants, g_{V0} and g_{A0} , describing the Zee vertex:

$$s_0^2 = \frac{1}{4} \left(1 - \frac{g_{V0}}{g_{A0}} \right). \quad (2.8)$$

Of course, many other definitions are possible, and all of them are equivalent to one another, but for our purposes these expressions are enough.

What we want to do now is to find the best way to relate these theoretical expressions to the experimental measurements. Let us start neglecting radiative corrections, so to check whether the

tree approximation is sufficient to describe the SM phenomenology at the present experimental accuracy.

At tree level, the bare quantities appearing on the r.h.s. of Eqs. (2.5-2.8) have a straightforward physical meaning, and all what we have to do is just to replace them with the corresponding experimental numbers. However, if we do this, we find that the values for the electroweak angle θ_0 which follow from these equations are in general in disagreement with one another. More exactly, the corresponding values for the parameter s_0^2 are just those reported in Eqs. (2.1-2.4), provided that the numerical value of $\bar{\alpha}$, rather than α , is used for α_0 in Eq. (2.7). The reason for this is that Eqs. (2.5), (2.6), (2.7) and (2.8), when considered as relations between physical quantities, are nothing but the definitions of the four different angles (2.2), (2.3), (2.1) and (2.4), respectively. In symbols:

$$\hat{s}^2 \equiv \frac{\hat{e}^2}{\hat{g}^2} \quad (\text{in the } \overline{\text{MS}} \text{ scheme, with } \mu = m_Z); \quad (2.9)$$

$$s_W^2 \equiv 1 - \frac{m_W^2}{m_Z^2}; \quad (2.10)$$

$$s^2 \equiv \frac{1}{2} \left(1 - \sqrt{1 - \frac{4\pi\bar{\alpha}}{\sqrt{2}G_F m_Z^2}} \right); \quad (2.11)$$

$$s_l^2 \equiv \frac{1}{4} \left(1 - \frac{g_V}{g_A} \right). \quad (2.12)$$

The disagreement among the numerical values (2.1-2.4) clearly proves that the tree approximation is not adequate to explain the experimental data, and radiative corrections should be taken into account. To do this, we need first of all to write down the relations between bare quantities and physical observables; therefore, in the rest of this section we will quickly review these formulas, addressing the reader to Ref. [22] for a more accurate analysis.

2.1.1 The fine structure constant

The fine structure constant α is defined from the γee vertex. The relevant Feynman diagrams, at one-loop level, are:

$$\quad \quad \quad (2.13)$$

From these graphs, it is easy to derive a relation between α and α_0 :

$$\alpha = \alpha_0 \left[1 - \Sigma'_\gamma(0) - 2\frac{s}{c} \Pi_{\gamma Z}(0) \right]. \quad (2.14)$$

Note that in Eq. (2.14) only photon self-energy and γZ mixing contribute. In principle, vertex corrections and electron self-energies should also be taken into account; however, due to Ward

identities, the sum of these contributions vanishes:

$$= 0 \quad (2.15)$$

For the present discussion, it is more convenient to relate α_0 to $\bar{\alpha}$, rather than to α . Making use of Eqs. (1.53) and (1.54), we can rewrite Eq. (2.14) as:

$$\bar{\alpha} = \alpha_0 \left[1 - 2 \frac{S}{c} \Pi_{\gamma Z}(0) - \Pi_{\gamma}(m_Z^2) - \delta\alpha_{t,W} \right]. \quad (2.16)$$

2.1.2 The W and Z pole masses

The relation between physical and bare W and Z masses are particularly simple. At the one-loop level, the relevant Feynman diagrams are:

$$(2.17)$$

Therefore:

$$m_W^2 = m_{W0}^2 [1 - \Pi_W(m_W^2)], \quad (2.18)$$

$$m_Z^2 = m_{Z0}^2 [1 - \Pi_Z(m_Z^2)]. \quad (2.19)$$

2.1.3 The Fermi coupling constant

The Fermi coupling constant G_F is defined from the process $\mu \rightarrow e \nu_{\mu} \bar{\nu}_e$. The Feynman diagrams are:

$$(2.20)$$

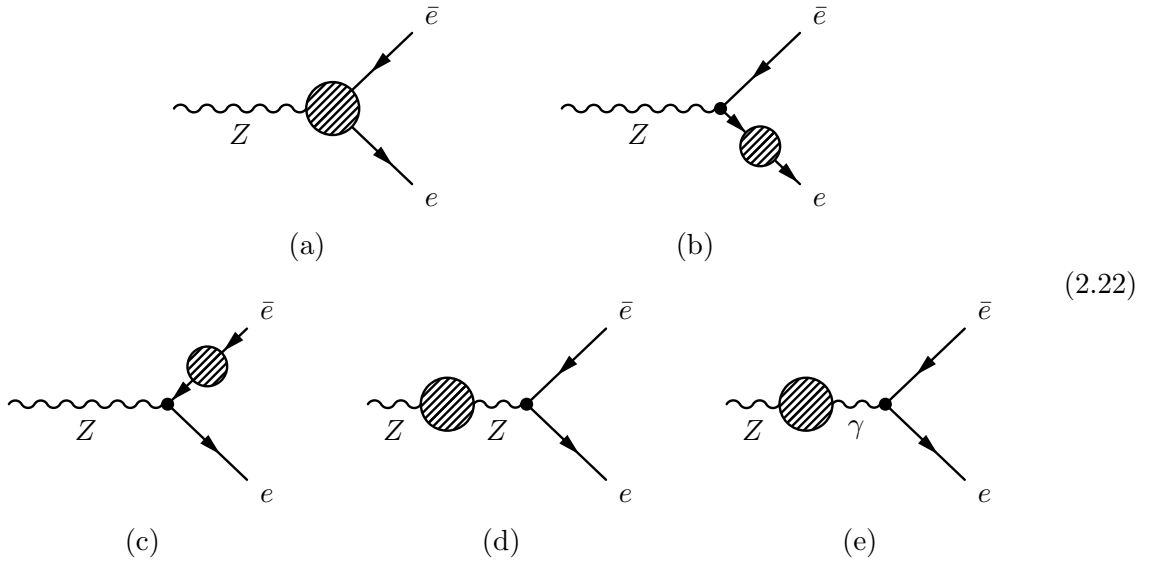
Therefore, the relation between G_F and G_{F0} is:

$$G_F = G_{F0} [1 + \Pi_W(0) + D], \quad (2.21)$$

where the term D denote the sum of the last three diagrams (c)-(e).

2.1.4 The g_V/g_A ratio

The last expressions we are interested in relate the bare parameters g_{V0} and g_{A0} to the physical observables g_V and g_A . These quantities describe the coupling of the Z boson field with the *vector* and *axial* part of the charged lepton current, respectively, and therefore the Feynman diagrams which are relevant for the present case are those affecting the Zll vertex:



In Ref. [22], accurate expressions relating g_{V0} to g_V and g_{A0} to g_A are derived. However, since in the present chapter the only place where g_V and g_A are used is the definition of the electroweak angle θ_l , it is enough for our purposes to consider just the *ratio* between them; therefore the only expression we report here is:

$$\frac{g_V}{g_A} = \frac{g_{V0}}{g_{A0}} \left(1 - \frac{4cs}{1-4s^2} [F_V^{Ze} - (1-4s^2) F_A^{Ze} + \Pi_{\gamma Z}(m_Z^2)] \right). \quad (2.23)$$

It is easy to understand *qualitatively* Eq. (2.23) by comparing it with the Feynman diagrams drawn above. The terms F_V^{Ze} and F_A^{Ze} describe the vector and axial part of the Zll vertex, and include both the contribution from the irreducible proper vertex (a) and the external lepton self-energies (b) and (c); the term $\Pi_{\gamma Z}(m_Z^2)$ comes from diagram (e). It is interesting to note that diagram (d), which is related to the wave function renormalization of the Z boson field, gives the same contribution both to g_V and to g_A , and therefore it cancels out (at one-loop level) from the ratio (2.23).

2.2 The one-loop approximation

Having proven that the tree approximation is not adequate to explain experimental data, let us now take into consideration the effects of radiative corrections. In the present section, we will derive relations which are correct up to the one-loop level, leaving for the next section the discussion of some higher-order contributions.

2.2.1 \hat{s}^2 versus s^2

The simplest way to relate \hat{s}^2 to s^2 is to start from Eq. (2.7) and substitute the bare parameters appearing on its r.h.s. with physical quantities, by means of Eqs. (2.16), (2.19) and (2.21). The final result is:

$$c_0^2 s_0^2 = \frac{\pi\bar{\alpha}}{\sqrt{2}G_F m_Z^2} \frac{[1 + \Pi_W(0) + D][1 - \Pi_Z(m_Z^2)]}{[1 - 2\frac{s}{c}\Pi_{\gamma Z}(0) - \Pi_{\gamma}(m_Z^2) - \delta\alpha_{t,W}]}. \quad (2.24)$$

Comparing this expression with Eq. (1.55), we see that the overall factor $\pi\bar{\alpha}/\sqrt{2}G_F m_Z^2$ is nothing but $c^2 s^2$. Moreover, since for the moment we are interested only in the one-loop approximation, we can expand the involved ratio of self-energies into an expression linear in the Π_i . In this way, we have:

$$c_0^2 s_0^2 = c^2 s^2 \left(1 + 2\frac{s}{c}\Pi_{\gamma Z}(0) + \Pi_{\gamma}(m_Z^2) - \Pi_Z(m_Z^2) + \Pi_W(0) + \delta\alpha_{t,W} + D \right). \quad (2.25)$$

It is straightforward to see that this angle θ_0 will coincide with $\hat{\theta}$ if D and Π_i are calculated in $\overline{\text{MS}}$ framework with $\mu = m_Z$. Therefore, from (2.25) we easily get:

$$\hat{s}^2 = s^2 + \frac{c^2 s^2}{c^2 - s^2} \left(2\frac{s}{c}\hat{\Pi}_{\gamma Z}(0) + \hat{\Pi}_{\gamma}(m_Z^2) - \hat{\Pi}_Z(m_Z^2) + \hat{\Pi}_W(0) + \delta\alpha_{t,W} + \hat{D} \right) \quad (2.26)$$

which is the relation we are interested in. Since the last equation is central for the present discussion, let us derive it in a different way. Substituting Eqs. (2.18) and (2.19) into Eq. (2.6) and assuming that Π_W and Π_Z are evaluated in the $\overline{\text{MS}}$ scheme, we get (see also Ref. [23]):

$$\begin{aligned} \hat{s}^2 &= 1 - \left[\frac{m_{W0}^2}{m_{Z0}^2} \right]_{\overline{\text{MS}}} = 1 - \frac{m_W^2 \left(1 - \hat{\Pi}_Z(m_Z^2) \right)}{m_Z^2 \left(1 - \hat{\Pi}_W(m_W^2) \right)} \\ &= 1 - \frac{m_W^2}{m_Z^2} + c^2 \left[\hat{\Pi}_Z(m_Z^2) - \hat{\Pi}_W(m_W^2) \right], \end{aligned} \quad (2.27)$$

where in the last expression we have substituted $(m_W/m_Z)^2$ with c^2 in the factor which multiplies Π_i , which is correct at one-loop level. Now for the ratio m_W/m_Z we should use a formula which takes radiative corrections into account. Since we are following the general approach to the electroweak radiative corrections which is presented partly in Ref. [22], we use Eq. (38) from that paper:

$$\begin{aligned} \frac{m_W^2}{m_Z^2} &= c^2 + \frac{c^2 s^2}{c^2 - s^2} \left(\frac{c^2}{s^2} [\Pi_Z(m_Z^2) - \Pi_W(m_W^2)] + \Pi_W(m_W^2) \right. \\ &\quad \left. - \Pi_W(0) - \Pi_{\gamma}(m_Z^2) - 2\frac{s}{c}\Pi_{\gamma Z}(0) - \delta\alpha_{t,W} - D \right). \end{aligned} \quad (2.28)$$

$\hat{D} \approx 96.083$	Heavy	Light	Bosons	Total
$\delta\alpha_{t,W}$	-0.623	0	5.326	4.703
$\hat{\Pi}_W(0)$	149.559	0	-18.891	130.669
$2\frac{s}{c}\hat{\Pi}_{\gamma Z}(0)$	0	0	-6.493	-6.493
$\hat{\Pi}_\gamma(m_Z^2)$	-8.964	86.902	-14.312	63.627
$-\hat{\Pi}_Z(m_Z^2)$	-244.399	-119.530	71.806	-292.123
Total	-104.427	-32.628	37.438	-99.617

Table 2.1: Contributions of the various self-energies appearing in Eq. (2.26), in units of 10^{-4} . The first column refers to *top* and *bottom*, the second to leptons and *up*, *down*, *charm*, *strange* quarks. The third column contains vector bosons, higgs and ghost loops, and the last one is the sum of the first three. We assumed $m_t = 173.8$ GeV and $m_H = 120$ GeV. The vertex-box contribution \hat{D} is reported in the upper-left corner.

The term $\delta\alpha_{t,W}$, which is absent in the original formula, has been added here to take explicitly into account the *top* and *W* loops, which contribute to Π_γ but are not included in the definition of $\bar{\alpha}$ (in Ref. [22], these contributions were accounted for by replacing s^2 with $s^2 + 0.00015$: see Ref. [15] for a detailed discussion on this subject).

Since both m_W/m_Z and c are finite, the expression for the sum of all the radiative corrections is finite as well and we can use $\overline{\text{MS}}$ quantities in it:

$$\begin{aligned} \frac{m_W^2}{m_Z^2} = c^2 + \frac{c^2 s^2}{c^2 - s^2} \left(\frac{c^2}{s^2} \left[\hat{\Pi}_Z(m_Z^2) - \hat{\Pi}_W(m_W^2) \right] + \hat{\Pi}_W(m_W^2) \right. \\ \left. - \hat{\Pi}_W(0) - \hat{\Pi}_\gamma(m_Z^2) - 2\frac{s}{c}\hat{\Pi}_{\gamma Z}(0) - \delta\alpha_{t,W} - \hat{D} \right). \end{aligned} \quad (2.29)$$

Substituting the last equation in (2.27), we obtain once more Eq. (2.26).

In Table 2.1 we provide some numerical estimate for all the polarization operators appearing in Eq. (2.26), together with the vertex-box term \hat{D} , for $m_t = 173.8$ GeV and $m_H = 120$ GeV. It is immediate to see that the contribution coming from top quark loops dominates over light fermions and gauge bosons, and that the overall result for all self-energies cancels quite exactly the vertex-box diagrams \hat{D} . The final expression for the difference $\hat{s}^2 - s^2$ at one-loop level is therefore:

$$\hat{s}^2 - s^2 \Big|_{\substack{m_t=173.8 \text{ GeV} \\ m_H=120 \text{ GeV}}} = -0.00329 + 0.00318 = -0.00011, \quad (2.30)$$

where the first term comes from polarization operators and the second from vertices and boxes.

To understand whether this strong cancellation has some physical meaning or is purely accidental, let's show in Figs. 2.1 and 2.2 the $\hat{s}^2 - s^2$ dependence on m_H and m_t , respectively. From Fig. 2.1, we see that the higgs mass play only a marginal role, since effects of varying it are in

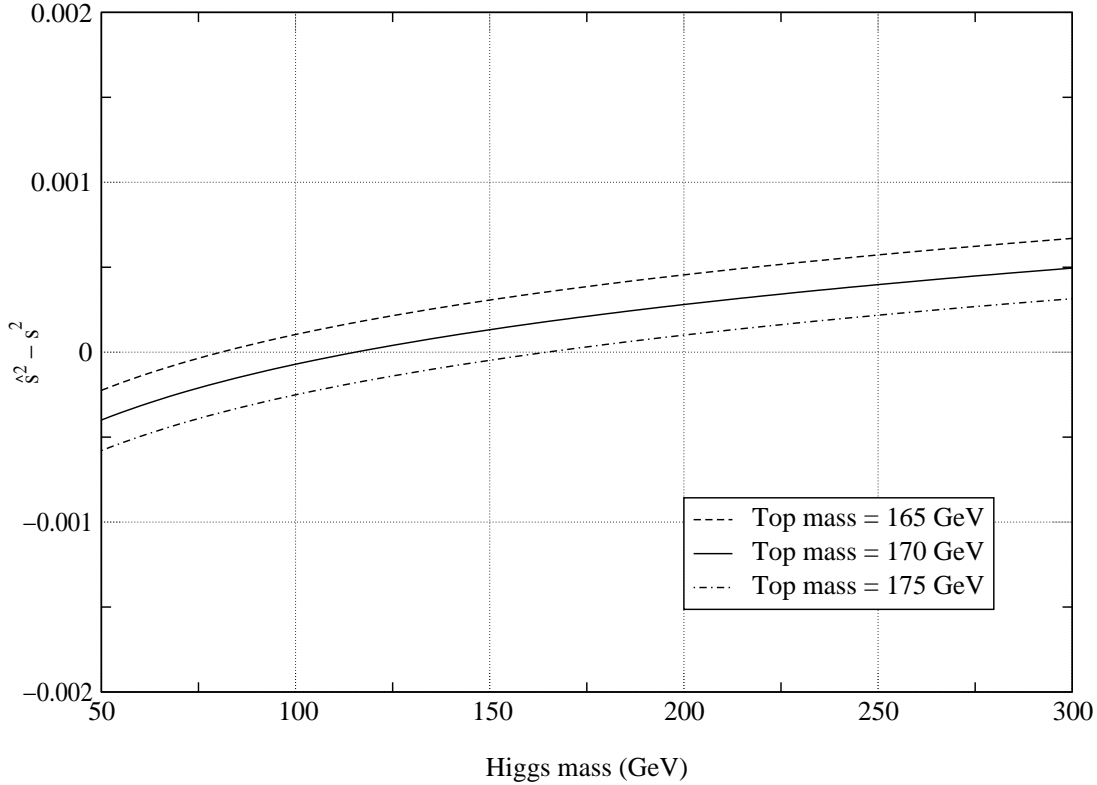


Figure 2.1: Numerical value of the difference $\hat{s}^2 - s^2$, at one-loop, as a function of the higgs mass m_H . Note that the dependence on m_H is only logarithmic.

general rather small. This can be verified straightforwardly by looking at the leading term in m_H which enters Eq. (2.26):

$$\hat{s}^2 - s^2|_{m_H \gg m_Z} \approx \frac{\bar{\alpha} (1 + 9s^2)}{48\pi (c^2 - s^2)} \ln \left(\frac{m_H}{m_Z} \right)^2. \quad (2.31)$$

From this formula one can see that the dependence of $\hat{s}^2 - s^2$ on the higgs mass is only logarithmic.

The situation completely changes if one consider the dependence on the top mass. From Fig. 2.2, it is clear that \hat{s}^2 is close to s^2 only for m_t around 170 GeV, so one cannot find any physical reason for the closeness of these two angles. The fact that $\hat{s}^2 - s^2$ rapidly varies with m_t can be figured out from the large m_t approximation:

$$\hat{s}^2 - s^2|_{m_t \gg m_Z} \approx -\frac{3\bar{\alpha}}{16\pi (c^2 - s^2)} \left(\frac{m_t}{m_Z} \right)^2. \quad (2.32)$$

At this point we conclude that the numerical closeness of \hat{s}^2 and s^2 is a mere coincidence without any deep physical reason.

2.2.2 s_l^2 versus s^2

Before going further, let us quickly review the relation between s_l^2 and s^2 . As stated in the introduction, and as can be seen directly comparing Eqs. (2.1) and (2.4), it turns out that these

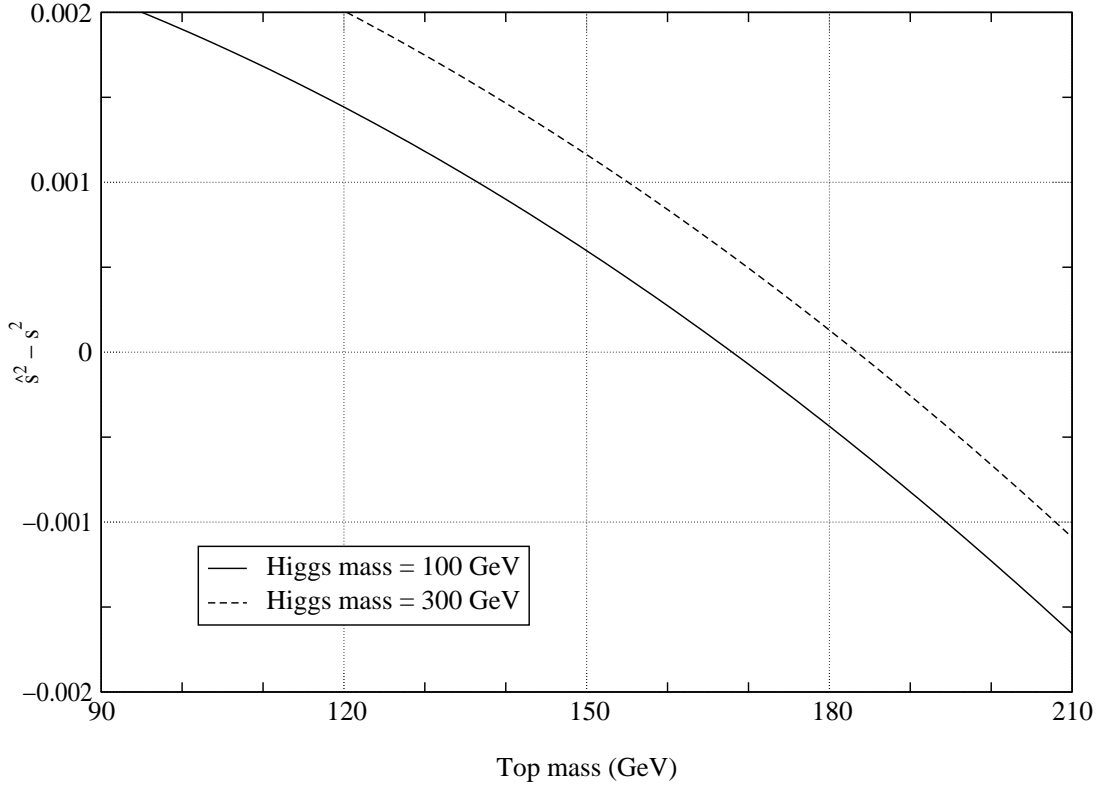


Figure 2.2: Numerical value of the difference $s_l^2 - s^2$, at one-loop, as a function of the top mass m_t . The strong dependence on m_t is clearly evident.

two angles are numerically very close; however, this degeneracy is known to be accidental. To check this, we need to derive an analytic expression for their difference, and this can be done in two steps by first substituting Eq. (2.23) into (2.8) and using Eq. (2.12):

$$s_0^2 = s_l^2 - cs \left[F_V^{Ze} - (1 - 4s^2) F_A^{Ze} + \Pi_{\gamma Z}(m_Z^2) \right], \quad (2.33)$$

and then eliminating s_0^2 in favor of s^2 by means of Eq. (2.25):

$$s_l^2 = s^2 + cs \left[F_V^{Ze} - (1 - 4s^2) F_A^{Ze} + cs \Pi_{\gamma Z}(m_Z^2) \right] + \frac{c^2 s^2}{c^2 - s^2} \left[\Pi_{\gamma}(m_Z^2) - \Pi_Z(m_Z^2) + \Pi_W(0) + 2\frac{s}{c} \Pi_{\gamma Z}(0) + \delta\alpha_{t,W} + D \right]. \quad (2.34)$$

Having this formula at our disposal, we can now investigate numerically the dependence of $s_l^2 - s^2$ on m_H and m_t , and the corresponding plots are shown in Fig. 2.3 and 2.4. As in the previous case, once again this difference depends logarithmically on m_H but linearly on $(m_t/m_Z)^2$, and so the coincidence occurs only for m_t close to 170 GeV. However, if now we evaluate the large m_H and m_t approximations and write down the corresponding asymptotic expressions, we find an interesting result:

$$s_l^2 - s^2|_{m_H \gg m_Z} \approx \frac{\bar{\alpha} (1 + 9s^2)}{48\pi (c^2 - s^2)} \ln \left(\frac{m_H}{m_Z} \right)^2, \quad (2.35)$$

$$s_l^2 - s^2|_{m_t \gg m_Z} \approx -\frac{3\bar{\alpha}}{16\pi (c^2 - s^2)} \left(\frac{m_t}{m_Z} \right)^2. \quad (2.36)$$

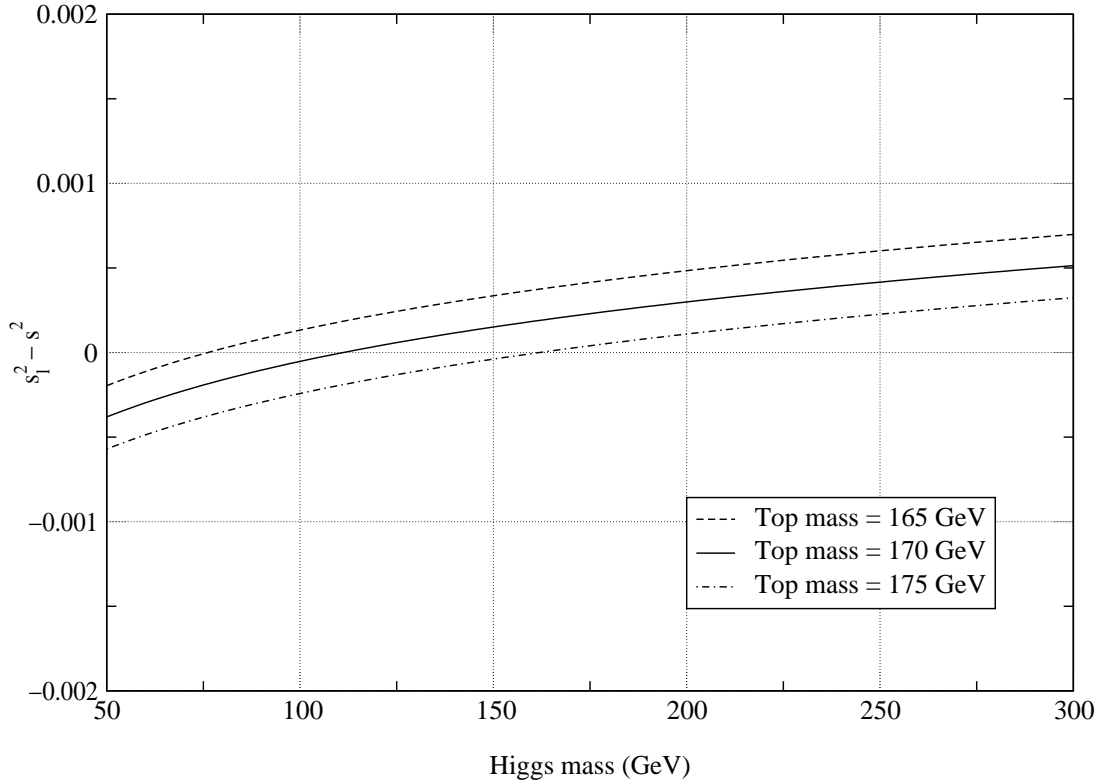


Figure 2.3: Numerical value of the difference $s_l^2 - s^2$, at one-loop, as a function of the higgs mass m_H . The dependence on m_H is only logarithmic.

which coincide with Eqs (2.31) and (2.32)! This immediately lead us to conclude that in the difference $(\hat{s}^2 - s^2) - (s_l^2 - s^2)$ the terms of order $\ln(m_H/m_Z)^2$ and $(m_t/m_Z)^2$ cancel, i.e. the dependence of $\hat{s}^2 - s_l^2$ on m_t is *weaker* than in the two cases analyzed so far. This is just the kind of relation we were looking for, and will be discussed widely in the next section.

2.2.3 \hat{s}^2 versus s_l^2

As explained in Sec. 2.1.4, the quantity s_l describes the asymmetries in Z boson decay; s_l , s_u and s_d refers to decays into pairs of leptons, up-quarks and down-quarks, respectively. Let us discuss s_l . Rewriting Eq. (2.33) in the $\overline{\text{MS}}$ scheme with $\mu = m_Z$, we immediately get (see also Ref. [24]):

$$\hat{s}^2 = s_l^2 - cs \left[\hat{F}_V^{Ze} - (1 - 4s^2) \hat{F}_A^{Ze} + \hat{\Pi}_{\gamma Z}(m_Z^2) \right] \quad (2.37)$$

The form of the last equation can be foreseen without any calculation. The point is that both $\hat{\theta}$ and θ_l are defined by the ratio of bare gauge coupling constants; the difference between them arises since θ_l describes $Z \rightarrow e^+e^-$ decays and in this case the additional vertex radiative corrections as well as $Z \rightarrow \gamma \rightarrow e^+e^-$ transition contribute to θ_l . In (2.37) these additional terms are subtracted from s_l^2 in order to get \hat{s}^2 . The vertex terms in (2.37) are mere numbers, while $\hat{\Pi}_{\gamma Z}$ depends on m_t only logarithmically due to the non-decoupling property of $\overline{\text{MS}}$ scheme

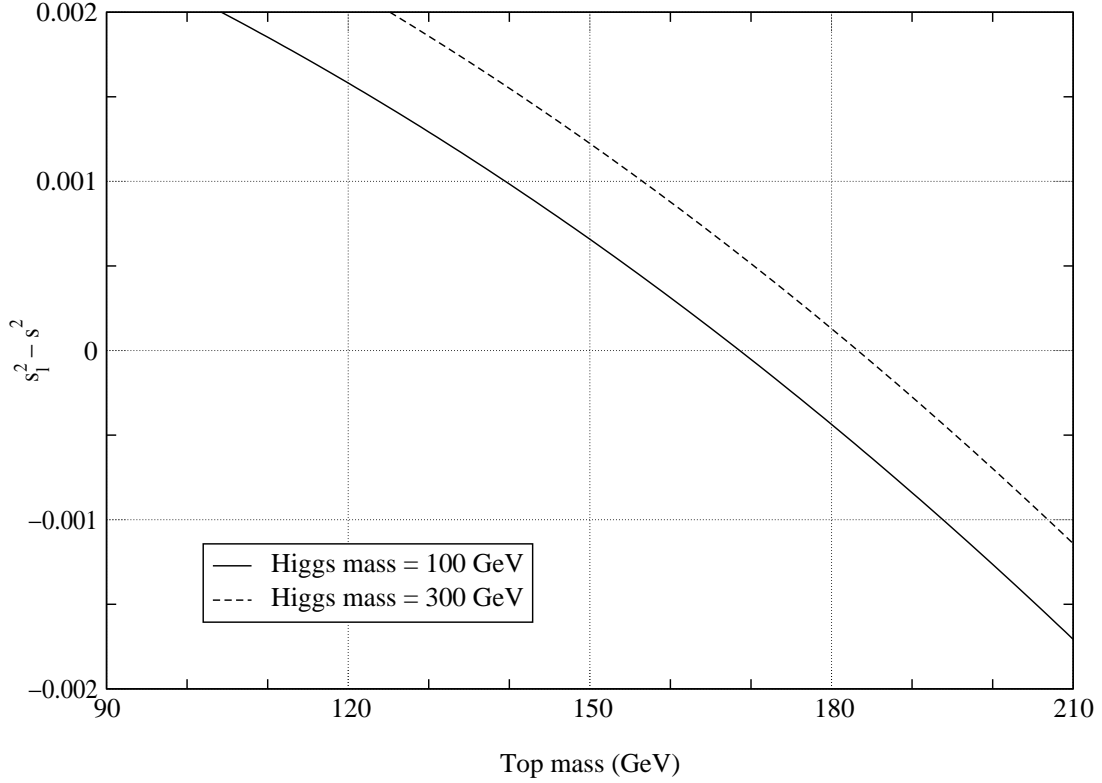


Figure 2.4: Numerical value of the difference $s_t^2 - s^2$, at one-loop, as a function of the top mass m_t . The strong dependence on m_t is clearly evident.

(since a diagonal vector current is conserved, there is no m_t^2 term in $\hat{\Pi}_{\gamma Z}$, that is why $\hat{\Pi}_{\gamma Z}$ is numerically small). There is also no m_H dependence in the difference $\hat{s}^2 - s_t^2$.

From the $\hat{\Pi}_{\gamma Z}(m_Z^2)$ term we get the following expression for the logarithmically enhanced contribution for $m_t \gg m_Z$:

$$\hat{s}^2 - s_t^2|_{m_t \gg m_Z} \approx \frac{\bar{\alpha}}{\pi} \left(\frac{1}{6} - \frac{4}{9} s^2 \right) \ln \left(\frac{m_t}{m_Z} \right)^2. \quad (2.38)$$

Having all the necessary formulas in our disposal, we are ready to make numerical estimates. Using expressions (93), (94) from Ref. [25] and formulas from Appendix G of Ref. [22], we get:

$$\hat{F}_V^{Ze} = 0.00197 + \frac{\bar{\alpha}}{8\pi} \frac{c}{s^3} \ln \left(\frac{m_W}{m_Z} \right)^2 = 0.00133, \quad (2.39)$$

$$\hat{F}_A^{Ze} = 0.00186 + \frac{\bar{\alpha}}{8\pi} \frac{c}{s^3} \ln \left(\frac{m_W}{m_Z} \right)^2 = 0.00122, \quad (2.40)$$

where the logarithmic terms arise from the divergent parts of vertex functions after imposing $\overline{\text{MS}}$ renormalization conditions with $\mu = m_Z$. Note that in numerical calculations we substituted c^2 for $(m_W/m_Z)^2$.

To calculate $\hat{\Pi}_{\gamma Z}(m_Z^2)$ we use formulas from Appendices of Ref. [22], which take into account

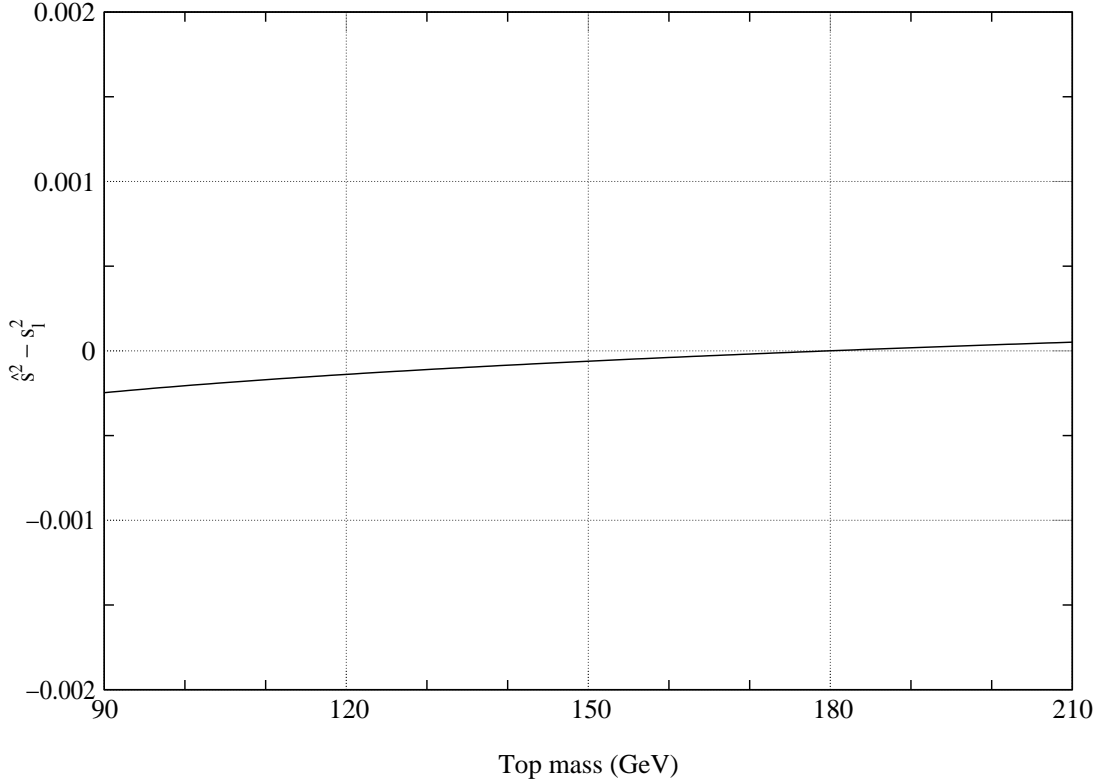


Figure 2.5: Numerical value of the difference $\hat{s}^2 - s_l^2$, at one-loop, as a function of the top mass m_t . This quantity does not depend on the higgs mass, and the dependence on m_t is only logarithmic.

W^+W^- , light fermions and (t, b) doublet contributions. For $m_t = 173.8$ GeV we obtain:

$$\hat{\Pi}_{\gamma Z}(m_Z^2) = -0.00121. \quad (2.41)$$

Substituting (2.39), (2.40) and (2.41) into (2.37), we finally obtain:

$$\hat{s}^2 - s_l^2 \Big|_{m_t=173.8 \text{ GeV}} = -0.00052 + 0.00051 = -0.00001, \quad (2.42)$$

where the first term comes from vertex diagrams and the second from $\hat{\Pi}_{\gamma Z}(m_Z^2)$. This expression should be compared with Eq. (2.30): once again, we see that a very small numerical value arises from two large contributions of opposite sign. Also for Eq. (2.42) we must conclude that this cancellation, which is peculiar to s_l and does not occur for s_u or s_d , is merely accidental (see also Ref. [24]); but it is essential to stress that, unlike the case of Eq. (2.30), here there is no dependence on the higgs mass, and yet more important the dependence on the top quark mass is now only logarithmic. As a consequence, even if the top mass would have been quite different from its actual value 173.8(5.2) GeV, a numerical closeness between \hat{s}^2 and s_l^2 would still have occurred, while no coincidence between \hat{s}^2 (or s_l^2) and s^2 would have appeared. This situation is clearly depicted in Fig. 2.5, where $\hat{s}^2 - s_l^2$ is plotted against m_t : one can easily see that, unlike the case of $\hat{s}^2 - s^2$ difference, here the dependence on m_t is really small for a large m_t values interval.

2.3 Higher-order corrections and numerical estimates

Due to the strong cancellation which occurs among one-loop diagrams in Eqs. (2.30) and (2.42), an accurate analysis of the differences $\hat{s}^2 - s^2$ and $\hat{s}^2 - s_l^2$ requires to take into consideration also the leading two-loop contributions, which can now be comparable or even larger than one-loop ones.

2.3.1 \hat{s}^2 versus s_l^2

For the case of $\hat{s}^2 - s_l^2$, the leading two-loop corrections are of the order of $\alpha\alpha_s$ and come from the insertion of a gluon into quark loops which contribute to $\hat{\Pi}_{\gamma Z}(m_Z^2)$:

(2.43)

There are two types of one-loop diagrams which we should consider: those with light quarks (u, d, c, s, b), and those with heavy top (t). The necessary two-loop formulas are widely discussed in Ref. [26]. However, in that article all the calculations were made with ultraviolet cutoff Λ . To rewrite Kniehl formulas in the usual dimensional regularization approach, in order to derive expressions for the boson self-energies in the $\overline{\text{MS}}$ renormalization scheme, we compare them with the calculations of Djouadi and Gambino reported in Ref. [27]. In this way we find the following replacement rule:

$$\ln\left(\frac{\Lambda^2}{m_Z^2}\right) \longrightarrow \Delta_Z + \frac{55}{12} - 4\zeta(3) \longrightarrow \frac{55}{12} - 4\zeta(3) \approx -0.225. \quad (2.44)$$

For the case of light quarks contribution (u, d, c, s, b), we get:

$$\delta_{\text{light}}^{\alpha\alpha_s} \hat{\Pi}_{\gamma Z}(m_Z^2) = \frac{\hat{\alpha}_s(m_Z)}{\pi} \frac{\bar{\alpha}}{\pi c s} \left(\frac{7}{12} - \frac{11}{9} s^2 \right) \left[\frac{55}{12} - 4\zeta(3) \right] \approx -0.00002, \quad (2.45)$$

where we used $\hat{\alpha}_s(m_Z) = 0.119$ for numerical estimate. For the contribution of the top quark we obtain:

$$\begin{aligned} \delta_t^{\alpha\alpha_s} \hat{\Pi}_{\gamma Z}(m_Z^2) &= \frac{\hat{\alpha}_s(m_t)}{\pi} \frac{\bar{\alpha}}{\pi c s} \left(\frac{1}{6} - \frac{4}{9} s^2 \right) \left[\frac{55}{12} - 4\zeta(3) - \ln t + 4tV_1 \left(\frac{1}{4t} \right) \right] \\ &\approx 0.00004, \end{aligned} \quad (2.46)$$

where $t \equiv (m_t/m_Z)^2$ and (see Refs. [28, 26]):

$$\hat{\alpha}_s(m_t) = \frac{\hat{\alpha}_s(m_Z)}{1 + \frac{23}{12\pi} \hat{\alpha}_s(m_Z) \ln t} \approx 0.109, \quad (2.47)$$

$$V_1(x) = \left[4\zeta(3) - \frac{5}{6} \right] x + \frac{328}{81} x^2 + \frac{1796}{675} x^3 + \dots, \quad (2.48)$$

$$\zeta(3) = 1.2020569\dots \quad (2.49)$$

Substituting (2.45) and (2.46) into (2.37), we have the overall $\alpha\alpha_s$ corrections:

$$\delta^{\alpha\alpha_s} (\hat{s}^2 - s_l^2) = -0.00001. \quad (2.50)$$

Since the leading $\sim \alpha$ correction cancel almost completely in (2.42), one start to worry about significance of two-loop α^2 corrections. Enhanced $\alpha^2 t$ corrections to Eq. (2.37) were calculated in Ref. [29], where it is stated that they are numerically negligible; α^2 corrections have not been calculated yet. However, according to Ref. [29] there exist enhanced two-loop $\alpha^2 \pi^2$ corrections, which come from the interference of the imaginary parts of $\Pi_{\gamma Z}$ and Π_γ :

$$\quad (2.51)$$

Numerically they give:

$$\delta_{\text{int}}^{\alpha^2} (\hat{s}^2 - s_l^2) = -0.00004. \quad (2.52)$$

Adding Eqs. (2.50) and (2.52) to the one-loop term given in Eq. (2.42), we finally get:

$$\delta(\hat{s}^2 - s_l^2) = -0.00005, \quad (2.53)$$

$$\hat{s}^2 - s_l^2 \Big|_{m_t=173.8 \text{ GeV}} = -0.00001 - 0.00005 = -0.00006, \quad (2.54)$$

in good agreement with Eqs. (2.2) and (2.4). It is instructive to compare the last formula with the corresponding numbers in Tables 1 and 2 from Ref. [30], as well as the last formula in Ref. [29].

2.3.2 \hat{s}^2 versus s^2

Coming back to the aim of the present chapter, we should study Eq. (2.26) in more details. Comparing Eq. (2.30), which is valid at the one-loop level, with Eqs. (2.1) and (2.2), we observe an evident inconsistency. To overcome it small higher loop corrections to Eq. (2.26) should be accounted for, in analogy with what was done for the case $\hat{s}^2 - s_l^2$. One can act straightforwardly, taking into account corrections to polarization operators entering (2.26). Another possible way is to rewrite the difference $\hat{s}^2 - s^2$ through s_l^2 , so to split the contributions of the higher order radiative corrections into two parts:

$$\delta(\hat{s}^2 - s^2) = \delta(\hat{s}^2 - s_l^2) + \delta(s_l^2 - s^2). \quad (2.55)$$

The first term was discussed in the previous section, and the leading two-loop contributions are given in Eq. (2.53). Concerning the second term, we follow the analysis presented in Refs. [25, 31, 32]:

$$\delta(s_l^2 - s^2) = -\frac{3\bar{\alpha}}{16\pi(c^2 - s^2)} (\delta_2 V_R + \delta_3 V_R + \delta_4 V_R + \delta_4' V_R) \quad (2.56)$$

where $\delta_2 V_R$ comes from gluon insertions into quark loops, $\delta_3 V_R$ accounts for three-loop $\alpha\alpha_s^2 t$ terms, and $\delta_4 V_R$ and $\delta'_4 V_R$ include the leading two-loop electroweak corrections of order $\alpha^2 t^2$ (δ_4 comes from irreducible diagrams and δ'_4 from reducible ones). Expressions for these functions are reported in Refs. [25, 31, 32]:

$$\delta_2 V_R(t, h) = \frac{4}{3} \frac{\hat{\alpha}_s(m_t)}{\pi} \left[t A_1 \left(\frac{1}{4t} \right) - \frac{5}{3} t V_1 \left(\frac{1}{4t} \right) - 4t F_1(0) + \frac{1}{6} \ln t \right], \quad (2.57)$$

$$\delta_3 V_R(t, h) = -14.594 \frac{\hat{\alpha}_s^2(m_t)}{\pi^2} t, \quad (2.58)$$

$$\delta_4 V_R(t, h) = -\frac{\bar{\alpha}}{16\pi s^2 c^2} A \left(\frac{m_H}{m_t} \right) t^2, \quad (2.59)$$

$$\delta'_4 V_R(t, h) = -\frac{3\bar{\alpha}}{16\pi (c^2 - s^2)^2} t^2, \quad (2.60)$$

where V_1 is given in (2.48), and A_1 , F_1 and A can be found in Refs. [25, 31, 32].

Substituting Eqs. (2.57-2.60) into (2.56), we have:

$$\delta(s_l^2 - s^2) = 0.00047, \quad (2.61)$$

which can be added to Eq. (2.53) into Eq. (2.55), and then to the one-loop term given in Eq. (2.30), to find the numerical value:

$$\delta(\hat{s}^2 - s^2) = 0.00042, \quad (2.62)$$

$$\hat{s}^2 - s^2 \Big|_{\substack{m_t=173.8 \text{ GeV} \\ m_H=120 \text{ GeV}}} = -0.00011 + 0.00042 = 0.00031, \quad (2.63)$$

in good agreement with Eqs. (2.1) and (2.2).

2.4 Conclusions

In this chapter we have investigated the origin of the numerical closeness among three different definitions of the electroweak mixing angle: s^2 , \hat{s}^2 , and s_l^2 . We have found that the degeneracy between \hat{s}^2 and s^2 , as well as between s_l^2 and s^2 , is merely accidental, while for the case of \hat{s}^2 and s_l^2 the dependence of their difference on the m_t is only logarithmic: therefore their closeness would have occurred even if the top quark mass would have been quite different from its actual value.

Moreover, Eq. (2.26) provides an explicit and very simple relation between the phenomenological quantity s^2 and the $\overline{\text{MS}}$ parameter \hat{s}^2 , and this relation will be very useful in the following chapter. The numerical estimates we did in Sec. 2.3 proves that our formulas are in good agreement with experimental data (or, for the case of \hat{s}^2 , with the theoretical calculations of other groups), provided that the leading two-loop contributions are taken into account.

Effects of new physics will be studied in the next chapter. However, let us mention since now that in generalizations of Standard Model a lot of new heavy particles occur, and all of them

contribute to \hat{s}^2 due to the non-decoupling property of $\overline{\text{MS}}$ renormalization. To avoid this non-universality of $\overline{\text{MS}}$ quantities, it was suggested to subtract from vector boson self-energies Π_i the contributions of all the particles heavier than m_Z . In this approach, not only new particles, but also the top quark is decoupled from \hat{s}^2 , and in particular the logarithmic term shown in (2.38) should not be included (see Refs. [33, 21]). According to the definition accepted in Ref. [21], the quantity \hat{s}^2 which has been discussed up to now is called \hat{s}_{ND}^2 , while a new “decoupled” $\overline{\text{MS}}$ parameter \hat{s}_Z^2 is introduced:

$$\hat{s}_Z^2 = \hat{s}^2 - \frac{\bar{\alpha}}{\pi} \left(\frac{1}{6} - \frac{4}{9}s^2 \right) \ln \left(\frac{m_t}{m_Z} \right)^2 = \hat{s}^2 - 0.00020. \quad (2.64)$$

From (2.2) and (2.64) we get:

$$\hat{s}_Z^2 = 0.23124(24), \quad (2.65)$$

where, unlike \hat{s}^2 , \hat{s}_Z^2 is uniquely defined both in the Standard Model and in its extensions.

Chapter 3

\hat{s}_{SM}^2 , \hat{s}_{ND}^2 and the value of $\hat{\alpha}_s(m_Z)$ from SUSY Grand Unification

Although Eq. (2.26) is very effective in providing a bridge between the experimentally measured quantity s^2 and the $\overline{\text{MS}}$ parameter \hat{s}^2 , a special care is required when leaving the SM domain to study the effects of New Physics. If this equation is used in the most straightforward and trivial way, allowing *all* particles of the model to participate to the vector boson self-energies $\hat{\Pi}_i$ as it seems natural, then a lot of new contributions appear and the numerical estimate (2.63) is no longer correct. On the other hand, it is clear that, as long as one takes care to artificially *not* include new particles into Eq. (2.26) and to consider only SM contributions, all the results found in the previous chapter remain valid. This apparent ambiguity suggests us to replace the $\overline{\text{MS}}$ parameter \hat{s} with two better defined quantities sharing its properties: \hat{s}_{SM}^2 , which lives within the SM and does not depend on New Physics, and \hat{s}_{ND}^2 , which also account for all new particles present in the model. However, having now at our disposal two different $\overline{\text{MS}}$ angles, one may wonder which one should be used when writing down the Renormalization Group equations, and how the Grand Unification mass scale m_{GUT} is affected by this choice.

In order to investigate the running of the $SU(3)$, $SU(2)$ and $U(1)$ gauge coupling constants, it is essential as a first step to implement a unified method for calculating their initial values. In the literature, the $\overline{\text{MS}}$ renormalization scheme is usually used. Since in this prescription heavy particles do not decouple, it happens that even at low μ the value of the coupling constants depends on the (unknown) contents of the theory at high energies. To avoid this evident inconvenience Marciano and Rosner introduced the so-called “ $\overline{\text{MS}}$ with heavy particles decoupling procedure”: when performing calculations at some value of μ the contribution of particles with masses larger than μ must be neglected [33]. In this approach, low-energy data and particle spectrum are all what is needed to determine initial values for coupling constants. This procedure is very reasonable: using $\overline{\text{MS}}$ without decoupling in GUT models will lead to the inconvenient result that all gauge couplings remain equal even *below* m_{GUT} , as far as they unify above m_{GUT} into unique α_5 value. This is why evolving below m_{GUT} it is desirable to decouple heavy degrees of freedom.

Going down in energy, we cross thresholds associated with superpartners and finally reach the

domain $\mu \sim m_Z$. Instead of this theoretically preferable up-down running, in practice down-up running is performed because what are experimentally measured are the values of gauge coupling constants at low energies, $\mu \sim m_Z$. Starting from this domain one has two different options: to use \hat{s}_{SM}^2 , where SUSY partners are decoupled, or \hat{s}_{ND}^2 , where they are taken into account and not decoupled. The same ambiguity take place for electromagnetic coupling $\bar{\alpha}$: $\hat{\alpha}_{\text{SM}}(m_Z)$ or $\hat{\alpha}_{\text{ND}}(m_Z)$. These two procedures lead to different initial values of coupling constants \hat{g}_1 and \hat{g}_2 and a natural question arise: how it is possible to get one and the same value of m_{GUT} (where \hat{g}_1 and \hat{g}_2 become equal) starting from different sets of initial values.

We will provide an answer to this question in Sec. 3.1, showing how calculations based on \hat{s}_{SM}^2 and \hat{s}_{ND}^2 produce just the same numerical value for the Grand Unification mass m_{GUT} . As an application of the techniques described there, in Sec. 3.2 we will quickly discuss what is the value of $\hat{\alpha}_s(m_Z)$ which can be predicted from the demand of SUSY Grand Unification.

3.1 RGE in the $\overline{\text{MS}}$ scheme and the concept of threshold

One of the most remarkable properties of the $\overline{\text{MS}}$ renormalization prescription is that the Renormalization Group equations for the gauge coupling constants do not contain explicitly the mass scale μ . As a consequence, in this scheme the RGE can be easily written and solved, at least within perturbation theory, and this is why it is very well suited for the study of Grand Unified theories.

On the other hand, it is well known that $\overline{\text{MS}}$ quantities have no simple interpretations in terms of physical quantities, so special care is required when setting the *initial value* (i.e., the value at some fixed scale μ_0) of $\overline{\text{MS}}$ parameters which will enter RGE. In particular, as already stated at the beginning of this chapter, $\overline{\text{MS}}$ quantities get radiative corrections from *any* particle in the model, no matter how light or heavy it is, and so heavy boson and higgs multiplets, with masses $\sim 10^{16}$ GeV, which are usually present in GUT models should be taken into account even when considering the low-scale ($\sim m_Z$) behavior of the theory.

Although not theoretically unacceptable (we remind that $\overline{\text{MS}}$ quantities have no physical meaning), this *non-decoupling* property is clearly unpractical, since it forces us to set different low-scale initial conditions for models which differ *only* in the high-energy particle contents and have the same low-energy limit (the $SU(3) \times SU(2) \times U(1)$ gauge group of the Standard Model and its particle content). Clearly, it would be much more attractive to split the study of GUT into two independent parts, namely a model-independent relation between physical observables and some variant of $\overline{\text{MS}}$ quantities (taking into consideration only the low-energy spectrum, for example the Standard Model or the MSSM) and a model-dependent way to run these quantities up to the GUT scale.

A way to realize this project, which has been widely used in literature for the accurate study of Grand Unified theories, make use of the concept of *threshold*. The purpose of the first part of this chapter is to review in an extensive but simple way how this idea arises.

3.1.1 Effects of new physics on the initial values

Let's start with the SM. In terms of the physical parameters G_F , $\bar{\alpha}$ and s^2 , the $\overline{\text{MS}}$ quantities \hat{s}^2 and $\hat{\alpha}^2$ at the scale $\mu = \mu_0 = m_Z$ can be written (at one-loop level) as:

$$\hat{s}^2 = s^2 + \frac{c^2 s^2}{c^2 - s^2} A, \quad (3.1)$$

$$A = 2 \frac{s}{c} \hat{\Pi}_{\gamma Z}(0) + \hat{\Pi}_{\gamma}(m_Z^2) - \hat{\Pi}_Z(m_Z^2) + \hat{\Pi}_W(0) + \delta\alpha_{t,W} + \hat{D} \Big|_{\mu=\mu_0};$$

$$\hat{\alpha} = \bar{\alpha} + \bar{\alpha} B,$$

$$B = 2 \frac{s}{c} \hat{\Pi}_{\gamma Z}(0) + \hat{\Pi}_{\gamma}(m_Z^2) + \delta\alpha_{t,W} \Big|_{\mu=\mu_0}. \quad (3.2)$$

Now, let's introduce some set of new particles, all with almost degenerate masses m , and let's assume that the new model obtained is still renormalizable. Due to their definitions, the value of $\bar{\alpha}$ and s^2 is clearly unaffected by the introduction of the new particles (they are defined directly from experimentally measured quantities), but the $\overline{\text{MS}}$ parameters $\hat{\alpha}$ and \hat{s}^2 will get new contributions from self-energies, vertices and boxes coming from new physics. If we denote with \hat{s}_{SM}^2 and $\hat{\alpha}_{\text{SM}}$ their old value, and with \hat{s}_{ND}^2 and $\hat{\alpha}_{\text{ND}}$ the new one, we can write:

$$\hat{s}_{\text{ND}}^2 = \hat{s}_{\text{SM}}^2 + \delta\hat{s}^2, \quad \delta\hat{s}^2 = \frac{c^2 s^2}{c^2 - s^2} \delta A; \quad (3.3)$$

$$\hat{\alpha}_{\text{ND}} = \hat{\alpha}_{\text{SM}} + \delta\alpha, \quad \delta\alpha = \bar{\alpha} \delta B; \quad (3.4)$$

where:

$$\delta A = 2 \frac{s}{c} \hat{\Pi}_{\gamma Z}(0) + \hat{\Pi}_{\gamma}(m_Z^2) - \hat{\Pi}_Z(m_Z^2) + \hat{\Pi}_W(0) + \delta\alpha_{t,W,X} + \hat{D} \Big|_{\mu=\mu_0}^{\text{New Physics}} \quad (3.5)$$

$$= 2 \frac{s}{c} \delta\hat{\Pi}_{\gamma Z}(0) + \delta\hat{\Sigma}'_{\gamma}(0) - \delta\hat{\Pi}_Z(m_Z^2) + \delta\hat{\Pi}_W(0) + \delta\hat{D};$$

$$\delta B = \delta\hat{\Sigma}'_{\gamma}(0) + 2 \frac{s}{c} \delta\hat{\Pi}_{\gamma Z}(0); \quad (3.6)$$

Since we are interested in application to GUT models, it is more convenient to deal with $\hat{\alpha}_1$ and $\hat{\alpha}_2$, rather than $\hat{\alpha}$ and \hat{s}^2 . We have:

$$\hat{\alpha}_1 = \frac{5}{3} \frac{\hat{\alpha}}{c^2}; \quad \delta\hat{\alpha}_1 = \hat{\alpha}_1 \left(\frac{\delta\hat{\alpha}}{\hat{\alpha}} - \frac{\delta\hat{c}^2}{c^2} \right); \quad (3.7)$$

$$\hat{\alpha}_2 = \frac{\hat{\alpha}}{\hat{s}^2}; \quad \delta\hat{\alpha}_2 = \hat{\alpha}_2 \left(\frac{\delta\hat{\alpha}}{\hat{\alpha}} - \frac{\delta\hat{s}^2}{\hat{s}^2} \right). \quad (3.8)$$

After some simple calculations, one finds:

$$\frac{\delta\hat{\alpha}_1}{\hat{\alpha}_1} = \frac{1}{c^2 - s^2} \left\{ c^2 \left(\delta\hat{\Sigma}'_{\gamma}(0) + 2 \frac{s}{c} \delta\hat{\Pi}_{\gamma Z}(0) \right) + s^2 \left(\delta\hat{\Pi}_W(0) - \delta\hat{\Pi}_Z(m_Z^2) + \delta\hat{D} \right) \right\}; \quad (3.9)$$

$$\frac{\delta\hat{\alpha}_2}{\hat{\alpha}_2} = -\frac{1}{c^2 - s^2} \left\{ s^2 \left(\delta\hat{\Sigma}'_{\gamma}(0) + 2 \frac{s}{c} \delta\hat{\Pi}_{\gamma Z}(0) \right) + c^2 \left(\delta\hat{\Pi}_W(0) - \delta\hat{\Pi}_Z(m_Z^2) + \delta\hat{D} \right) \right\}. \quad (3.10)$$

Although these formulae has been derived with the assumption that $\mu = \mu_0 \equiv m_Z$ (cfr. Eqs. (3.5) and (3.6)), it is straightforward to note that the condition $\mu_0 = m_Z$ has never been used for

deriving them, and so they are correct for *any* possible value of μ_0 ; therefore, we can conclude they provide a relation between $\hat{\alpha}_i^{\text{SM}}$ and $\hat{\alpha}_i^{\text{ND}}$ for *any* value of μ . As a consequence, there is no need for writing down RGE for $\hat{\alpha}_i^{\text{ND}}$, since we already know their solution; the only thing which we should do is to write down explicitly the dependence of $\hat{\alpha}_i^{\text{ND}}$ on the mass parameter μ . Although this would be the simplest approach, since the goal of this article is to give a simple presentation of how the concept of threshold arises, in the following sections we will forget about this and keep on assuming that $\mu = \mu_0$ in Eqs. (3.9) and (3.10), so that their meaning is simply to set the *shift* in the *initial value* of $\hat{\alpha}_i^{\text{ND}}$; instead, the running of the coupling constants will be derived from the RGE.

3.1.2 Writing and solving the RGE

Now let's consider in more detail which kind of contribution the new set of particles gives to the initial value of the coupling constants and to their running. It is well known that any unrenormalized self-energy, vertex or box diagram can be written as a sum of three parts:

- (1) a purely divergent contribution, proportional to $\frac{1}{\epsilon}$ and independent of μ , coming from dimensional regularization ($\delta\hat{Z}$);
- (2) a finite μ -dependent part, also arising from dimensional regularization ($\delta\tilde{Z}$);
- (3) a finite and μ -independent part.

Only the third term is physically relevant and contributes to physical observables; the second one has no physical meaning, but is present in the definition of $\overline{\text{MS}}$ quantities and contributes to $\delta\hat{\alpha}_i$. On the other hand, the first term ($\delta\hat{Z}$) is directly involved when writing the RG equations. In general, $\delta\hat{Z}$ and $\delta\tilde{Z}$ are not independent, but (at one-loop level) can be written as:

$$\delta\hat{Z} = 4\pi\hat{\alpha}\delta C\frac{1}{\epsilon}, \quad (3.11)$$

$$\delta\tilde{Z} = -4\pi\hat{\alpha}\delta C \ln \frac{m^2}{\mu_0^2}. \quad (3.12)$$

where δC is a constant which depends on the particular Feynman diagram.

Since in Eqs. (3.9) and (3.10) the contributions of the new particles enter through the $\overline{\text{MS}}$ *renormalized* vertex-box and self-energies, the term (1) is absent by definition. On the other hand, the term (3) directly affects physical observables, so a large value (larger for example than the experimental error of some measured quantity) will result either in the discovery of new physics or in the rejection of the model; therefore, we will assume that this term is small, and neglect it.

Now, let $2\delta\tilde{Z}_i$ be the sum of the μ -dependent part (2) coming from all the renormalized self-energies and vertex-box contributions appearing in Eqs. (3.9) and (3.10), and let $2\delta\hat{Z}_i$ be the sum of all the divergent part (1) of the corresponding unrenormalized diagrams. Using Eqs. (3.11)

and (3.12), we have:

$$\frac{\delta\hat{\alpha}_i}{\hat{\alpha}_i} \equiv 2\delta\tilde{Z}_i, \quad (3.13)$$

$$\delta\tilde{Z}_i \equiv -4\pi\hat{\alpha}_i\delta C_i \ln \frac{m^2}{\mu_0^2}, \quad (3.14)$$

$$\delta\hat{Z}_i \equiv 4\pi\hat{\alpha}_i\delta C_i \frac{1}{\epsilon}. \quad (3.15)$$

Substituting Eq. (3.14) into Eq. (3.13), we have that the shift in the starting point induced by the new particles in the coupling constants is:

$$\begin{aligned} \delta \left(\frac{1}{\hat{\alpha}_i} \right) &= -\frac{1}{\hat{\alpha}_i} \left(\frac{\delta\hat{\alpha}_i}{\hat{\alpha}_i} \right) = -\frac{2}{\hat{\alpha}_i} \delta\tilde{Z}_i = -\frac{2}{\hat{\alpha}_i} 4\pi\hat{\alpha}_i\delta C_i \left(-\ln \frac{m^2}{\mu_0^2} \right) \\ &= 8\pi\delta C_i \ln \frac{m^2}{\mu_0^2}. \end{aligned} \quad (3.16)$$

On the other hand, due to the presence of the $\delta\hat{Z}_i$ contribution, the RG equation changes, and the running of the $\overline{\text{MS}}$ quantities $\hat{\alpha}_i$ is consequently modified. At one-loop:

$$\mu^2 \frac{d\hat{\alpha}_i}{d\mu^2} = -\hat{\alpha}_i\epsilon - 2\frac{\mu^2}{Z_i} \frac{d\hat{Z}_i}{d\mu^2} \hat{\alpha}_i. \quad (3.17)$$

The solution of this equation, both in the case when only SM is considered and when new particles are included, is:

$$\frac{1}{\hat{\alpha}_i^{\text{SM}}(\mu^2)} = 8\pi C_i^{\text{SM}} \ln \frac{K_i^{\text{SM}}}{\mu^2}, \quad (3.18)$$

$$\frac{1}{\hat{\alpha}_i^{\text{ND}}(\mu^2)} = 8\pi C_i^{\text{ND}} \ln \frac{K_i^{\text{ND}}}{\mu^2}. \quad (3.19)$$

where K_i^{SM} and K_i^{ND} are integration constants, and C_i have the same meaning as δC_i appearing in Eq. (3.15) and (3.14) (and, in particular, $\delta C_i = C_i^{\text{ND}} - C_i^{\text{SM}}$). Subtracting Eq. (3.18) from Eq. (3.19) and after some algebra, we find:

$$\frac{1}{\hat{\alpha}_i^{\text{ND}}(\mu^2)} - \frac{1}{\hat{\alpha}_i^{\text{SM}}(\mu^2)} = 8\pi\delta C_i \ln \frac{K_i}{\mu^2}, \quad (3.20)$$

$$K_i = K_i^{\text{SM}} \left(\frac{K_i^{\text{ND}}}{K_i^{\text{SM}}} \right)^{C_i^{\text{SM}}/\delta C_i}. \quad (3.21)$$

The constants K_i can be determined by remembering that, for $\mu = \mu_0$, the value of $1/\hat{\alpha}_i^{\text{ND}}(\mu_0) - 1/\hat{\alpha}_i^{\text{SM}}(\mu_0)$ is given by Eq. (3.16). The solution is then:

$$\frac{1}{\hat{\alpha}_i^{\text{ND}}(\mu)} = \frac{1}{\hat{\alpha}_i^{\text{SM}}(\mu)} + 8\pi\delta C_i \ln \frac{m^2}{\mu^2}. \quad (3.22)$$

This result, although mathematically trivial, is nevertheless rather interesting, since it put into clear light the effects of the introduction of new particles on the running of the $\overline{\text{MS}}$ coupling

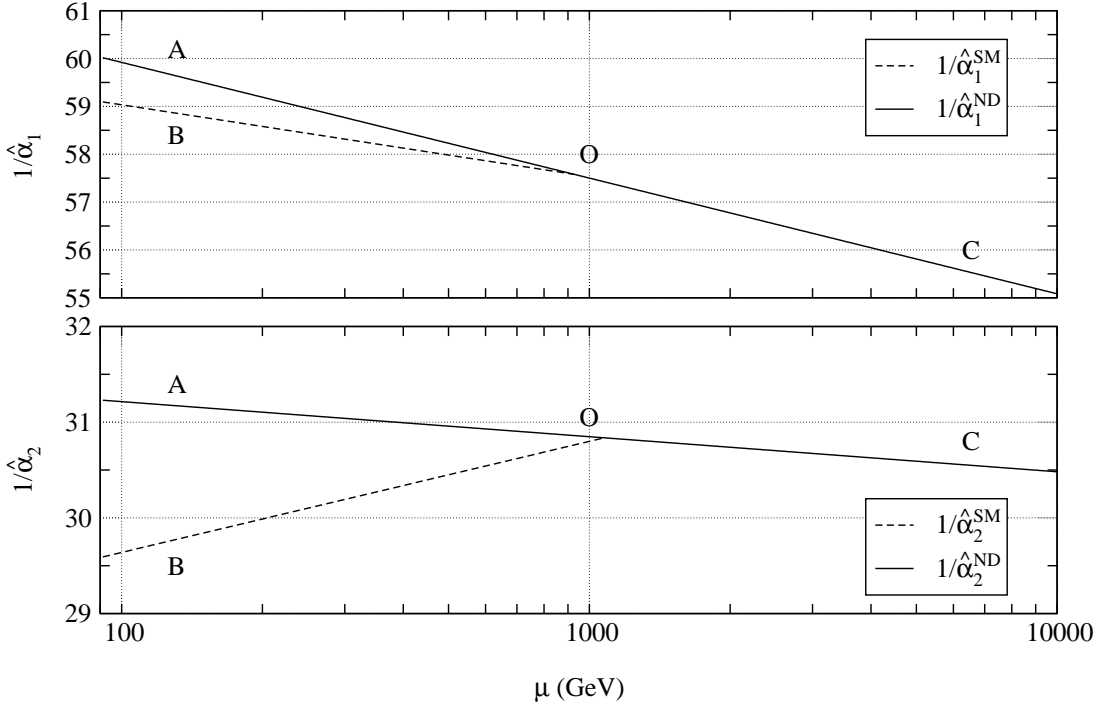


Figure 3.1: Running of $\hat{\alpha}_1$ and $\hat{\alpha}_2$ coupling constants, at one-loop, as a function of the mass scale parameter μ , both in the *non-decoupling* (paths \overline{AOC}) and *decoupling* (paths \overline{BOC}) approaches. As SM model extension, MSSM with $m_{\text{SUSY}} = 1000$ GeV is used. The small shift of the $\hat{\alpha}_i^{\text{SM}} - \hat{\alpha}_i^{\text{ND}}$ crossing point with respect to m_{SUSY} is due to the term (3) which was neglected in equations.

constants. First of all, as expected, the coefficients of the logarithmic term are changed, so the running occurs with a different slope. But it can be seen that absolutely nothing happens when crossing the new particles mass threshold: the running of $\hat{\alpha}_i$ is always the same, both below and above m . Instead, an extra contribution to the *initial value* $\hat{\alpha}_i(\mu_0)$ should be accounted for, due to the non-decoupling property of $\overline{\text{MS}}$ scheme. This behavior corresponds to paths \overline{AOC} in Fig. 3.1. It is straightforward to see that, for $\mu = m$, we have $\alpha_i^{\text{ND}} = \alpha_i^{\text{SM}}$: here, as expected, the contribution of the new particles to the value of $\hat{\alpha}_i$ vanishes.

3.1.3 Running in the decoupling approach

We started this chapter stating that we would have shown how it could be possible to split the study of GUT models into two independent parts, namely a model-independent relation between physical quantities and some variant of $\overline{\text{MS}}$ quantities, and a model-dependent way to run these quantities up to the GUT scale. We have seen in the previous section that new particles contributes both to the setting of the initial point (the relation between physical quantities and $\overline{\text{MS}}$ coupling constants) and to the running of $\hat{\alpha}_i$, but we also noted that $\hat{\alpha}_i^{\text{SM}}$ and $\hat{\alpha}_i^{\text{ND}}$ become equals when $\mu = m$. This provides us with the solution to our problem: up to small μ -independent contributions (see beginning of Sec. 3.1.2, term (3) in the list), it is possible to use *ordinary* (i.e. accounting only for the contribution of SM particles) RGE, without introducing any extra initial shift, to run coupling constants up to the scale $\mu = m$, and then to run them up

to the GUT scale by means of the *full* (i.e. accounting also for the new particles) RG equations. This behavior corresponds to paths $\overline{\text{BOC}}$ in Fig. 3.1.

This approach has also a very simple physical interpretation: it corresponds to working with a variant of $\overline{\text{MS}}$ scheme, in which the contribution of particles heavier than the considered mass scale μ is decoupled from the very beginning. In other words, Eqs. (3.11) and (3.12) are replaced by:

$$\delta\hat{Z} = 4\pi\hat{\alpha}C \left[\frac{1}{\epsilon} - \theta(m - \mu) \ln \frac{m^2}{\mu^2} \right], \quad (3.23)$$

$$\delta\tilde{Z} = -4\pi\hat{\alpha}\delta C\theta(\mu - m) \ln \frac{m^2}{\mu^2}. \quad (3.24)$$

Solving the RGE, it is easy to see that, for $\mu < m$, the one-loop contribution of the new particles is now canceled by the logarithmic μ -dependent term in $\delta\hat{Z}_i$, so that the total result is now zero; for $\mu > m$, nothing is changed and the running of the coupling constants simply reflects the usual behavior.

3.2 The numerical value of $\hat{\alpha}_s(m_Z)$ from SUSY GUT

As an application of the results found in the previous section, we will now present a short overview of the prediction on $\hat{\alpha}_s(m_Z)$ from the demand of SUSY Grand Unification. Since our purpose is simplicity, rather than completeness, we will consider in some detail only effects related to low energy physics, and in particular we will analyze the dependence of $\hat{\alpha}_s(m_Z)$ on the Standard Model parameters $\hat{\alpha}_{\text{SM}}$, \hat{s}_{SM}^2 , and \hat{m}_t^{SM} . Instead, we will not consider the contributions of heavy vector bosons and higgs multiplets which usually occur close to the unification scale in any reasonable GUT model; effects of unknown non-renormalizable operators which may be induced by (possible) new physics above m_{GUT} will be neglected as well. Also, we will assume the complete degeneracy of all SUSY particles at a common mass scale m_{SUSY} ; therefore, in our approach (which is based on Ref. [34]) the superpartners enter the RGE and affect $\hat{\alpha}_s(m_Z)$ only through the two parameters m_{SUSY} and $\tan\beta$. Although these assumption are very restrictive and physically unrealistic, they will allow us to keep our discussion at a very simple level; for a detailed analysis of all possible contributions which may affect the prediction of $\hat{\alpha}_s(m_Z)$, we address the reader to the literature (see for example Refs. [34, 35, 36]).

In our approach, we start from the value of the gauge coupling constants $\hat{\alpha}_1^{\text{SM}}$ and $\hat{\alpha}_2^{\text{SM}}$, the Yukawa couplings $\hat{\lambda}_t^{\text{SM}}$, $\hat{\lambda}_b^{\text{SM}}$ and $\hat{\lambda}_\tau^{\text{SM}}$, and the quartic higgs coupling $\hat{\lambda}^{\text{SM}}$, at the $\mu = m_Z$ scale; then we run them up to $\mu = m_{\text{SUSY}}$ using the SM two-loop RGE (Eqs. (35-43), (A17-A20) and (A25-A26) of Ref. [34]), evaluate the corresponding ND quantities, and finally run them up to $\mu = m_{\text{GUT}}$ using the MSSM two-loop RGE (Eqs. (1-4) and (A5-A11) of Ref. [34]). The mass scale m_{GUT} is defined by the condition $\hat{\alpha}_1^{\text{ND}}(m_{\text{GUT}}) = \hat{\alpha}_2^{\text{ND}}(m_{\text{GUT}})$; imposing the requirement $\hat{\alpha}_3^{\text{ND}}(m_{\text{GUT}}) = \hat{\alpha}_{1,2}^{\text{ND}}(m_{\text{GUT}})$ and running down all quantities back to $\mu = m_Z$, we obtain a prediction for $\hat{\alpha}_3^{\text{SM}}(m_Z)$. When crossing the SUSY threshold, both upwards and downwards, the following conditions between SM and ND quantities are imposed (see Eqs. (34), (44) and (45-49) from

Ref. [34]):

$$\hat{\alpha}_i^{\text{SM}}(m_{\text{SUSY}}) = \hat{\alpha}_i^{\text{ND}}(m_{\text{SUSY}}), \quad (3.25)$$

$$\hat{m}_j^{\text{SM}}(m_{\text{SUSY}}) = \hat{m}_j^{\text{ND}}(m_{\text{SUSY}}), \quad (3.26)$$

$$\hat{\lambda}^{\text{SM}}(m_{\text{SUSY}}) = \pi \left(\frac{3}{5} \hat{\alpha}_1^{\text{ND}}(m_{\text{SUSY}}) + \hat{\alpha}_2^{\text{ND}}(m_{\text{SUSY}}) \right) \cos^2 2\beta. \quad (3.27)$$

Let us add that, for small values of $\tan \beta$, the contributions of $\hat{\lambda}_b$ and $\hat{\lambda}_\tau$ to the running of $\hat{\alpha}_i$ are usually very small and could safely be neglected; however, since they are already included in formulas given in Ref. [34], we decided to take them into account as well.

While we are using explicitly the decoupling procedure described in Sec. 3.1.3 for taking SUSY particles into account, our approach is completely non-decoupling for what concerns the top quark: for example, the quantity \hat{s}^2 discussed in Chapter 2 depends strongly on m_t . On the other hand, the $\overline{\text{MS}}$ parameter $\hat{\alpha}_s(m_Z)$ used in literature accounts only for quarks lighter than m_Z . To allow comparison of our numerical calculations with experimental data, we need to subtract t contributions from $\hat{\alpha}_3^{\text{SM}}(m_Z)$, and this can be done by means of the following relation:

$$\hat{\alpha}_s(m_Z) = \frac{\hat{\alpha}_3^{\text{SM}}(m_Z)}{1 - \frac{1}{3\pi} \hat{\alpha}_3^{\text{SM}}(m_Z) \ln \frac{m_t}{m_Z}}, \quad (3.28)$$

which is valid at the one-loop level.

3.2.1 The SUSY parameters $\tan \beta$ and m_{SUSY}

We are now ready to investigate the dependence of $\hat{\alpha}_s(m_Z)$ on the only two SUSY parameters, m_{SUSY} and $\tan \beta$, which are relevant in our approximation. From Fig. 3.2, we immediately see that varying $\tan \beta$ do not introduce any relevant effect, and the value of $\hat{\alpha}_s$ remains almost the same for a large window of $\tan \beta$ values.

The situation is rather different if one considers the dependence of $\hat{\alpha}_s$ on m_{SUSY} , which is shown in Fig. 3.3. One can see that, when changing m_{SUSY} from 200 GeV to 10 TeV, the value of $\hat{\alpha}_s$ varies of about 0.012, which is much more than its experimental error. Since the mass scale at which supersymmetry occurs is unknown, this shift should be regarded as a theoretical uncertainty in the prediction of $\hat{\alpha}_s$. Therefore, we must conclude that, up to a concrete discovery of superpartners, it will not be possible to reduce the error on the *predicted* value of $\hat{\alpha}_s$ to less than $\sim 10\%$. However, we should note that SUSY Grand Unification is not in disagreement with the experimental value 0.119(2), and in particular $m_{\text{SUSY}} \sim 1$ TeV reproduce nicely this number (although it is well known that the effects of *mass splitting* among superpartners can change drastically this picture, and so m_{SUSY} should be regarded only as an *effective* parameter without any physical meaning).

Fig. 3.3 also shows us that the dependence of $\hat{\alpha}_s$ on m_{SUSY} is almost logarithmic. From this plot we can derive an useful approximate relation:

$$\hat{\alpha}_s(m_Z) = \begin{cases} 0.12014 - 0.0073934 \log_{10}(m_{\text{SUSY}}/\text{TeV}) & \text{for } \tan \beta = 2, \\ 0.12051 - 0.0075748 \log_{10}(m_{\text{SUSY}}/\text{TeV}) & \text{for } \tan \beta = 10, \\ 0.11981 - 0.0074000 \log_{10}(m_{\text{SUSY}}/\text{TeV}) & \text{for } \tan \beta = 50. \end{cases} \quad (3.29)$$

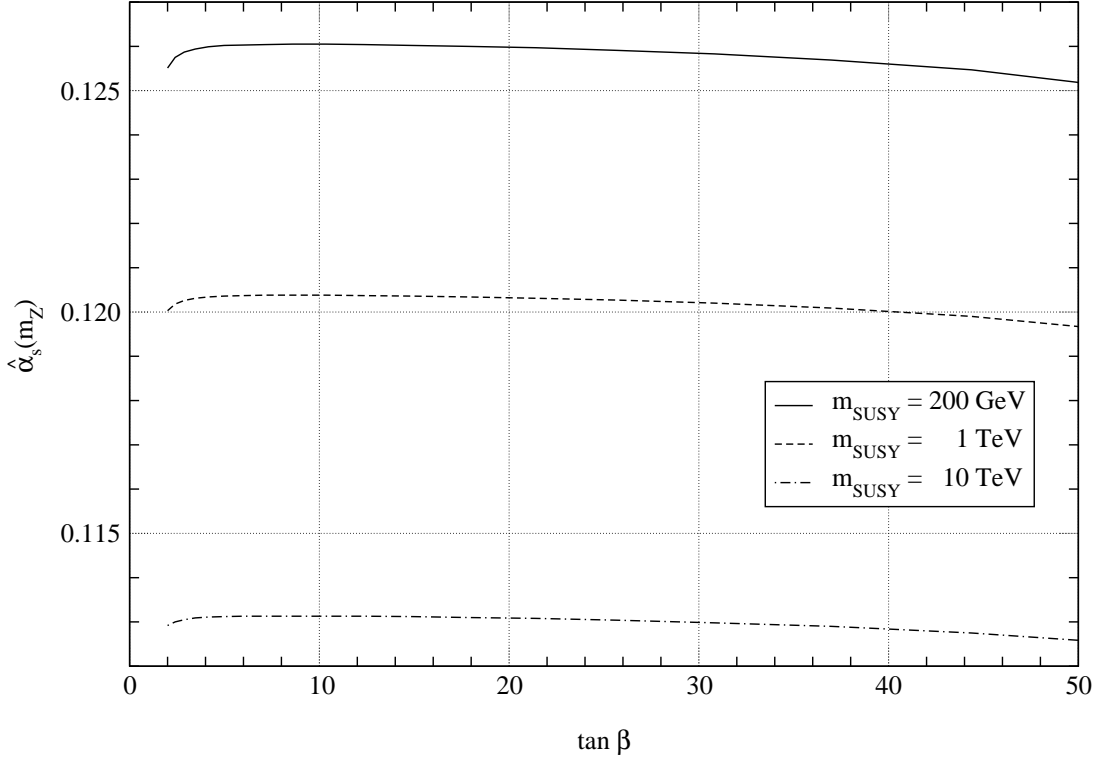


Figure 3.2: Dependence of $\hat{\alpha}_s$ on $\tan \beta$, for $\bar{\alpha} = 1/128.878$, $s^2 = 0.23116$, $m_Z = 91.1867 \text{ GeV}$, $m_H = 120 \text{ GeV}$, $m_t = 173.8 \text{ GeV}$.

3.2.2 The SM parameters $\hat{\alpha}$, \hat{s}^2 and \hat{m}_t

As already stated, before dealing with the running of $\overline{\text{MS}}$ coupling constants up to the GUT scale we need first of all to set their initial values. Since our original project of splitting the study of SUSY GUT into two independent parts, one dealing with “low-energy” SM quantities and one accounting for “high-energy” MSSM effects, has been successfully realized by the introduction of one SUSY threshold, we can now forget about superpartners when setting the starting point. As a consequence, all formulas derived in Chapter 2 for the case of SM are now perfectly adequate for our purposes, and we can use them.

As reference values for the relevant physical observables, we use $\bar{\alpha} = 1/128.878$, $s^2 = 0.23116$, $m_Z = 91.1867 \text{ GeV}$, $m_H = 120 \text{ GeV}$ and $m_t = 173.8 \text{ GeV}$. From Eqs. (2.1) and (2.63) given in the previous chapter, we get $\hat{s}^2(m_Z) = 0.23147$, while the value of $\hat{\alpha}$ at the one-loop order can be derived by Eq. (3.2) leading to $\hat{\alpha}(m_Z) = 1/128.1$. Concerning \hat{m}_t the situation is slightly more difficult: Eq. (17) from Ref. [34] is valid at the scale $\mu = m_t$, and to get an estimation for $\hat{m}_t(m_Z)$ we need to run it down to the Z scale. However, doing this one finds that the big splitting between m_t and $\hat{m}_t(m_t)$ which occurs at the top scale due to the large value of $\hat{\alpha}_s$ is completely compensated by the running effects, and for m_t in the range $165 \div 185 \text{ GeV}$ it follows that $\hat{m}_t(m_Z)$ is about 1 GeV larger than m_t . This complete the analysis of the initial conditions.

Now let’s consider the prediction of $\hat{\alpha}_s$ coming from the demand of gauge coupling unification

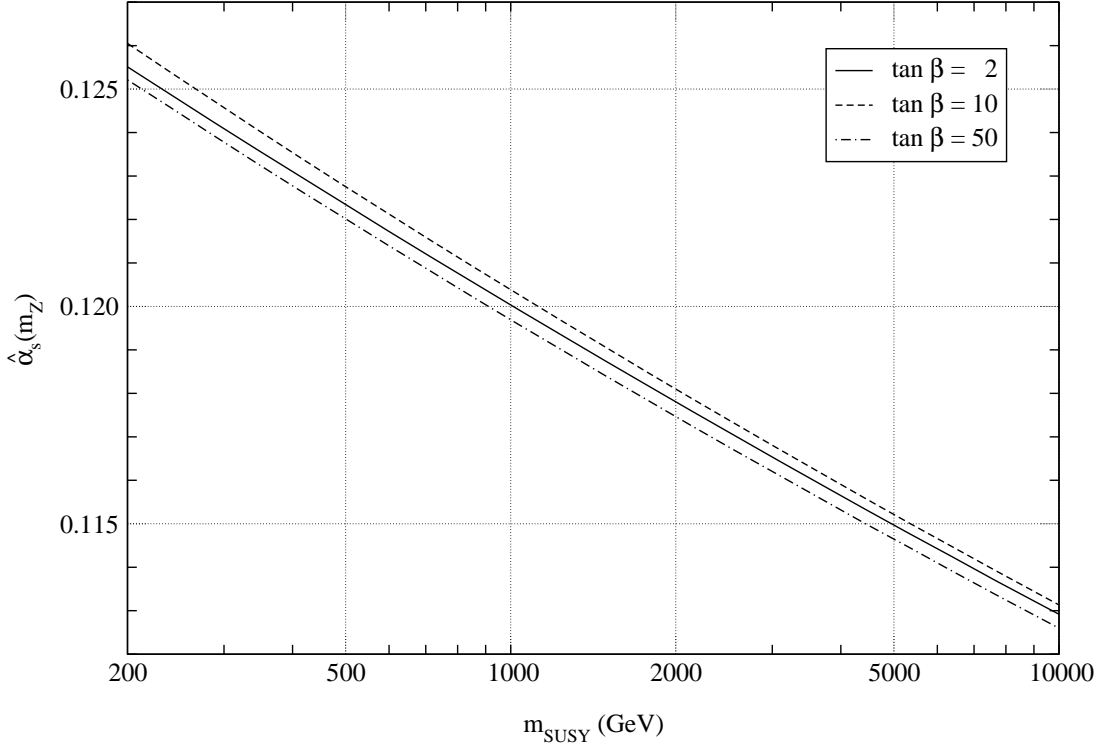


Figure 3.3: Dependence of $\hat{\alpha}_s$ on m_{SUSY} , for $\bar{\alpha} = 1/128.878$, $s^2 = 0.23116$, $m_Z = 91.1867$ GeV, $m_H = 120$ GeV, $m_t = 173.8$ GeV.

at the GUT scale. In Figs. 3.4, 3.5 and 3.6 we show the dependence of $\hat{\alpha}_s$ on the $\overline{\text{MS}}$ quantities $\hat{\alpha}$, \hat{s}^2 and \hat{m}_t , respectively. One can see immediately that, unlike the case of the completely unbounded parameter m_{SUSY} , here the small theoretical uncertainty on these quantities induces a correspondingly small error on $\hat{\alpha}_s$. The largest effect is due to \hat{s}^2 , and in particular from Eq. (2.63) and Fig. 3.5 one can see that inclusion of the leading two-loop contributions in the relation between \hat{s}^2 and s^2 produce a sensible change in $\hat{\alpha}_s$ (about half of the experimental error). On the contrary, from Fig. 3.4 and Eq. (43) of Ref. [15] we see that contributions of order $\alpha\alpha_s$ into $\hat{\alpha}$ have negligible consequences on $\hat{\alpha}_s$, and this is why we used the one-loop relation (3.2) to set the initial value of $\hat{\alpha}$. Finally, Fig. 3.6 proves that changing $\hat{m}_t(m_Z)$ does not induce any relevant effect on $\hat{\alpha}_s$.

Figs. 3.4 and 3.5 also show that $\hat{\alpha}_s$ depends almost linearly on $1/\hat{\alpha}$ and \hat{s}^2 ; therefore, we can derive the following approximate relations:

$$\hat{\alpha}_s(m_Z) = \begin{cases} 0.12003 - 0.00097812 [1/\hat{\alpha}(m_Z) - 128.1] & \text{for } \tan \beta = 2, \\ 0.12038 - 0.00098094 [1/\hat{\alpha}(m_Z) - 128.1] & \text{for } \tan \beta = 10, \\ 0.11971 - 0.00097153 [1/\hat{\alpha}(m_Z) - 128.1] & \text{for } \tan \beta = 50; \end{cases} \quad (3.30)$$

$$\hat{\alpha}_s(m_Z) = \begin{cases} 0.12006 - 4.2340 [\hat{s}^2(m_Z) - 0.23147] & \text{for } \tan \beta = 2, \\ 0.12044 - 4.2306 [\hat{s}^2(m_Z) - 0.23147] & \text{for } \tan \beta = 10, \\ 0.11973 - 4.2000 [\hat{s}^2(m_Z) - 0.23147] & \text{for } \tan \beta = 50. \end{cases} \quad (3.31)$$

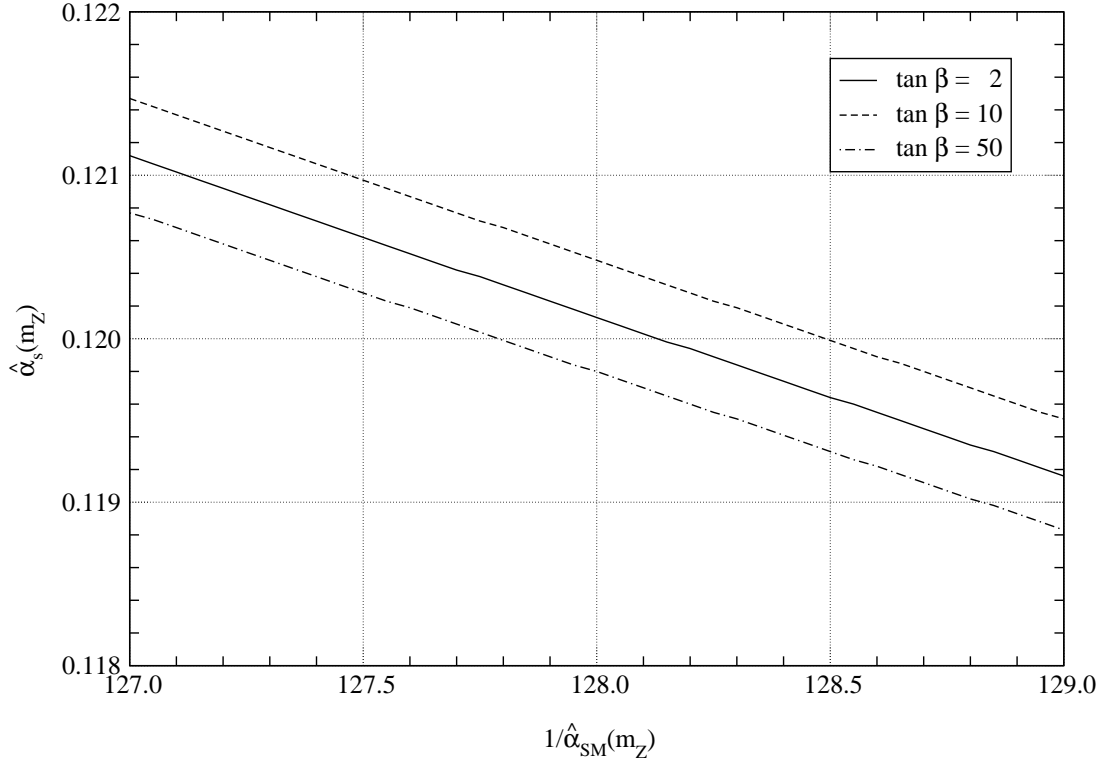


Figure 3.4: Dependence of $\hat{\alpha}_s$ on $1/\hat{\alpha}$, for $m_{\text{SUSY}} = 1$ TeV, $\hat{s}^2(m_Z) = 0.23147$, $\hat{m}_t(m_Z) = 175$ GeV.

It is interesting to discuss explicitly how effects of varying the *physical observables* $\bar{\alpha}$, s^2 and m_t on $\hat{\alpha}_s$ may be derived from comparing Figs. 3.4, 3.5 and 3.6 with Figs. 2.1 and 2.2 from the previous chapter. As an example, let us consider m_t . Changing it induces shifts on the initial values of $\hat{\alpha}$, \hat{s}^2 and \hat{m}_t , and these shifts will result in a different prediction for $\hat{\alpha}_s$. However, from Fig. 3.6 we immediately see that the variation of \hat{m}_t does not produce any sensible effect on $\hat{\alpha}_s$, while since $\hat{\alpha}$ depends on m_t only logarithmically its variation itself is very small. Therefore, in our approach the only relevant contribution of m_t into $\hat{\alpha}_s$ happens *through* \hat{s}^2 , and can easily be estimated from Figs. 2.2 and 3.5. An analogous situation holds for the higgs mass m_H .

3.3 Conclusions

In this chapter we have discussed in detail how both the decoupling and the non-decoupling approach to the running of coupling constants in the $\overline{\text{MS}}$ scheme produce the same numerical value of m_{GUT} despite of the different initial conditions. The concept of threshold has been introduced in Sec. 3.1 and used in Sec. 3.2, where the dependence of $\hat{\alpha}_s$ on the SM parameters $\hat{\alpha}$, \hat{s}^2 and \hat{m}_t and the MSSM quantities m_{SUSY} and $\tan \beta$ has been studied. Combining the results obtained in this chapter with analysis of \hat{s}^2 carried out in Chapter 2 it is straightforward to evaluate the impact of the numerical value of the physical observables $\bar{\alpha}$, s^2 and m_t on the prediction of $\hat{\alpha}_s$ from the demand of SUSY Grand Unification.

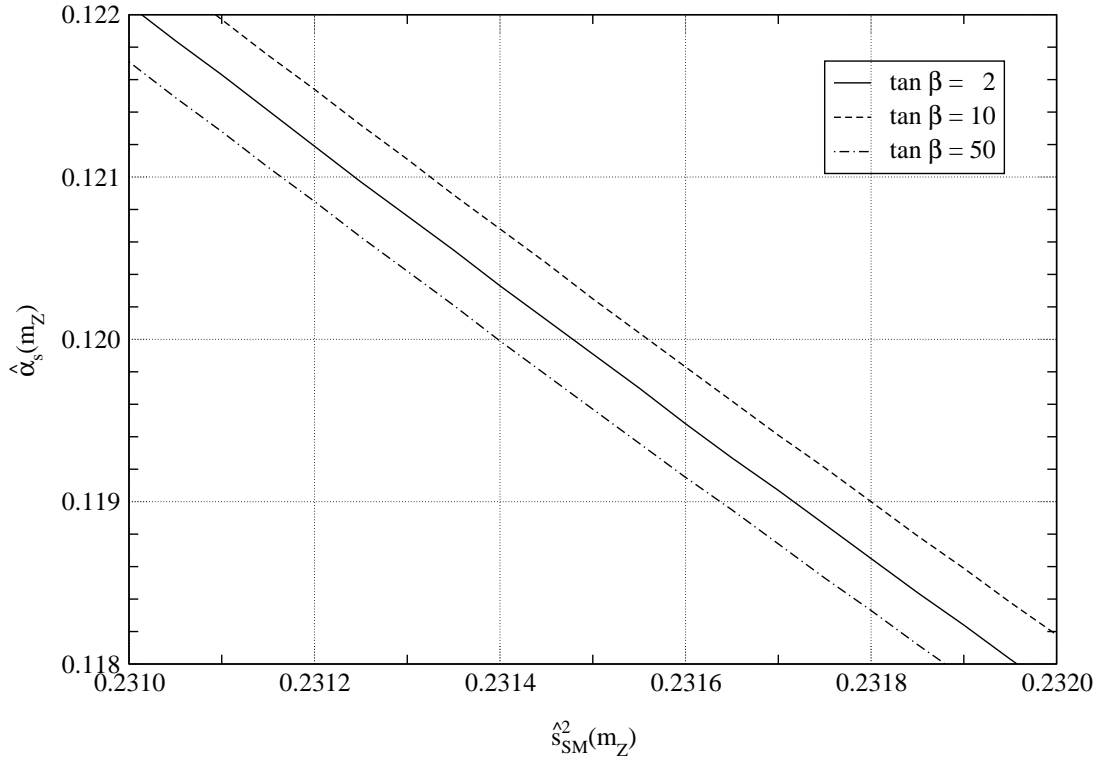


Figure 3.5: Dependence of $\hat{\alpha}_s$ on \hat{s}^2 , for $m_{\text{SUSY}} = 1$ TeV, $\hat{\alpha}(m_Z) = 1/128.1$, $\hat{m}_t(m_Z) = 175$ GeV.

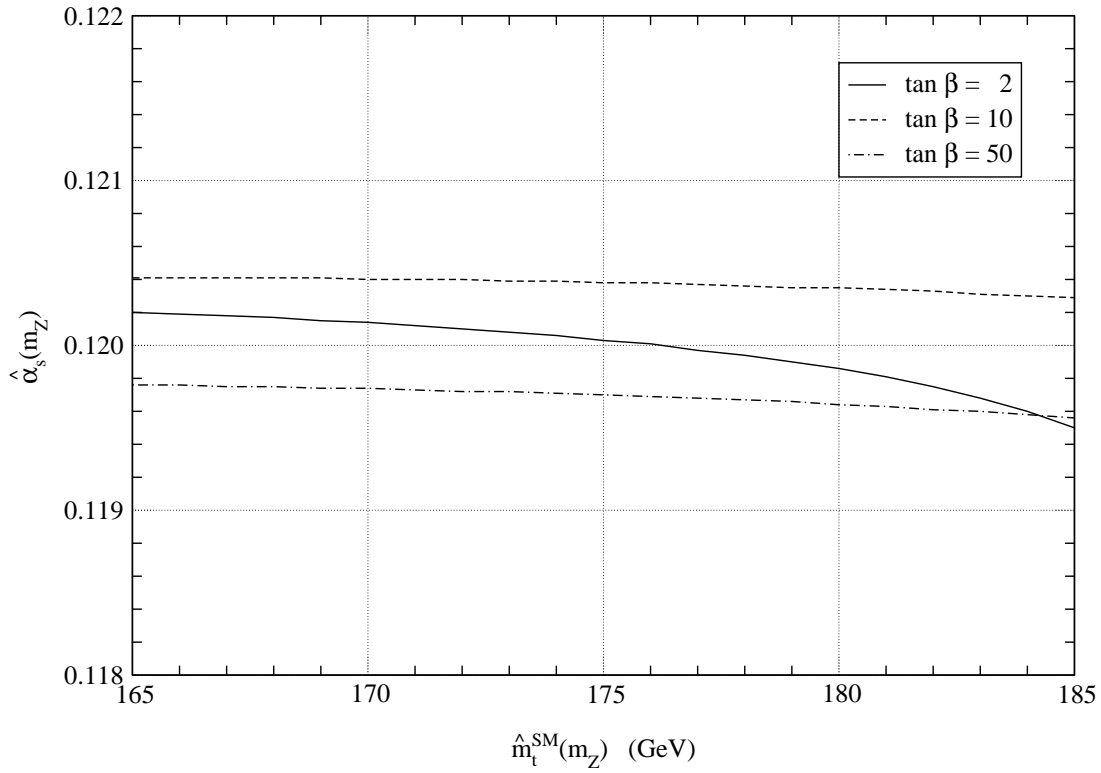


Figure 3.6: Dependence of $\hat{\alpha}_s$ on \hat{m}_t , for $m_{\text{SUSY}} = 1$ TeV, $\hat{\alpha}(m_Z) = 1/128.1$, $\hat{s}^2(m_Z) = 0.23147$.

Chapter 4

Charginos nearly degenerate with the lightest neutralino

Despite of its success in predicting the correct value of $\hat{\alpha}_s(m_Z)$ from the hypothesis of gauge coupling unification at the GUT scale, the MSSM still lacks a direct confirmation from experimental search. None of the many new particles expected in SUSY models have yet been observed, and the high energy and luminosity reached at LEP II and Tevatron in the last years allow now to put stringent bounds on the masses of most of the superpartners. However, to further constrain SUSY parameters, or alternatively to determine them through the discovery of new particles, more powerful accelerators are required, and they won't be available till the construction of LHC - i.e. many years.

To overcome this limitation of direct search experiments, one may try to find *indirect* evidence of the superpartners analyzing their impact on precision measurements through radiative corrections. Since no deviation from the predictions of the SM has so far been observed, nowadays precision data can only provide further bounds on MSSM parameters. Unfortunately, unlike other kind of New Physics (for example, an extra generation of fermions, which we will discuss in the next chapter), SUSY particles have the remarkable property to *decouple* from low-energy physical observables when their masses are pushed to a high energy scale. This means that loop effects may be appreciable only if superpartners are light, but this possibility is strongly constrained by the results of direct observations. Therefore, one is led to answer the following question: is there still something to learn about supersymmetry from precision measurements *after* having imposed all bounds required by direct search?

In most of the cases, the answer is negative. Concerning sfermions, radiative corrections could be large if the mass splitting between the up-left and down-left superpartners were big enough, but this situation never occurs in the MSSM (except for the third generations of squarks, see [37]). Concerning gauginos, radiative corrections are *always* small, at least in the region still allowed by LEP II bounds.

However, there is still one class of situations where precision measurements can be useful, and it occurs when direct search analysis, for some particular reason, fails, leaving a hole in a domain

which would otherwise have been closed. This is just what happens in the gaugino sector when the neutralino is the LSP and the lightest chargino is only ~ 1 GeV heavier: in this case, the chargino is too short-lived to be identified as a stable heavy particle, and its decay products are too soft to be distinguished from the background, so it escapes detection and no bound other than LEP I can be applied.

In the present chapter, we will discuss in detail the impact on precision measurements of a chargino almost degenerate in mass with the lightest neutralino. In particular, we will show that the bound $m_{\tilde{\chi}} \gtrsim 45$ GeV which follows from direct searches can be improved up to 51 GeV for the higgsino-dominated case, and 56 GeV for the wino-dominated case, by analyzing the precision data. Also, we will derive explicit formulas for the oblique electroweak radiative corrections.

In Sec. 4.1, we will quickly review the present experimental situation, showing the results found by the DELPHI collaboration [38]. Secs. 4.2 and 4.3 are based on the published paper [3]. In Sec. 4.4 we will discuss the latest (preliminary) results presented by A. Perrotta (DELPHI Collab.) at the conference PASCOS99 [39], together with an improved analysis of χ^2 that we also presented there [5].

4.1 Experimental bounds

LEP II is very effective in bounding from below the masses of charginos which, if kinematically allowed, should be produced in a pair in $e^+e^- \rightarrow \chi^+\chi^-$ annihilation. This process can be mediated by either a gauge boson or a sneutrino, and the relevant Feynman diagrams fall into two classes:

(a)

(b)

(4.1)

The relevance of each graph changes depending on the nature of the outgoing chargino. In the higgsino-dominated case, diagram (4.1b) gives negligible contribution, and only diagram (4.1a) should be considered. On the other hand, in the gaugino-dominated case both these graphs contribute, but the second is suppressed if the sneutrino is heavy. Since the interference term between (4.1a) and (4.1b) is negative, the total cross section in the gaugino-dominated scenario will be smaller if the sneutrino is light, and the corresponding lower limit on $m_{\tilde{\chi}}$ will be weaker. According to Refs. [40, 38], the present bound is $m_{\tilde{\chi}^\pm} \gtrsim 90$ GeV for the higgsino-dominated case or when the sneutrino is heavy, while if the sneutrino is light and the chargino is mainly a gaugino this bound is reduced to $m_{\tilde{\chi}^\pm} \gtrsim 70$ GeV.

However, when the lightest chargino and neutralino (the latter being the LSP) are almost de-

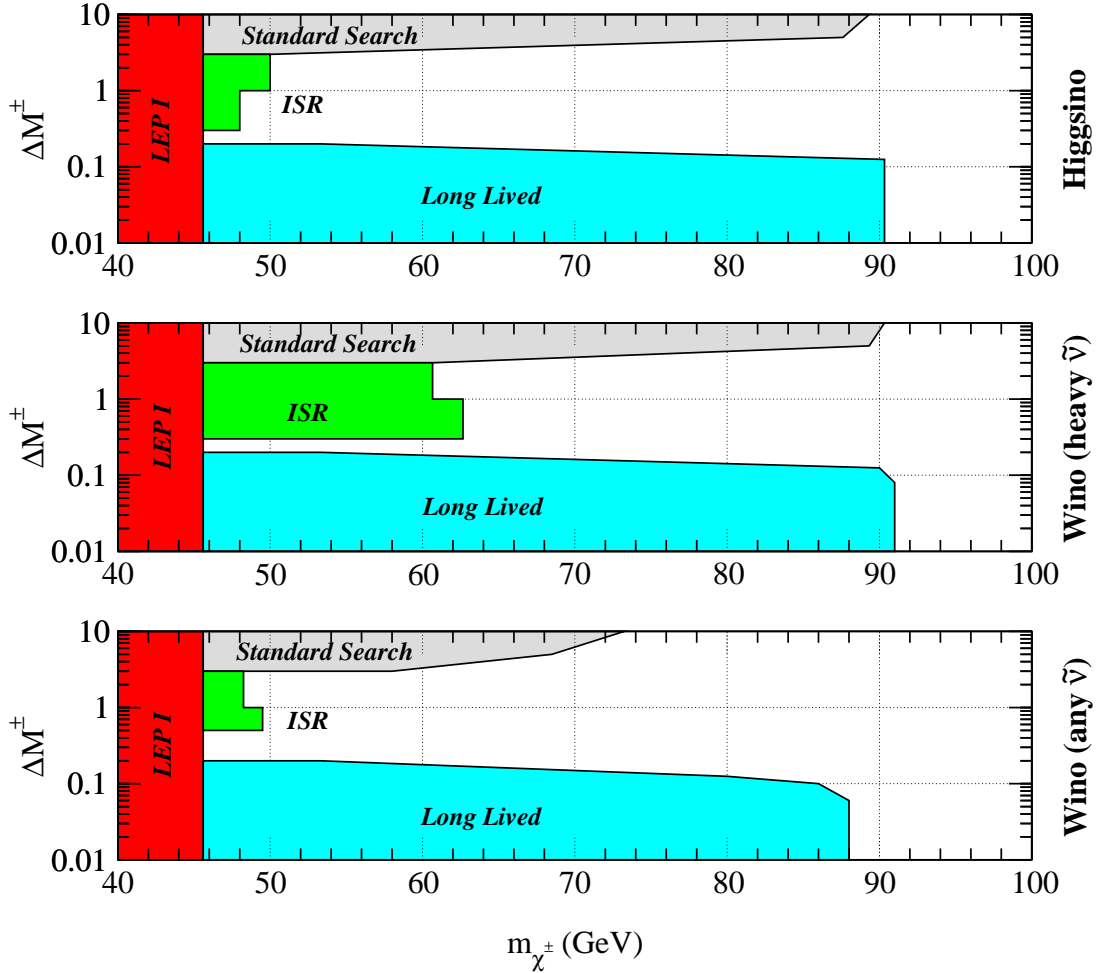


Figure 4.1: Regions in the plane $(m_{\tilde{\chi}}, \Delta M^\pm)$ excluded at 95% C.L. by the DELPHI collaboration. The upper panel refers to the Higgsino-dominated case, and the lower ones to the wino-dominated scenario with and without assuming $m_{\tilde{\nu}_e} > 500$ GeV. This figure reproduces schematically Fig. 12 of Ref. [38].

generate in mass, the charged decay products of the light chargino are very soft, and the above quoted bounds are no longer valid. A special search for such light chargino has been performed recently by the DELPHI collaboration, and the case of $\Delta M^\pm \equiv m_{\tilde{\chi}_1^\pm} - m_{\tilde{\chi}_1^0} \lesssim 100$ MeV is now excluded [38]. However, still in the case of $\Delta M^\pm \sim 1$ GeV LEP II does not provide a lower bound and charginos as light as 45 GeV are allowed (this bound comes from the measurements of Z decays at LEP I and SLC). The case of almost degenerate chargino and neutralino can be naturally realized in SUSY and the possibilities to find such particles are discussed in literature [41].

In Fig. 4.1 we summarize the present experimental bounds on the chargino mass for different values of the chargino-neutralino mass splitting ΔM^\pm . One can see that, for 0.2 GeV $\lesssim \Delta M^\pm \lesssim 3$ GeV, not much more than $m_{\tilde{\chi}^\pm} < 45$ GeV can be excluded. However, some interesting results can be obtained by looking at the so-called Initial State Radiation (ISR), which consists in the emission of a single photon from the initial e^+ or e^- . In the analysis presented in Ref. [38], the use of ISR does not led to relevant improvements of the chargino mass bounds in the region

$0.2 \text{ GeV} \lesssim \Delta M^\pm \lesssim 3 \text{ GeV}$, except for the case of gaugino domination with a heavy sneutrino. However, recently many progresses have been done in this direction, and some preliminary results found by the DELPHI collaboration [39] will be discussed in Sec. 4.4.

4.2 Theoretical analysis

In the simplest supersymmetric extensions of the Standard Model, the chargino-neutralino sector is characterized by the numerical values of four parameters: M_1 , M_2 , μ and $\tan \beta$. The particle contents of the model includes one $SU(2)$ singlet (bino), one $SU(2)$ triplet (wino) and two $SU(2)$ doublets (higgsinos):

$$\tilde{B}, \quad \begin{pmatrix} \tilde{W}_1 \\ \tilde{W}_2 \\ \tilde{W}_3 \end{pmatrix}, \quad \begin{pmatrix} \tilde{H}_1^0 \\ \tilde{H}_1^- \end{pmatrix}, \quad \begin{pmatrix} \tilde{H}_2^+ \\ \tilde{H}_2^0 \end{pmatrix}, \quad (4.2)$$

where all the fields are Weyl spinors. For later convenience, let us also define the Weyl fields \tilde{W}^\pm and the charged Dirac fields \tilde{W} and \tilde{H} :

$$\tilde{W}^\pm \equiv \frac{\tilde{W}_1 \mp i\tilde{W}_2}{\sqrt{2}}, \quad \tilde{W} \equiv \begin{pmatrix} -i\tilde{W}^+ \\ i\tilde{W}^- \end{pmatrix}, \quad \tilde{H} \equiv \begin{pmatrix} \tilde{H}_2^+ \\ \tilde{H}_1^- \end{pmatrix}. \quad (4.3)$$

The terms of the SUSY Lagrangean which are relevant for our purposes are those describing the coupling of gauginos with the electroweak gauge bosons (which we will discuss in the following sections), and of course the mass terms:

$$\begin{aligned} \mathcal{L}_m = & \frac{1}{2}M_1\tilde{B}\tilde{B} + \frac{1}{2}M_2\tilde{W}_i\tilde{W}_i + \mu \left(\tilde{H}_1^0\tilde{H}_2^0 - \tilde{H}_1^+\tilde{H}_2^- \right) - i\frac{g'}{2}\tilde{B} \left(v_1\tilde{H}_1^0 - v_2\tilde{H}_2^0 \right) \\ & + i\frac{g}{2} \left[v_1 \left(\sqrt{2}\tilde{W}^+\tilde{H}_1^- + \tilde{W}_3\tilde{H}_1^0 \right) + v_2 \left(\sqrt{2}\tilde{W}^-\tilde{H}_2^+ - \tilde{W}_3\tilde{H}_2^0 \right) \right] + \text{h.c.} \end{aligned} \quad (4.4)$$

Looking at Eq. (4.4), it is straightforward to see that the states (4.2) are *not* mass eigenstates. To find mass eigenstates, it is convenient to introduce the following definitions:

$$\mathbf{X} = \begin{pmatrix} M_2 & \sqrt{2}m_W \sin \beta \\ \sqrt{2}m_W \cos \beta & \mu \end{pmatrix}, \quad \psi^+ = \begin{pmatrix} -i\tilde{W}^+ \\ \tilde{H}_2^+ \end{pmatrix}, \quad \psi^- = \begin{pmatrix} -i\tilde{W}^- \\ \tilde{H}_1^- \end{pmatrix}, \quad (4.5)$$

$$\mathbf{Y} = \begin{pmatrix} M_1 & 0 & -m_Z s \cos \beta & m_Z s \sin \beta \\ 0 & M_2 & m_Z c \cos \beta & -m_Z c \sin \beta \\ -m_Z s \cos \beta & m_Z s \sin \beta & 0 & -\mu \\ m_Z c \cos \beta & -m_Z c \sin \beta & -\mu & 0 \end{pmatrix}, \quad \psi^0 = \begin{pmatrix} -i\tilde{B} \\ -i\tilde{W}_3 \\ \tilde{H}_1^0 \\ \tilde{H}_2^0 \end{pmatrix}. \quad (4.6)$$

Now the mass Lagrangean \mathcal{L}_m can be written in a more compact form:

$$\mathcal{L}_m = -\frac{1}{2}(\psi^+ \ \psi^-) \begin{pmatrix} 0 & \mathbf{X}^T \\ \mathbf{X} & 0 \end{pmatrix} \begin{pmatrix} \psi^+ \\ \psi^- \end{pmatrix} - \frac{1}{2}(\psi^0)^T \mathbf{Y} \psi^0 + \text{h.c.}, \quad (4.7)$$

and the mass eigenstates can be obtained from (4.2) by means of a unitary transformation, chosen in such a way that the new mass matrices (4.5, 4.6) will be diagonal:

$$\mathbf{U}^* \mathbf{X} \mathbf{V}^{-1} = \text{diag}(m_{\tilde{\chi}_1^\pm}, m_{\tilde{\chi}_2^\pm}), \quad \mathbf{N}^* \mathbf{Y} \mathbf{N}^{-1} = \text{diag}(m_{\tilde{\chi}_1^0}, m_{\tilde{\chi}_2^0}, m_{\tilde{\chi}_3^0}, m_{\tilde{\chi}_4^0}). \quad (4.8)$$

At this point, let us note that, while it is rather simple to find the eigenstates for the (2×2) chargino matrix \mathbf{X} , the (4×4) neutralino matrix \mathbf{Y} cannot in general be diagonalized analytically; therefore, no results written explicitly through the SUSY parameters M_1 , M_2 , μ and $\tan \beta$ can usually be obtained when discussing the neutralino sector.

From Eqs. (4.5) and (4.6) it is easy to see that the case of a nearly degenerate lightest chargino and neutralino naturally arises under two different circumstances:

- (1) $M_2 \gg \mu$: in this case the particles of interest form an $SU(2)$ doublet of Dirac fermions, whose wave functions are dominated by higgsinos;
- (2) $\mu \gg M_2$: in this way we get an $SU(2)$ triplet of Majorana fermions, with the wave functions dominated by winos.

Although physically different, the mathematical description of these two cases is the same. In fact, it is simple to prove that, given an arbitrary matrix, if a diagonal element dominates over the others then the corresponding non-diagonal elements which lie on the same line or column may be neglected in the first approximation (even if they are comparable in size with the other diagonal elements). For what concerns the mass matrices (4.5, 4.6), limits (1) and (2) are mathematically equivalent to setting $m_{W,Z} = 0$ (or equivalently $v_1 = v_2 = 0$ in Eq. (4.4)), and this has some straightforward consequences:

- the SUSY parameter $\tan \beta$ disappears from Eqs. (4.5) and (4.6);
- the matrices \mathbf{X} and \mathbf{Y} are now automatically diagonal (except for the (2×2) block involving higgsinos in the neutralino matrix \mathbf{Y}), therefore the states (4.2) are now mass eigenstates;
- the two neutral Weyl higgsinos merge to form a Dirac particle with mass μ ;
- for each neutralino it exists a chargino with the same mass, except for the bino which has no charged counterpart.

Being \mathbf{X} and \mathbf{Y} in both the cases already in the desired form, it is now possible to choose the matrices \mathbf{U} , \mathbf{V} and \mathbf{N} to be simply the identity matrix, so in these particular limits we can derive *analytical* expressions for the radiative corrections. The coupling Lagrangean is naturally split into two parts, one describing the interactions of the wino components (with mass M_2), and the other describing the interactions of the higgsino components (with mass μ); depending on whether limit (1) or (2) is considered, either the former or the latter part will describe the low-energy spectrum of the model.

In the following sections, we will analyze in detail both these cases and the corresponding relevant parts of the coupling Lagrangean. Let us note since now that the bino is decoupled from gauge bosons, therefore the mass parameter M_1 never enters in the expressions for the oblique corrections.

4.2.1 The higgsino-dominated case

As already noted, the two neutral Weyl higgsinos \tilde{H}_1^0 and \tilde{H}_2^0 can be seen as components of a neutral Dirac fermion \tilde{H}^0 , which together with the charged higgsino \tilde{H} form an $SU(2)$ doublet with mass μ . The interesting parts of the mass and coupling Lagrangean are:

$$\mathcal{L}_m^{\tilde{H}} = -\mu\tilde{H}\tilde{H} - \mu\tilde{H}^0\tilde{H}^0, \quad (4.9)$$

$$\mathcal{L}_\gamma^{\tilde{H}} = -eA_\mu\tilde{H}\gamma^\mu\tilde{H}, \quad (4.10)$$

$$\mathcal{L}_Z^{\tilde{H}} = \frac{e}{cs} \left(s^2 - \frac{1}{2} \right) Z_\mu\tilde{H}\gamma^\mu\tilde{H} + \frac{e}{2cs} Z_\mu\tilde{H}^0\gamma^\mu\tilde{H}^0, \quad (4.11)$$

$$\mathcal{L}_W^{\tilde{H}} = -\frac{e}{\sqrt{2}s} W_\mu\tilde{H}^0\gamma^\mu\tilde{H} + \text{h.c.} \quad (4.12)$$

It is immediate to note that all the couplings are vector-like. As a consequence, all the gauge boson self-energies are simply proportional to the photon self-energy $\Sigma_\gamma(q^2)$, and the proportionality factor can be easily derived from the coupling constants entering Eqs. (4.10-4.12). We have:

$$\Sigma_W^{\tilde{H}}(q^2) = \frac{1}{2s^2}\Sigma_\gamma(q^2), \quad (4.13)$$

$$\Sigma_Z^{\tilde{H}}(q^2) = \frac{1 + (c^2 - s^2)^2}{4c^2s^2}\Sigma_\gamma(q^2), \quad (4.14)$$

$$\Sigma_{\gamma Z}^{\tilde{H}}(q^2) = \frac{c^2 - s^2}{2cs}\Sigma_\gamma(q^2). \quad (4.15)$$

The expression for the photon self-energy $\Sigma_\gamma(q^2)$ due to a charged Dirac fermion with mass m is known from QED:

$$\Sigma_\gamma(q^2) = \frac{\bar{\alpha}}{3\pi} \left\{ q^2 \left(\Delta - \ln \frac{m^2}{m_Z^2} \right) + (q^2 + 2m^2) F\left(\frac{q^2}{m_Z^2}\right) - \frac{q^2}{3} \right\}, \quad (4.16)$$

where the function $F(x)$ is defined in Eq. (A.11). Now, looking at Eqs. (A.4-A.6) and using Eqs. (4.13-4.15), we see that the quantities which are relevant for evaluating the V_i functions are $\Sigma'_\gamma(0)$, $\Sigma'_\gamma(m_Z^2)$, $\Pi_\gamma(m_Z^2)$ and $\Pi_\gamma(m_W^2)$:

$$\Sigma'_\gamma(0) = \frac{\bar{\alpha}}{3\pi}\Delta_\chi, \quad (4.17)$$

$$\Sigma'_\gamma(m_Z^2) = \frac{\bar{\alpha}}{3\pi} \left\{ \Delta_\chi + F(\chi) + (1 + 2\chi) F'(\chi) - \frac{1}{3} \right\}, \quad (4.18)$$

$$\Pi_\gamma(m_Z^2) = \frac{\bar{\alpha}}{3\pi} \left\{ \Delta_\chi + (1 + 2\chi) F(\chi) - \frac{1}{3} \right\}, \quad (4.19)$$

$$\Pi_\gamma(m_W^2) = \frac{\bar{\alpha}c^2}{3\pi} \left\{ \Delta_\chi + \left(1 + 2\frac{\chi}{c^2} \right) F\left(\frac{\chi}{c^2}\right) - \frac{1}{3} \right\}, \quad (4.20)$$

where $\chi \equiv (m_{\tilde{\chi}}/m_Z)^2$ and $m_{\tilde{\chi}} = \mu$ is the common mass of the light chargino and neutralino. Finally, substituting Eqs. (4.13-4.15) and (4.17-4.20) into Eqs. (A.4-A.6), we find:

$$\delta^{\tilde{H}}V_m = \frac{16}{9} \left[\left(\frac{1}{2} - s^2 + s^4 \right) (1 + 2\chi) F(\chi) - \left(\frac{1}{2} - s^2 \right) \left(1 + 2\frac{\chi}{c^2} \right) F\left(\frac{\chi}{c^2}\right) - \frac{s^4}{3} \right], \quad (4.21)$$

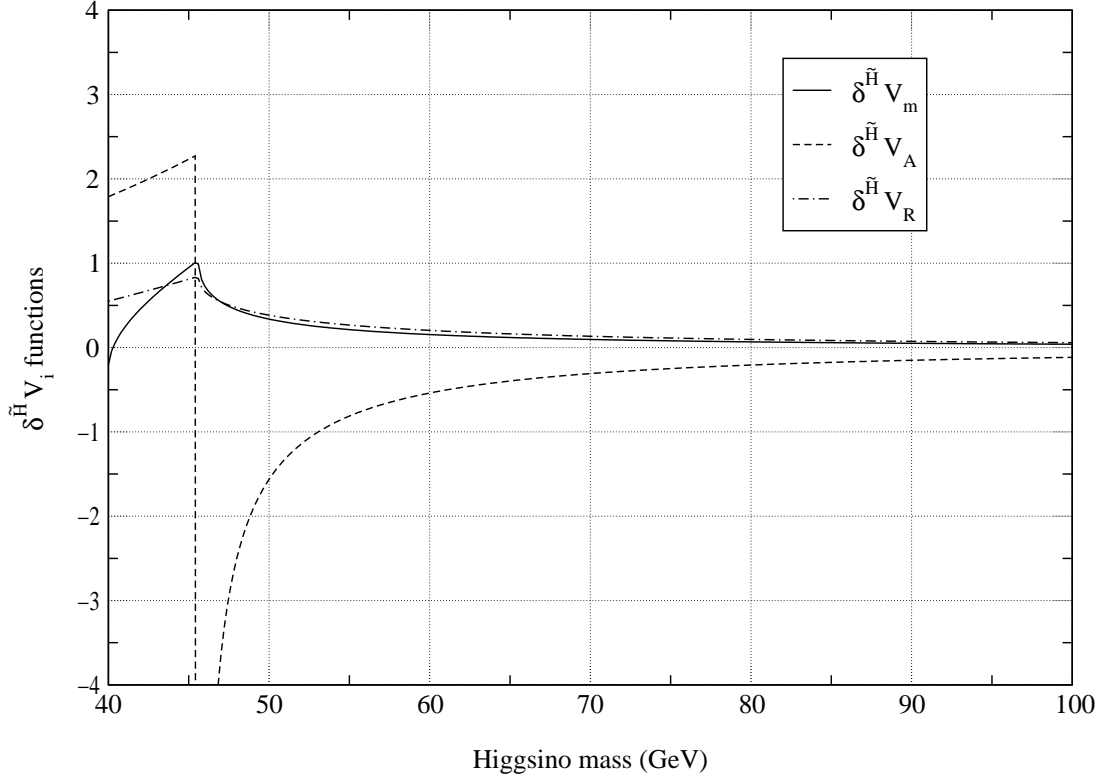


Figure 4.2: Dependence of the $\delta^{\tilde{H}} V_i$ functions on the light gaugino mass $m_{\tilde{\chi}}$, in the limit $M_{1,2} \gg \mu$ (higgsino-dominated case).

$$\delta^{\tilde{H}} V_A = \frac{16}{9} \left(\frac{1}{2} - s^2 + s^4 \right) \left[\frac{12\chi^2 F(\chi) - 2\chi - 1}{4\chi - 1} \right], \quad (4.22)$$

$$\delta^{\tilde{H}} V_R = \frac{16}{9} c^2 s^2 \left[(1 + 2\chi) F(\chi) - \frac{1}{3} \right], \quad (4.23)$$

In Fig. 4.2 the V_i functions are plotted against the chargino-neutralino mass $m_{\tilde{\chi}}$. Looking at it we can see that the numerical values of $\delta^{\tilde{H}} V_m$ and $\delta^{\tilde{H}} V_R$ are always rather small, and the main contribution comes from $\delta^{\tilde{H}} V_A$ which is singular at $m_{\tilde{\chi}} = m_Z/2$. This singularity is not physical and our formulas are valid only for $2m_{\tilde{\chi}} \gtrsim m_Z + \Gamma_Z$; the existence of χ^\pm with a mass closer to $m_Z/2$ will change Z-boson Breit-Wigner curve, therefore it is also not allowed. The importance of the Z wave function renormalization for the case of light charginos was emphasized in [42].

4.2.2 The wino-dominated case

Let us now discuss case (2). The charged Dirac wino \tilde{W} and the neutral Weyl zino \tilde{Z} form an $SU(2)$ triplet of Majorana fermions, with mass M_2 . The relevant Lagrangean in this case is:

$$\mathcal{L}_m^{\tilde{W}} = -M_2 \tilde{W} \tilde{W} - \frac{1}{2} M_2 \tilde{Z} \tilde{Z}, \quad (4.24)$$

$$\mathcal{L}_\gamma^{\tilde{W}} = -e A_\mu \tilde{W} \gamma^\mu \tilde{W}, \quad (4.25)$$

$$\mathcal{L}_{\tilde{Z}}^{\tilde{W}} = -e \frac{c}{s} Z_\mu \tilde{\bar{W}} \gamma^\mu \tilde{W}, \quad (4.26)$$

$$\mathcal{L}_{\tilde{W}}^{\tilde{W}} = \frac{e}{s} W_\mu \tilde{\bar{Z}} \gamma^\mu \tilde{W} + \text{h.c.} \quad (4.27)$$

Again, we see that in Eqs. (4.25-4.27) we have only vector currents. Therefore, as in the previous case all gauge boson self-energies can be written through $\Sigma_\gamma(q^2)$, but the coefficients are now different:

$$\Sigma_{\tilde{W}}^{\tilde{W}}(q^2) = \frac{1}{s^2} \Sigma_\gamma(q^2), \quad (4.28)$$

$$\Sigma_{\tilde{Z}}^{\tilde{W}}(q^2) = \frac{c^2}{s^2} \Sigma_\gamma(q^2), \quad (4.29)$$

$$\Sigma_{\gamma\tilde{Z}}^{\tilde{W}}(q^2) = \frac{1}{c^2 s^2} \Sigma_\gamma(q^2). \quad (4.30)$$

Substituting Eqs. (4.28-4.30) into (A.4-A.6) and using once more Eqs. (4.17-4.20), we find the expressions for $\delta^{\tilde{W}} V_i$:

$$\delta^{\tilde{W}} V_m = \frac{16}{9} \left[c^4 (1 + 2\chi) F(\chi) - (1 - 2s^2) \left(1 + 2\frac{\chi}{c^2} \right) F\left(\frac{\chi}{c^2}\right) - \frac{s^4}{3} \right], \quad (4.31)$$

$$\delta^{\tilde{W}} V_A = \frac{16}{9} c^4 \left[\frac{12\chi^2 F(\chi) - 2\chi - 1}{4\chi - 1} \right], \quad (4.32)$$

$$\delta^{\tilde{W}} V_R = \frac{16}{9} c^2 s^2 \left[(1 + 2\chi) F(\chi) - \frac{1}{3} \right]. \quad (4.33)$$

Comparing Eqs. (4.31-4.33) with Eqs. (4.21-4.23), we see that the corresponding formulas for $\delta^{\tilde{H}} V_i$ and $\delta^{\tilde{W}} V_i$ are very similar, differing from each other only in some constant numerical coefficients. In particular, $\delta^{\tilde{H}} V_R$ and $\delta^{\tilde{W}} V_R$ are exactly identical, while for the case of δV_A the ratio $\delta^{\tilde{W}} V_A / \delta^{\tilde{H}} V_A$ does not depend on χ and its numerical value is $2c^4 / (c^4 + s^4) \approx 1.8$.

In Fig. 4.3 we show the dependence of $\delta^{\tilde{W}} V_i$ on the chargino-neutralino mass $m_{\tilde{\chi}}$. Note that for $m_{\tilde{\chi}} \gtrsim 50$ GeV we have $\delta^{\tilde{W}} V_m > \delta^{\tilde{W}} V_R$, while in the previous case it was $\delta^{\tilde{H}} V_m < \delta^{\tilde{H}} V_R$: this fact is irrelevant for the present discussion, but will be useful in the next chapter to explain why higgsinos help to improve fits for an extra generation of fermions more than winos do. Also, note that in the limit $m_{\tilde{\chi}} \rightarrow \infty$ all δV_i vanish, as expected due to the *decoupling* property of SUSY mentioned in the introduction.

At this point, one may wonder whether the results found so far are really useful for the problem under investigation or not. Formulae (4.21-4.23) and (4.31-4.33) are valid in the case of *exactly* degenerate chargino and neutralino, and we know from Sec. 4.1 that the experimental bounds are very strong for $\Delta M^\pm < 0.2$ GeV. However, it is important to note that, while for the direct search experiments the crucial quantity is the *mass difference* between the lightest chargino and neutralino (because it is on this parameter that the chargino life time and the energy of its decay products depend), for the case of precision measurements what really matters is the *mass* itself of the particles involved. This imply that, when the masses of chargino and neutralino are slightly moved from each other, the consequences on the results of direct search may be drastic, but effects on radiative corrections are very small and the overall picture does not change.

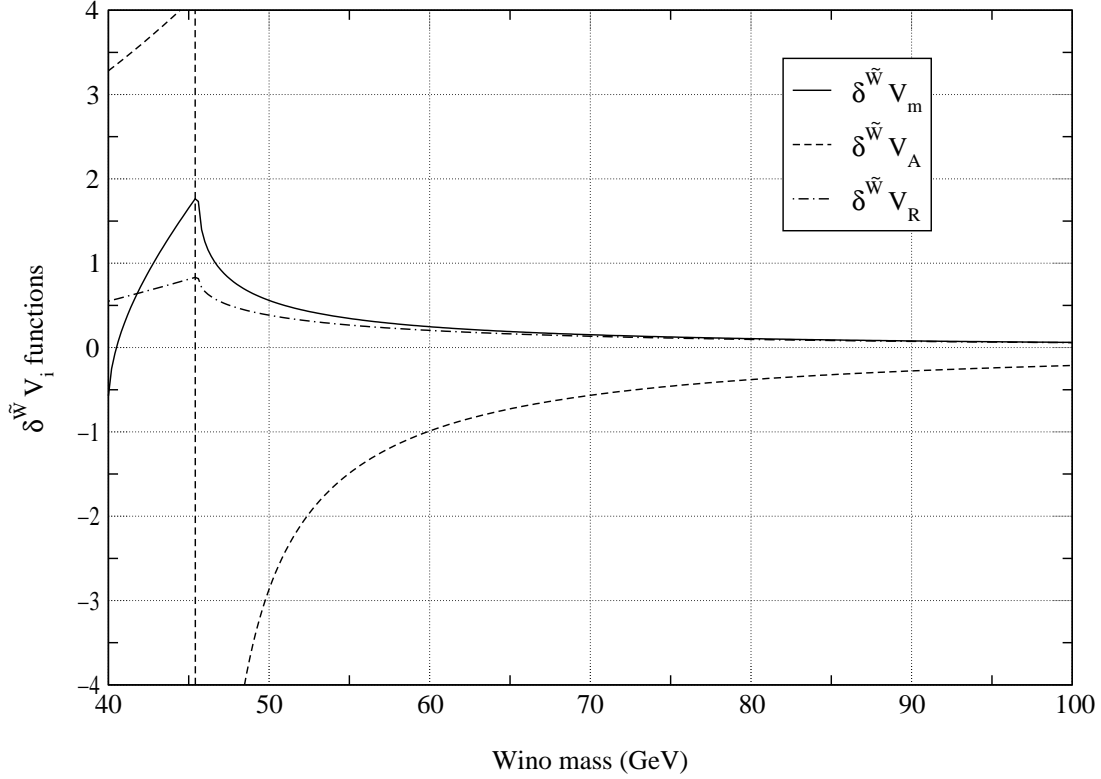
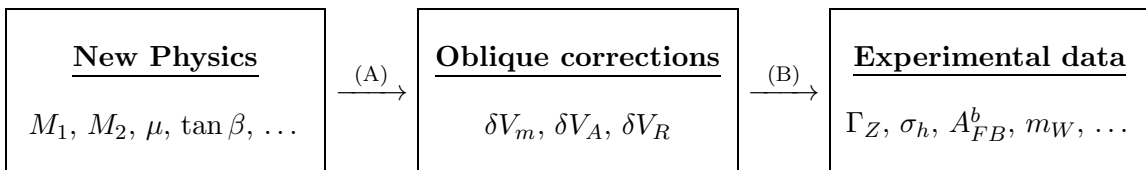


Figure 4.3: Dependence of the $\delta^{\tilde{W}} V_i$ functions on the light gaugino mass $m_{\tilde{\chi}}$, in the limit $\mu \gg M_{1,2}$ (wino-dominated case).

Therefore, even in the case of not-complete degeneracy Eqs. (4.21-4.23) and (4.31-4.33) provide a very good approximation to the exact numerical results and the conclusions still hold. This has been verified numerically using equations from Ref. [43].

4.3 Data analysis and fits

Having all the necessary formulas at our disposal, we can now analyze the impact of a chargino almost degenerate with the lightest neutralino on precision measurements, so to derive a lower limit for its mass. In Table 4.1, which we extracted from Table 7 of Ref. [16], we report the present experimental value of many electroweak observables, together with their SM expectation. The key point is that the contribution of New Physics into these observables occurs mostly *through* the oblique corrections, which are fully parameterized by the three functions V_i described above. This situation is summarized in the following diagram:



Observable	Experimental data	Theoretical fit	Pull	V_i function
Γ_Z (GeV)	2.4939(24)	2.4960(18)	-0.9	V_A, V_R
σ_h (nb)	41.491(58)	41.472(16)	0.3	V_A, V_R
R_l	20.765(26)	20.746(20)	0.7	V_A, V_R
R_b	0.2166(7)	0.2158(2)	1.1	V_A, V_R
R_c	0.1735(44)	0.1723(1)	0.3	V_A, V_R
A_τ	0.1431(45)	0.1467(16)	-0.8	V_R
A_e	0.1479(51)	0.1467(16)	0.2	V_R
A_b	0.8670(350)	0.9348(2)	-1.9	V_R
A_c	0.6470(400)	0.6677(7)	-0.5	V_R
A_{FB}^l	0.0168(10)	0.0161(4)	0.7	V_R
A_{FB}^b	0.0990(21)	0.1028(12)	-1.8	V_R
A_{FB}^c	0.0709(44)	0.0734(9)	-0.6	V_R
A_{LR}	0.1504(23)	0.1467(16)	1.6	V_R
$s_l^2(Q_{FB})$	0.2321(10)	0.2316(2)	0.5	V_R
m_W (GeV)	80.390(64)	80.366(34)	0.4	V_m
s_W^2	0.2254(21)	0.2233(7)	1.0	V_m
m_t (GeV)	173.8(5.0)	170.8(4.9)	0.6	

Table 4.1: Experimental value and SM theoretical prediction of the electroweak precision measurements, as reported in Tab. 7 of Ref. [16]. In the last column we list the V_i functions which are relevant for evaluating each observable.

Step (A) is clearly model dependent, and was performed in the previous sections by deriving Eqs. (4.21-4.23) and (4.31-4.33). On the contrary, step (B) is model independent, and can be done once for all by summarizing all the experimental data into three “best fit” values $\overline{\delta V_i}$ and a (3×3) correlation matrix C_{ij} . Using formulas from Ref. [16] and the numerical values from Table 4.1, we get:

$$\begin{pmatrix} C_{mm} & C_{mA} & C_{mR} \\ C_{mA} & C_{AA} & C_{AR} \\ C_{mR} & C_{AR} & C_{RR} \end{pmatrix} = \begin{pmatrix} 7.28 & 0 & 0 \\ 0 & 7.24 & 2.54 \\ 0 & 2.54 & 23.03 \end{pmatrix}; \quad \begin{pmatrix} \overline{\delta V_m} \\ \overline{\delta V_A} \\ \overline{\delta V_R} \end{pmatrix} = \begin{pmatrix} -0.07 \\ -0.33 \\ +0.01 \end{pmatrix}. \quad (4.34)$$

Now it is very easy to evaluate the χ^2 :

$$\chi^2 = C_{ij} (\delta^{\text{NP}} V_i - \overline{\delta V_i}) (\delta^{\text{NP}} V_j - \overline{\delta V_j}). \quad (4.35)$$

In Fig. 4.4 we report the confidence level curve for both the higgsino-dominated and the wino-dominated case. At 95% C.L., we have:

$$m_\chi \gtrsim 54 \text{ GeV for the higgsino-dominated case}; \quad (4.36)$$

$$m_\chi \gtrsim 60 \text{ GeV for the wino-dominated case}. \quad (4.37)$$

Since there are a number of new additional particles in SUSY extensions, we will briefly discuss their contributions to the functions V_i . In the considered limits the remaining charginos and

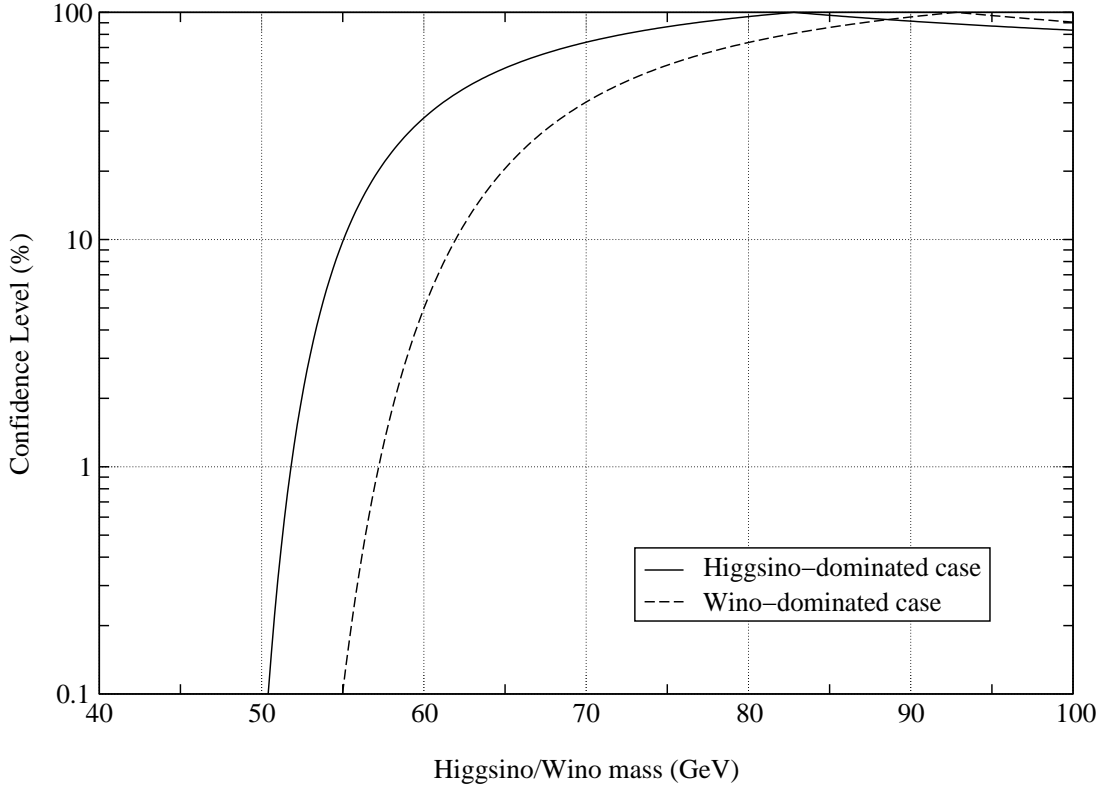


Figure 4.4: Dependence of the confidence level on the light gaugino mass $m_{\tilde{\chi}}$, both in the limit $M_{1,2} \gg \mu$ (higgsino-dominated case) and $\mu \gg M_{1,2}$ (wino-dominated case).

neutralinos are very heavy, so they simply decouple and produce negligible contributions. The contributions of the three generations of sleptons (with masses larger than 90 GeV) into V_A are smaller than 0.1, so they can be safely neglected. The contributions of squarks of the first two generations are also negligible since they should be heavier than Tevatron direct search bounds; taking $m_{\tilde{q}} \gtrsim 200$ GeV, we have $|\delta^{\tilde{q}} V_i| \lesssim 0.1$. Concerning the contributions of the third generation squarks, they are enhanced by the large top-bottom mass difference and are not negligible. However, being positive and almost universal [37], they do not affect our analysis: compensating negative contributions of chargino-neutralino into V_A they will generate positive contributions to V_R and V_m , and χ^2 will not be better. When squarks are heavy enough (for $m_{\tilde{q}} \gtrsim 300$ GeV), they simply decouple and their contributions become negligible as well.

The last sector of the theory to be discussed is Higgs bosons. Unlike the case of Standard Model now we have one extra charged higgs and two extra neutral higgses. Their contributions to radiative corrections were studied in detail in [44]. According to Fig. 2 from that paper it is clear that the contributions of MSSM higgses (and $SU(2) \times U(1)$ gauge bosons) equal with very good accuracy those of the Standard Model with the mass of SM higgs being equal to that of the lightest neutral higgs in SUSY generalization. That is why the contributions from the higgs sector of the theory also cannot compensate those of the light chargino-neutralino.

In addition to SUSY particles, one may wonder about the possibility of improving the overall χ^2 by shifting a bit some of the SM parameters from their central values. The most important

contributions of this kind are those coming from the worst-measured quantities, i.e. the top mass and the higgs mass. However, concerning the top its contributions are almost universal, just as for the case of the third generation squarks, therefore they also cannot affect our analysis. Concerning the higgs, in our model it is bounded to be heavier than 90 GeV by direct search experiments and lighter than $120 \div 130$ GeV by the basic assumption that SUSY exists (otherwise, we wouldn't discuss chargino mass!), and since its contributions to physical observables are only logarithmic, we do not expect them to be relevant.

Apart from oblique corrections (those arising from vector bosons self energies) which have been considered in this letter, there are process dependent vertex and box corrections. However, due to LEP II and Tevatron low bounds on squarks and sleptons masses they are small.

4.4 Recent developments and new fits

The analysis of the χ^2 done in the previous section is not completely satisfactory for two main reasons:

- the data reported in Table 4.1 are not independent from one another, since many of them come from the same experiment and therefore are strongly correlated. In the analysis performed in Sec. 4.3, the cross correlations have been neglected. This led to a small underestimation of the errors associated to each $\overline{\delta V}_i$ (or equivalently to an overestimation of the coefficients C_{ij}), so bounds (4.36-4.37) may be slightly stronger than the correct ones;
- effects of changing the higgs mass, although known to be small, may affect the precise numerical value of bounds (4.36-4.37).

To overcome these problems, we asked to A. Rozanov to repeat our analysis using the program LEPTOP. In Fig. 4.5 we show the new profile for the confidence level curve, which now account both for all the cross correlations among experimental data and for the effects of varying the SM parameters m_t , m_H and $\hat{\alpha}_s$. The new bounds at 95% C.L. for the chargino-neutralino mass are:

$$m_\chi \gtrsim 51 \text{ GeV for the higgsino-dominated case;} \quad (4.38)$$

$$m_\chi \gtrsim 56 \text{ GeV for the wino-dominated case.} \quad (4.39)$$

Although these limits are slightly weaker than the previous one, the main conclusion still hold.

Recently, the DELPHI collaboration has strongly improved its analysis of the ISR in the region $0.2 \text{ GeV} \lesssim \Delta M^\pm \lesssim 3 \text{ GeV}$. The preliminary results were presented in [39], and are summarized in Fig. 4.6. It can immediately be seen that the narrow window for a light chargino-neutralino has now be completely closed (up to 80 GeV) for the higgsino-dominated case, and for the wino-dominated case with a sneutrino heavier than 500 GeV. However, for a light sneutrino the negative interference between diagrams (4.1a) and (4.1b) makes the total cross section very

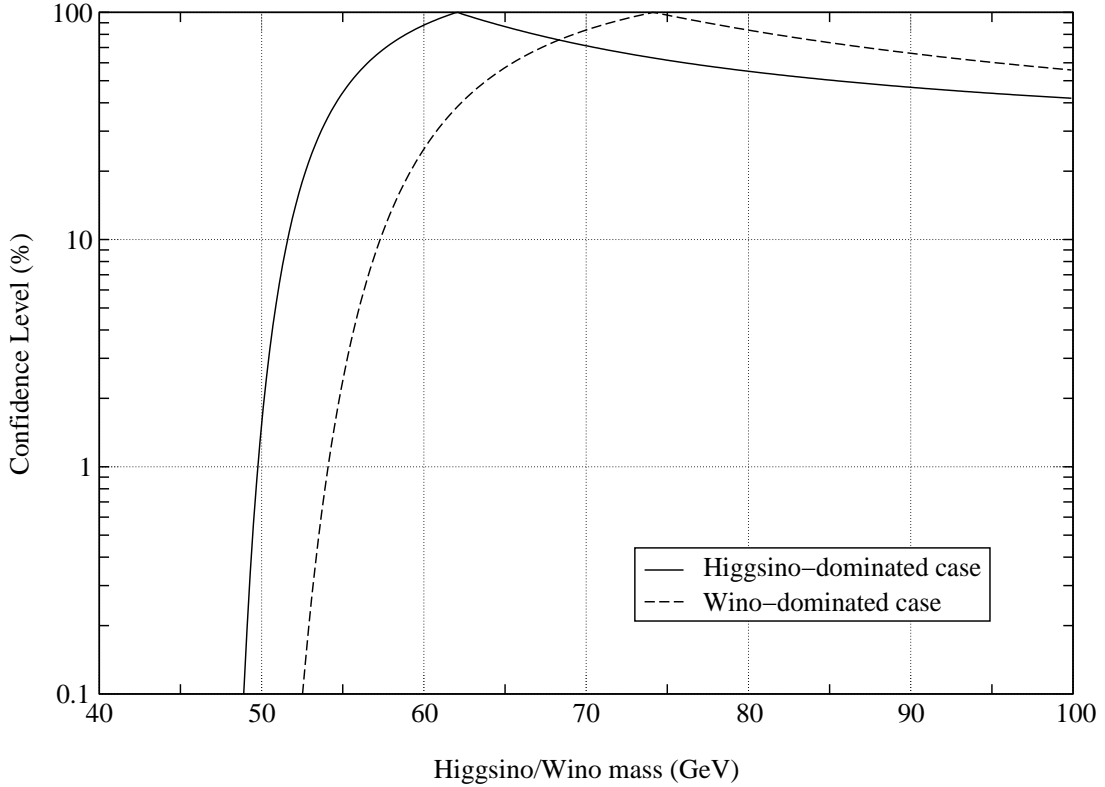


Figure 4.5: Dependence of the confidence level, evaluated with the program LEPTOP, on the light gaugino mass $m_{\tilde{\chi}}$, both in the limit $M_{1,2} \gg \mu$ (higgsino-dominated case) and $\mu \gg M_{1,2}$ (wino-dominated case).

small, and analysis based on ISR becomes impossible. Therefore, in the wino-dominated scenario with unconstrained sneutrino mass the study of radiative corrections is currently the only way to go beyond LEP I bound.

4.5 Conclusions

In this chapter, we analyzed in detail the effects of radiative corrections for the case of a chargino almost degenerate with the lightest neutralino on the electroweak precision measurements. Both the higgsino-dominated and the wino-dominated scenario have been studied, and for these limits simple analytical formulae have been derived. For the case of wino domination, the bound $m_{\tilde{\chi}} \gtrsim 56$ GeV is presently the strongest constraint which can be imposed without making any assumption on the mass spectrum of other superpartners.

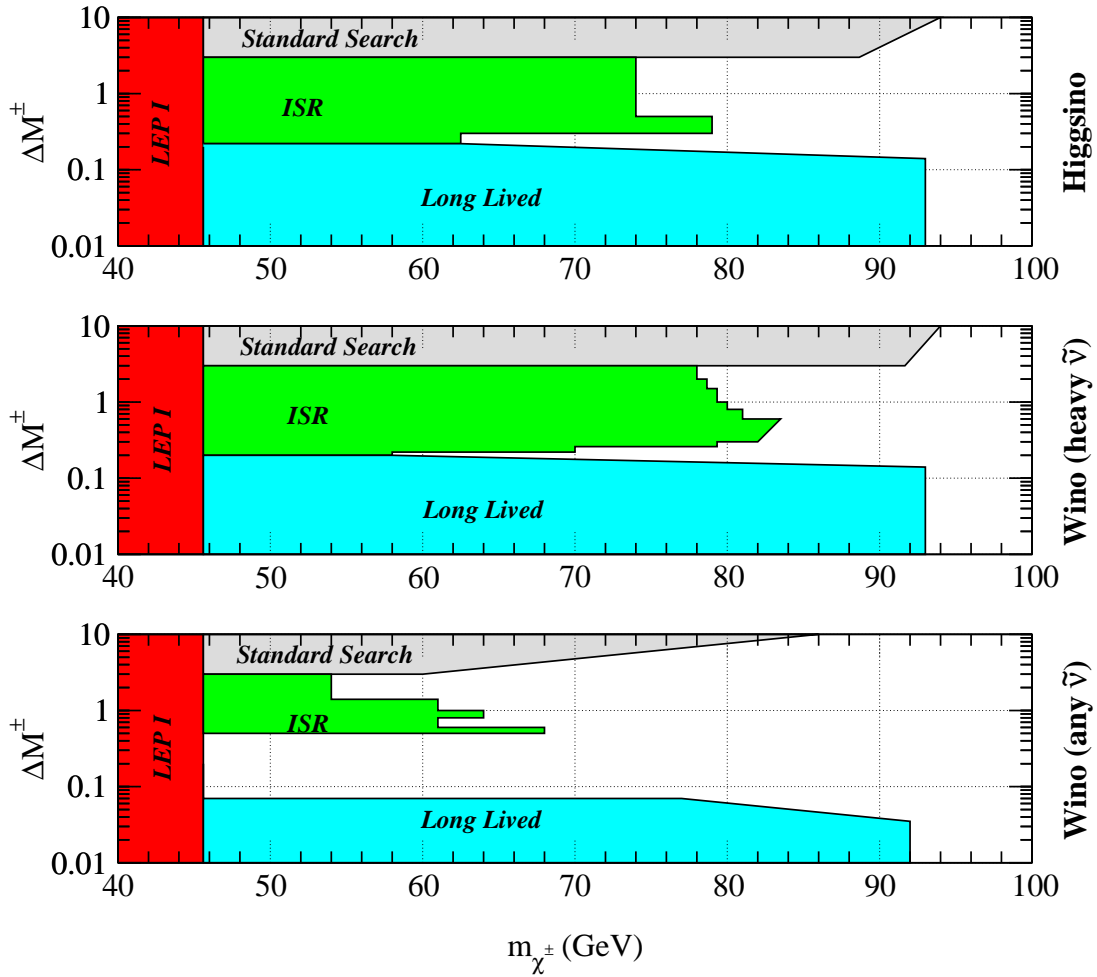


Figure 4.6: Regions in the plane $(m_{\tilde{\chi}^\pm}, \Delta M^\pm)$ excluded at 95% C.L. by the DELPHI collaboration. The upper panel refers to the Higgsino-dominated case, and the lower ones to the wino-dominated scenario with and without assuming $m_{\tilde{\nu}_e} > 500$ GeV. This figure reproduces schematically the results presented by A. Perrotta at the conference PASCOS99 [39].

Chapter 5

Extra quark-lepton generations and precision measurements

The analysis performed in the previous chapter has shown that, except for special cases when direct search experiments fail for some peculiar reason, at the present time precision measurements are not very useful to investigate those extensions of the SM which, like SUSY, exhibit the *de-coupling* property. However, the situation completely changes when dealing with *non-decoupling* New Physics, since in this framework even particles far too heavy to be directly produced and observed at accelerators may give relevant contributions to “low” ($\sim m_Z$) energy observables through radiative corrections. The most straightforward generalization of the Standard Model through inclusion of extra chiral generations of heavy fermions, both quarks ($q = U, D$) and leptons ($l = N, E$), is an example of such non decoupled New Physics.

The aim of this chapter is to understand to what extent the existing data on the Z -boson parameters, the W -boson and the top quark masses allow to bound effectively high energy models which do not decouple at low energies. In particular, we will analyze in detail the case of extra generations of fermions, showing that it is excluded by the electroweak precision measurements if all the new particles are heavier than m_Z . We find however that if masses of extra neutrinos are close to 50 GeV, then additional generations can exist, and in this case up to three extra families are allowed within 2σ . Finally, inclusion of new generations in SUSY extensions of the Standard Model is discussed.

When speaking of extra generations, the first thing to bother about is the extra neutrinos, N : being coupled to Z -boson they would increase the invisible Z -width, so to avoid contradiction with experimental data their masses should be larger than 45 GeV [45]. In order to meet this condition, one has to introduce not only left-handed states N_L but also right-handed states N_R , and supply new “neutrinos” with Dirac masses analogously to the case of charged leptons and quarks. Unfortunately, gauge symmetries do not forbid a Majorana mass term for N_R , and if it is large one would get light N_L through the see-saw mechanism. To avoid such a failure we will suppose that the Majorana mass of N_R is negligible, closing eyes on the emerging (un)naturalness problem. Thus, our neutral lepton N is a heavy Dirac particle.

Contributions of extra generations to the electroweak radiative corrections were considered in Refs. [46, 47, 48, 49, 50, 21]. In what follows we will assume that the mixing among new generations and the three existing ones is small, hence new fermions contribute only to oblique corrections (vector boson self-energies). This case is discussed in Ref. [21] and the authors come to the conclusion that one extra generation of heavy fermions is excluded at 99.2% C.L. The authors of [21] follow a two step procedure: first, they show that experimental bounds on parameter ρ exclude the existence of non-degenerate extra generations (a degenerate generation is decoupled from ρ); then, they consider the parameter S [51], which is sensitive also to degenerate families, and find that its experimental value excludes the existence of extra degenerate generation as well. Such procedure is not general enough: it does not use all precision data. In the present chapter we perform global fits of all precision measurements.

We study both degenerate and non-degenerate extra generations on the equal footing. By considering the contributions of new families into all precision electroweak observables simultaneously we see that the fit of the data is worsened by them if all the new particles are heavy. Taking the number of new generations N_g as a continuous parameter (just as it was done with the determination of the number of neutrinos from invisible Z width) we get a bound on it. The best χ^2 corresponds to $N_g \simeq -0.5$, while $N_g = 1$ is excluded by more than 2 standard deviations.

This chapter is based on Ref. [4], currently submitted for publication on PLB, and on the talk recently presented at the conference PASCOS99 [6]. Sec. 5.1 contains general formulas for oblique radiative corrections caused by an extra doublet of quarks or leptons. In Sec. 5.2 we consider the case when *all* the extra fermions are heavy ($m \gtrsim m_Z$), while in Sec. 5.3 we allow the extra neutrino to be “light” ($m_N \simeq 50$ GeV): in this case, the contribution of N compensates that of U , D , E . Finally, in Sec. 5.4 we analyze the SUSY version of four generations.

5.1 General formulas

New particles contribute to physical observables through the self-energies of vector and axial currents: this induces extra corrections δV_i to the functions V_i which are used to describe the theoretical relations among precision measurements (see Sec. 4.3 and Ref. [16]). In this section we present explicit expressions for these corrections. Eqs. (5.3-5.16) are valid both for lepton and quark contributions, provided that the values of Q_U , Q_D , Y , N_c , u and d are correctly set according to the following table:

	Q_U	Q_D	Y	N_c	u	d
leptons	0	-1	-1	1	$(m_N/m_Z)^2$	$(m_E/m_Z)^2$
quarks	2/3	-1/3	1/3	3	$(m_U/m_Z)^2$	$(m_D/m_Z)^2$

(5.1)

where Q_U and Q_D are the electric charges of the up and down component of the $SU(2)_L$ doublet, $Y = Q_U + Q_D$ is the doublet hypercharge (the hypercharge of isosinglets being equal to its doubled electric charge), and N_c is the number of colors. Corrections produced by the whole extra generation are given by the sum of lepton and quark contributions:

$$\Delta V_i = \delta V_i^q + \delta V_i^l \quad (5.2)$$

Contributions of quark or lepton doublets to V_i functions are:

$$\begin{aligned}
\delta V_m^{q,l} = & \frac{2}{9} N_c \left(1 - \frac{s^2}{c^2} \right) \left\{ -F(m_W^2, m_U^2, m_D^2) \left[2c^2 - u - d - \frac{(u-d)^2}{c^2} \right] + u + d - \frac{4}{3} c^2 \right\} \\
& - \frac{4s^2}{9} N_c Y \left\{ (1+2u)F(u) - (1+2d)F(d) - \ln\left(\frac{u}{d}\right) \right\} \\
& + \frac{16}{9} N_c s^4 \left\{ Q_U^2 \left[(1+2u)F(u) - \frac{1}{3} \right] + Q_D^2 \left[(1+2d)F(d) - \frac{1}{3} \right] \right\} \\
& + \frac{2}{9} N_c \left\{ (1-u)F(u) + (1-d)F(d) - \frac{2}{3} \right\} + \frac{s^2}{3c^2} N_c (u+d) \\
& - \frac{4}{9} N_c s^2 \left\{ (1+2u)F(u) + (1+2d)F(d) - \frac{2}{3} \right\} \\
& - \frac{2}{9} N_c \ln\left(\frac{u}{d}\right) \left\{ \left(1 + \frac{1}{c^2} \right) \frac{ud}{u-d} - (c^2 - s^2) \frac{u+d}{u-d} \right\},
\end{aligned} \tag{5.3}$$

$$\begin{aligned}
\delta V_A^{q,l} = & \frac{1}{3} N_c \left[u + d - 2 \frac{ud}{u-d} \ln\left(\frac{u}{d}\right) - F'(u) - F'(d) \right] \\
& - N_c \left(\frac{4}{9} s^2 + \frac{1}{9} \right) \left\{ [2uF(u) - (1+2u)F'(u)] + [2dF(d) - (1+2d)F'(d)] \right\} \\
& + \frac{16}{9} N_c s^4 \left\{ Q_U^2 [2uF(u) - (1+2u)F'(u)] + Q_D^2 [2dF(d) - (1+2d)F'(d)] \right\} \\
& - \frac{4}{9} N_c Y s^2 \left\{ [2uF(u) - (1+2u)F'(u)] - [2dF(d) - (1+2d)F'(d)] \right\},
\end{aligned} \tag{5.4}$$

$$\begin{aligned}
\delta V_R^{q,l} = & -\frac{2}{3} N_c \left[uF(u) + dF(d) + \frac{ud}{u-d} \ln\left(\frac{u}{d}\right) - \frac{u+d}{2} \right] \\
& + \frac{16}{9} N_c s^2 c^2 \left\{ Q_U^2 \left[(1+2u)F(u) - \frac{1}{3} \right] + Q_D^2 \left[(1+2d)F(d) - \frac{1}{3} \right] \right\} \\
& - \frac{2Y}{9} N_c \left\{ (1+2u)F(u) - (1+2d)F(d) - \ln\left(\frac{u}{d}\right) \right\},
\end{aligned} \tag{5.5}$$

where the expressions for $F(m_W^2, m_U^2, m_D^2)$, $F(x)$ and $F'(x)$ are given in Eqs. (A.10-A.12).

In the asymptotic limit (denoted by prime) where the extra generation particles are much heavier than Z -boson ($u, d \gg 1$), power suppressed terms can be neglected and Eqs. (5.3-5.5) reduce to:

$$\begin{aligned}
\delta' V_m^{q,l} = & \delta' V_A^{q,l} - \frac{2}{9} N_c + \frac{4}{9} N_c Y s^2 \ln\left(\frac{u}{d}\right) - \frac{4}{9} N_c (c^2 - s^2) \cdot \\
& \cdot \left\{ \frac{1}{3} - 2 \frac{ud}{(u-d)^2} - \frac{u^3 - 3u^2d - 3ud^2 + d^3}{2(u-d)^3} \ln\left(\frac{u}{d}\right) \right\},
\end{aligned} \tag{5.6}$$

$$\delta' V_A^{q,l} = \frac{1}{3} N_c \left[u + d - 2 \frac{ud}{u-d} \ln\left(\frac{u}{d}\right) \right], \tag{5.7}$$

$$\delta' V_R^{q,l} = \delta' V_A^{q,l} - \frac{2}{9} N_c + \frac{2}{9} N_c Y \ln\left(\frac{u}{d}\right). \tag{5.8}$$

A stronger approximation can be used when the mass differences $|m_N - m_E|$ and $|m_U - m_D|$ are small with respect to the masses of the extra particles, i.e. the total amount of $SU(2)_V$ breaking is not too large. In this case, further terms can be omitted from Eqs. (5.6-5.8) and the resulting expressions are almost trivial:

$$\delta'' V_m^{q,l} = \delta'' V_A^{q,l} - \frac{4}{9} N_c s^2 \left[1 - Y \ln \left(\frac{u}{d} \right) \right], \quad (5.9)$$

$$\delta'' V_A^{q,l} = \frac{4}{9} N_c \left[\sqrt{u} - \sqrt{d} \right]^2, \quad (5.10)$$

$$\delta'' V_R^{q,l} = \delta'' V_A^{q,l} - \frac{2}{9} N_c \left[1 - Y \ln \left(\frac{u}{d} \right) \right]. \quad (5.11)$$

From these formulas we can see that the $SU(2)_V$ breaking terms are universal, i.e. their contribution is the same for all the three V_i functions. Also, they are even under the exchange $u \leftrightarrow d$, while terms proportional to the doublet hypercharge Y are odd.

In the opposite case, when $SU(2)_V$ is strongly violated ($m_U \gg m_D$ or $m_U \ll m_D$), Eqs. (5.9-5.11) are no longer valid. However, also in this limit the $SU(2)_V$ breaking terms are universal and even under $u \leftrightarrow d$:

$$\delta' V_i = \frac{1}{3} N_c |u - d|. \quad (5.12)$$

In order to obtain the contributions of the whole generation, one should sum those of quarks and leptons, as shown in Eq. (5.2). Looking at (5.1), it is easy to see that in the ‘‘horizontally degenerate’’ case ($m_N = m_U$ and $m_E = m_D$) terms proportional to the doublet hypercharge cancel between quarks and leptons and the overall result is:

$$\left. \begin{aligned} \Delta'' V_m &= -\frac{16}{9} s^2 \\ \Delta'' V_A &= 0 \\ \Delta'' V_R &= -\frac{8}{9} \end{aligned} \right\} + \frac{16}{9} \left(\frac{m_{N,U} - m_{E,D}}{m_Z} \right)^2. \quad (5.13)$$

In the present chapter we consider the general case described *not* by asymptotic formulas (5.6-5.8), but by general formulas (5.3-5.5), which will allow us to study the case of ‘‘light’’ new neutrinos ($m_N \approx m_Z/2$). Effects of extra generations with masses heavier than m_Z were already analyzed in Refs. [48, 49, 50] using asymptotic expressions (5.6-5.8); however, with new experimental data the bounds we get are much more restrictive than those obtained in [50]. Concerning Eqs. (5.9-5.11), they are so simple that using them it will be possible to understand qualitatively many aspects of the numerical results produced by fits: this is the reason why we presented them here.

In Figs. 5.1-5.3 we show the u dependence of the functions δV_i , $\delta' V_i$ and $\delta'' V_i$ for $d = 1$, for the case of leptons alone (Fig. 5.1), quarks alone (Fig. 5.2), and horizontally degenerate quarks and leptons (Fig. 5.3, see also Eqs. (5.14-5.16)). It is clear that accuracy of equations (5.6-5.8) is very good as soon as new fermions are heavier than Z -boson. Also, we see that Eqs. (5.9-5.11) perfectly approximate the exact functions if the value of $|m_U - m_D|$ or $|m_N - m_E|$ is

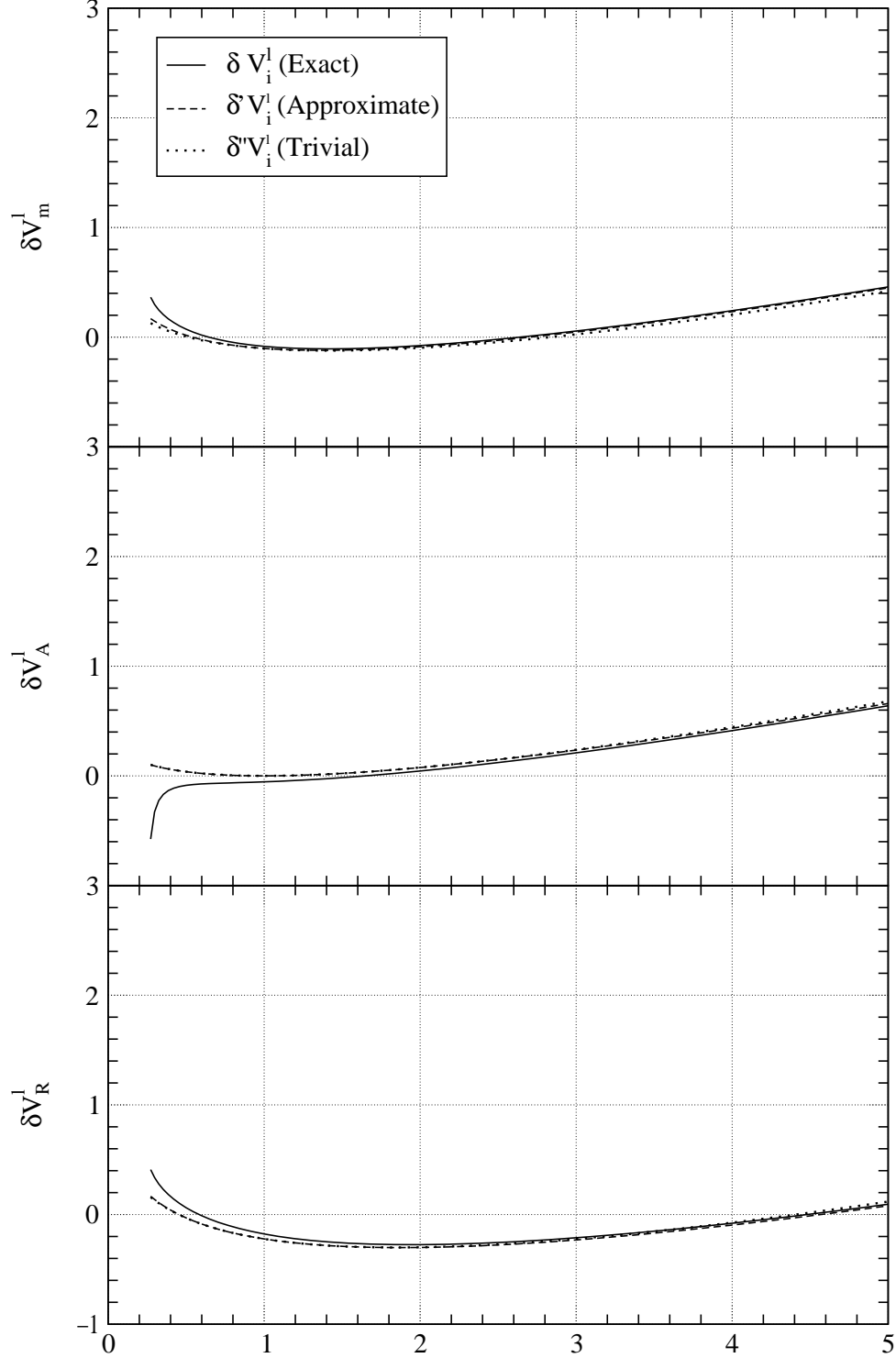


Figure 5.1: Contributions of an extra lepton doublet to δV_i^l as a function of $u \equiv (m_N/m_Z)^2$. We assume $m_E = m_Z$. Solid lines correspond to exact formulas (5.3-5.5), dashed lines to approximated expressions (5.6-5.8), and dotted lines to even more approximated relations (5.9-5.11).

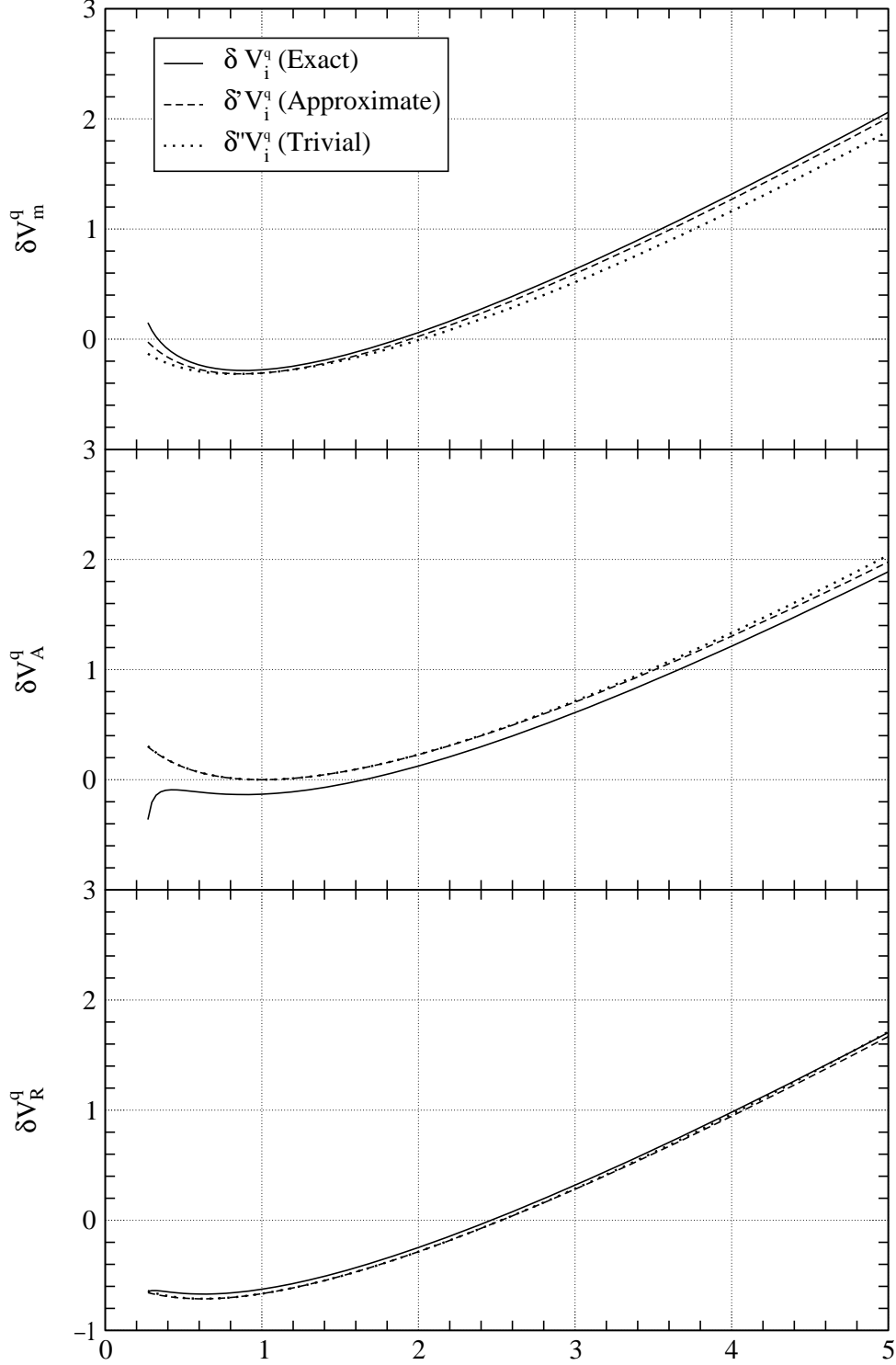


Figure 5.2: Contributions of an extra quark doublet to δV_i^q as a function of $u \equiv (m_U/m_Z)^2$. We assume $m_D = m_Z$. Solid lines correspond to exact formulas (5.3-5.5), dashed lines to approximated expressions (5.6-5.8), and dotted lines to even more approximated relations (5.9-5.11).

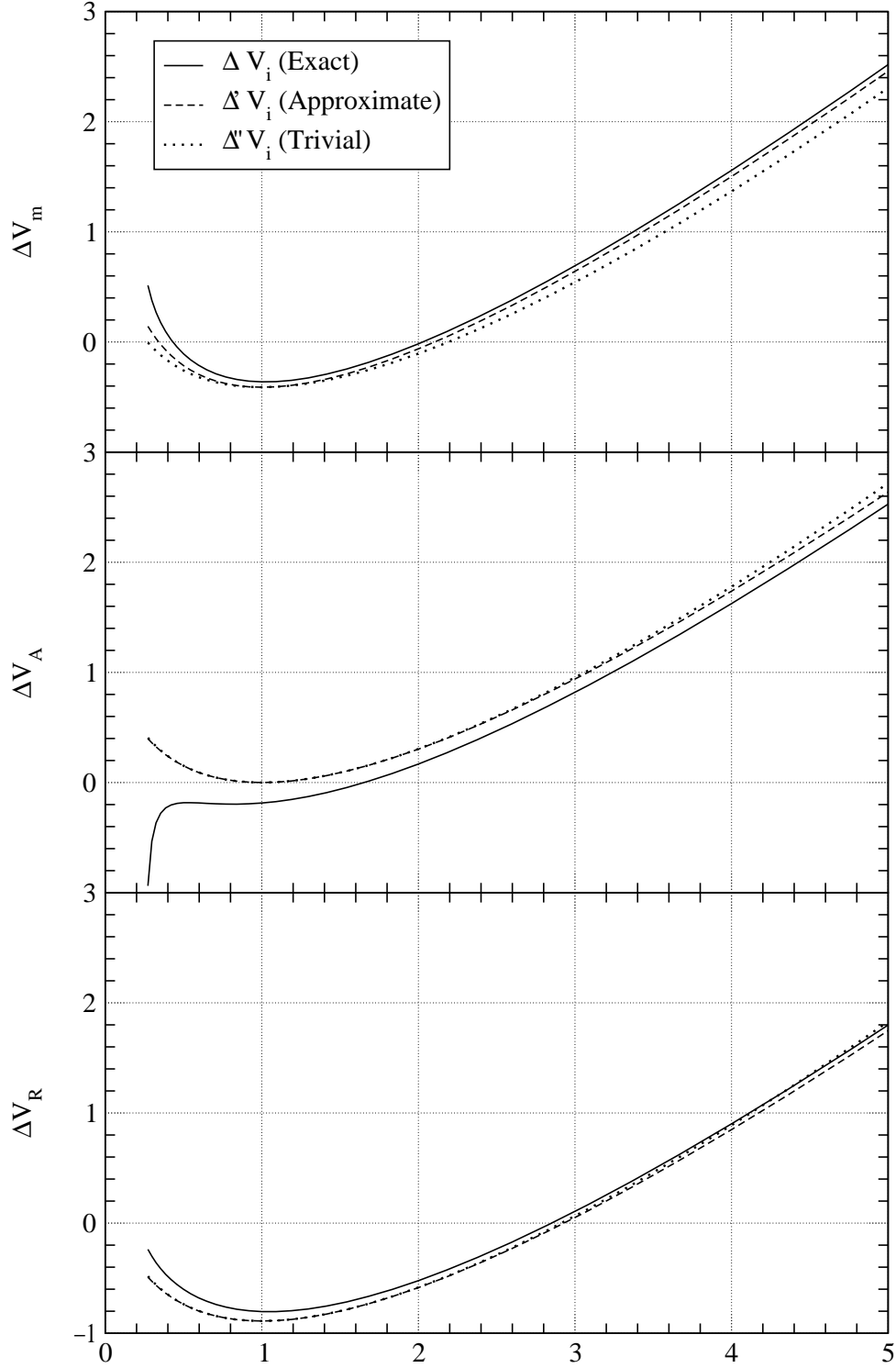


Figure 5.3: Contributions of an extra generation of fermions to ΔV_i as a function of $u \equiv (m_{N,U}/m_Z)^2$. We assume $m_N = m_U$ and $m_E = m_D = m_Z$. Solid lines correspond to exact formulas (5.3-5.5), dashed lines to approximated expressions (5.6-5.8), and dotted lines to even more approximated relations (5.9-5.11). These plots help to study accuracy of approximations (5.6-5.11) *outside* its formal domain of validity, that is why we neglect experimental bounds on m_U and m_D .

small enough. For larger $SU(2)_V$ breaking, corresponding to the (not shown) region $u \gg 1$ in Figs. 5.1-5.3, there is a discrepancy; however, in this limit the contributions to δV_i which are correctly described by Eq. (5.12) are so large that the quality of χ^2 is awful. Therefore this region is not interesting for our analysis.

Since in the rest of this chapter we will frequently assume horizontal degeneracy between lepton and quark doublets, let us conclude this section giving explicit formulas for this case:

$$\begin{aligned} \Delta V_m = & \frac{16}{9}s^2 \left(\frac{4}{9}s^2 - 1 \right) \left\{ (1+2u)F(u) + (1+2d)F(d) - \frac{2}{3} \right\} \\ & + \frac{8}{9} \left\{ (1-u)F(u) + (1-d)F(d) - \frac{2}{3} \right\} + \frac{4s^2}{3c^2} \left\{ u+d - 2\frac{ud}{u-d} \ln\left(\frac{u}{d}\right) \right\} \\ & + \frac{8}{9} \left(1 - \frac{s^2}{c^2} \right) \left\{ \frac{u-d}{2} \ln\left(\frac{u}{d}\right) + u+d + \left(c^2 - \frac{u+d}{2} \right) \frac{u+d}{u-d} \ln\left(\frac{u}{d}\right) - \frac{4}{3}c^2 \right\} \\ & - \frac{8}{9} \left(1 - \frac{s^2}{c^2} \right) \left[2c^2 - u - d - \frac{(u-d)^2}{c^2} \right] F(m_W^2, m_U^2, m_D^2), \end{aligned} \quad (5.14)$$

$$\begin{aligned} \Delta V_A = & \frac{4}{9} \left(\frac{16}{3}s^4 - 4s^2 - 1 \right) \left\{ [2uF(u) - (1+2u)F'(u)] + [2dF(d) - (1+2d)F'(d)] \right\} \\ & + \frac{4}{3} \left\{ u+d - 2\frac{ud}{u-d} \ln\left(\frac{u}{d}\right) - F'(u) - F'(d) \right\}, \end{aligned} \quad (5.15)$$

$$\begin{aligned} \Delta V_R = & -\frac{8}{3} \left\{ uF(u) + dF(d) + \frac{ud}{u-d} \ln\left(\frac{u}{d}\right) - \frac{u+d}{2} \right\} \\ & + \frac{64}{27}s^2c^2 \left\{ (1+2u)F(u) + (1+2d)F(d) - \frac{2}{3} \right\}. \end{aligned} \quad (5.16)$$

It is worth noting that these expressions are exactly even under the exchange $u \leftrightarrow d$. This happens since the cancellation of odd terms proportional to the doublet hypercharge Y between leptons and quarks, which we noted when deriving the approximate formula (5.13), occurs also for the exact relations (5.3-5.5).

5.2 Comparison with experimental data: heavy fermions

We compare theoretical predictions for the case of extra generations with experimental data using the computer program LEPTOP (see Refs. [32, 16]). We take $m_D = 130$ GeV - the lowest value allowed for the new quark mass from Tevatron search [52] - and assume $m_U \gtrsim m_D$. As for the extra leptons, their masses are independent parameters. To simplify the analysis, we start with the horizontally degenerate case, setting $m_N = m_U$ and $m_E = m_D$. Any value of higgs mass above 90 GeV is allowed in our fits, however χ^2 appears to be minimal for $m_H = 90$ GeV. In Fig. 5.4 the excluded domains in coordinates $(N_g, \Delta m)$ are shown (here $\Delta m = (m_U^2 - m_D^2)^{1/2}$). Minimum of χ^2 corresponds to $N_g = -0.5$ and the case $N_g = 0$ is in the 1 standard deviation domain. We see that one extra generation corresponds to 2.5σ approximately. The behavior of division lines in Fig. 5.4 can be understood qualitatively looking at Eq. (5.13). For degenerate extra generations the corrections ΔV_i are negative. They become

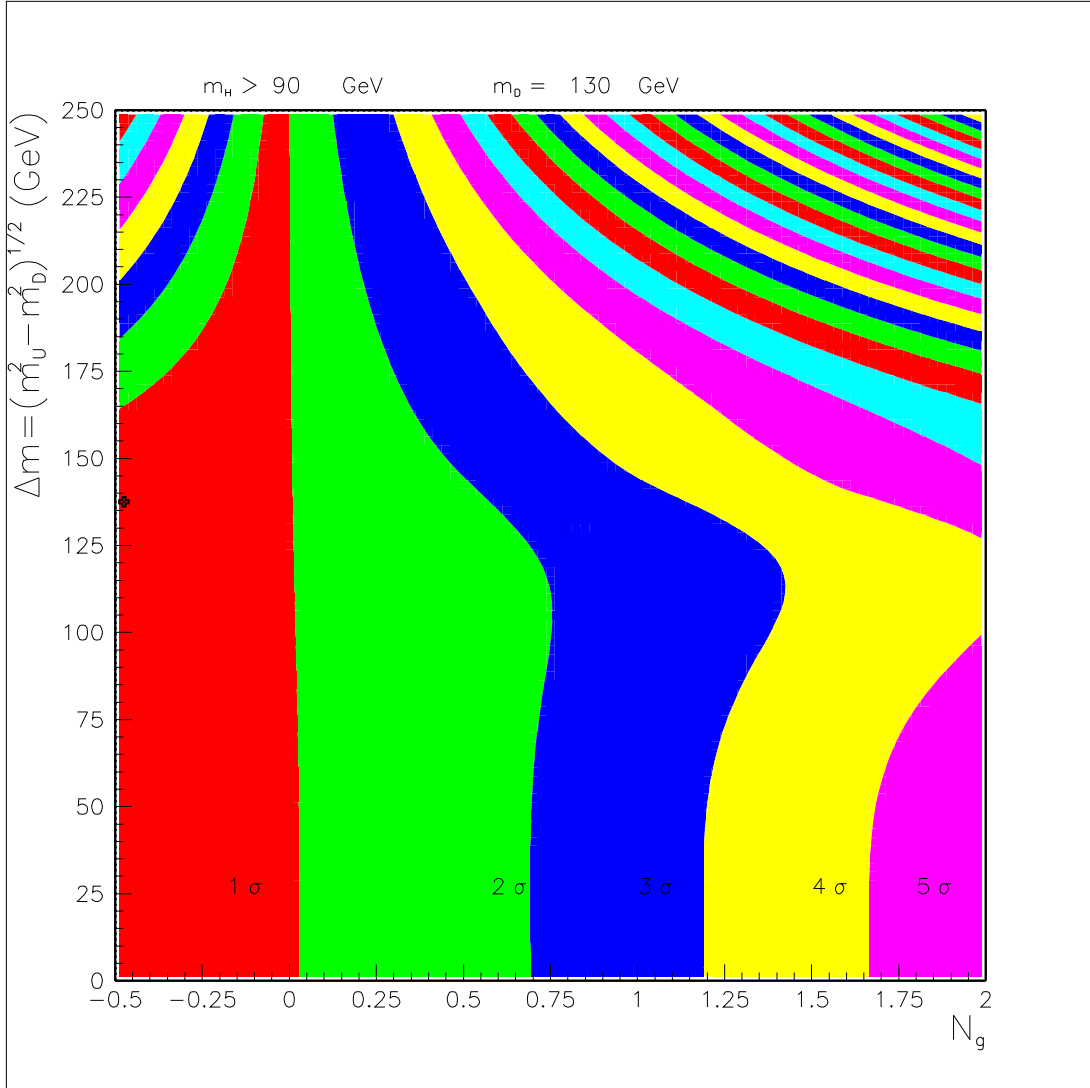


Figure 5.4: Constraints on the number of extra generations N_g and the mass difference Δm in the horizontally degenerate case: $(m_N = m_U) > (m_E = m_D = 130 \text{ GeV})$. The lower bound $m_{U,D} > 130 \text{ GeV}$ comes from Tevatron search [52]. All electroweak precision data and $m_H > 90 \text{ GeV}$ at 95% C.L. [53] were used in the fit. The cross corresponds to χ^2 minimum; regions show $< 1\sigma$, $< 2\sigma$, etc. allowed domains.

positive and large when Δm increases: this is why at large Δm division lines approach $N_g = 0$ value. In the intermediate region ($\Delta m \approx 125 \text{ GeV}$) ΔV_i cross zero and this explains the turn to the right of the division lines. However, for different i zero is reached for different Δm values, that is why extra generations are excluded even for $\Delta m \approx 125 \text{ GeV}$ (see Ref. [50]).

At this point, we have to check whether similar bounds are valid for the general choice of heavy fermion masses or they are peculiar to the special case shown in Fig. 5.4. To see this, one should perform a general scan of the whole 4-dimensional parameter space (m_N, m_E, m_U, m_D) , integrating out fermion masses and looking at the overall χ^2 . However, to do this accurately with LEPTOP, taking properly into account effects of changing m_t , m_H and other SM parameters, one would require a huge amount of computer time, so this way is precluded.

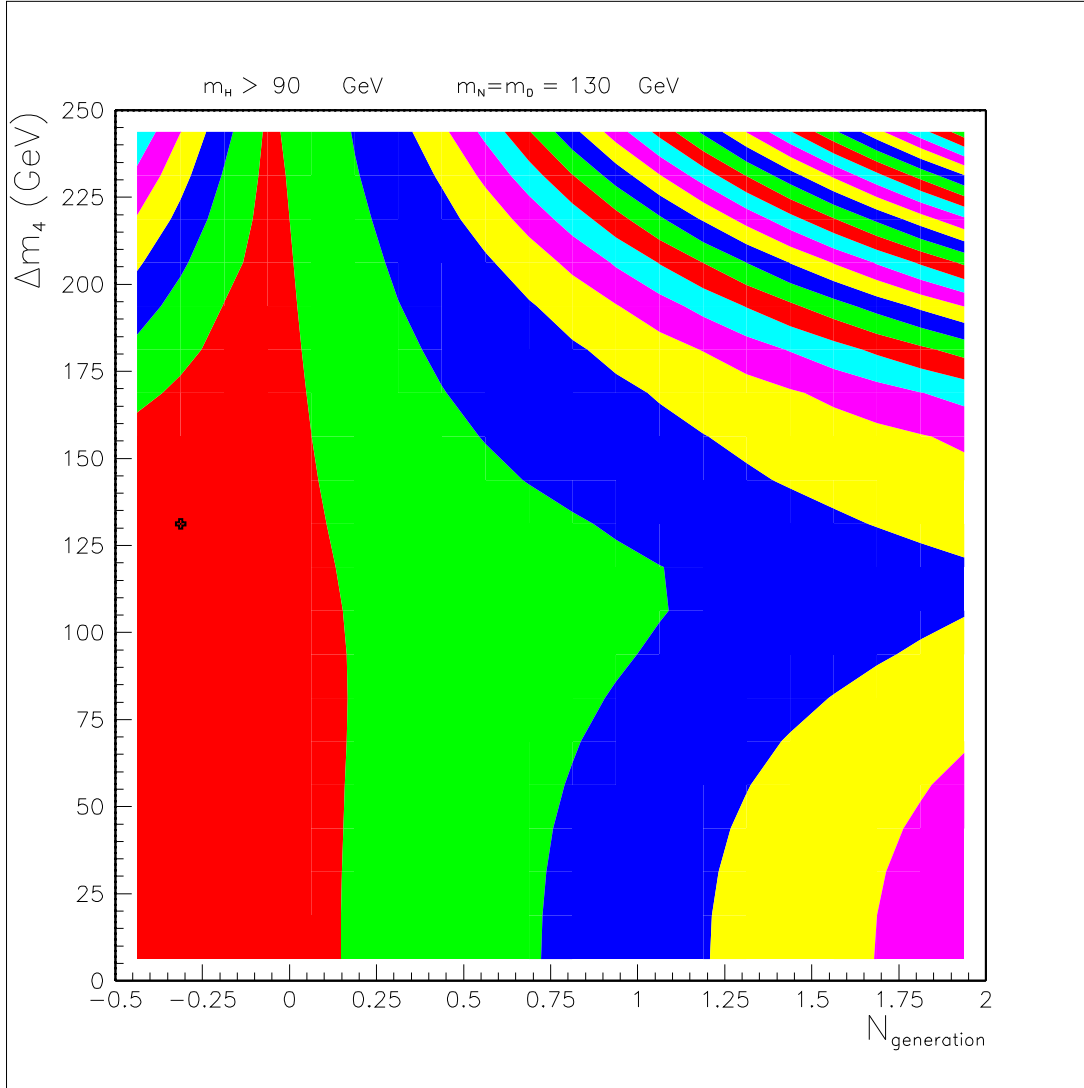


Figure 5.5: Constraints on the number of extra generations N_g and the mass difference Δm in the cross degenerate case: $(m_E = m_U) > (m_N = m_D = 130 \text{ GeV})$. The lower bound $m_{U,D} > 130 \text{ GeV}$ comes from Tevatron search [52]. All electroweak precision data and $m_H > 90 \text{ GeV}$ at 95% C.L. [53] were used in the fit. The cross corresponds to χ^2 minimum; regions show $< 1\sigma$, $< 2\sigma$, etc. allowed domains.

To overcome this problem, as a first step we analyzed two more cases which are somewhat complementary to Fig. 5.4: the “cross degenerate” case $(m_E = m_U) > (m_N = m_D = 130 \text{ GeV})$ and the “anti-cross degenerate” case $(m_N = m_D) > (m_E = m_U = 130 \text{ GeV})$. Results are shown in Figs. 5.5 and 5.6, respectively. It is immediate to see that, although in the cross degenerate case the χ^2 is slightly better than in the horizontally degenerate one and bounds on a fourth generation are consequently weaker, nevertheless the case of an extra heavy family is excluded almost at 2σ . On the other hand, the anti-cross degenerate case is strongly disfavored, and this shows that the mass hierarchy preferred by precision measurements for a new fermion generation is the same as in the third SM generation. The reason for this will be explained later.

As already stated, to go beyond these results one needs to perform a full scan of the whole

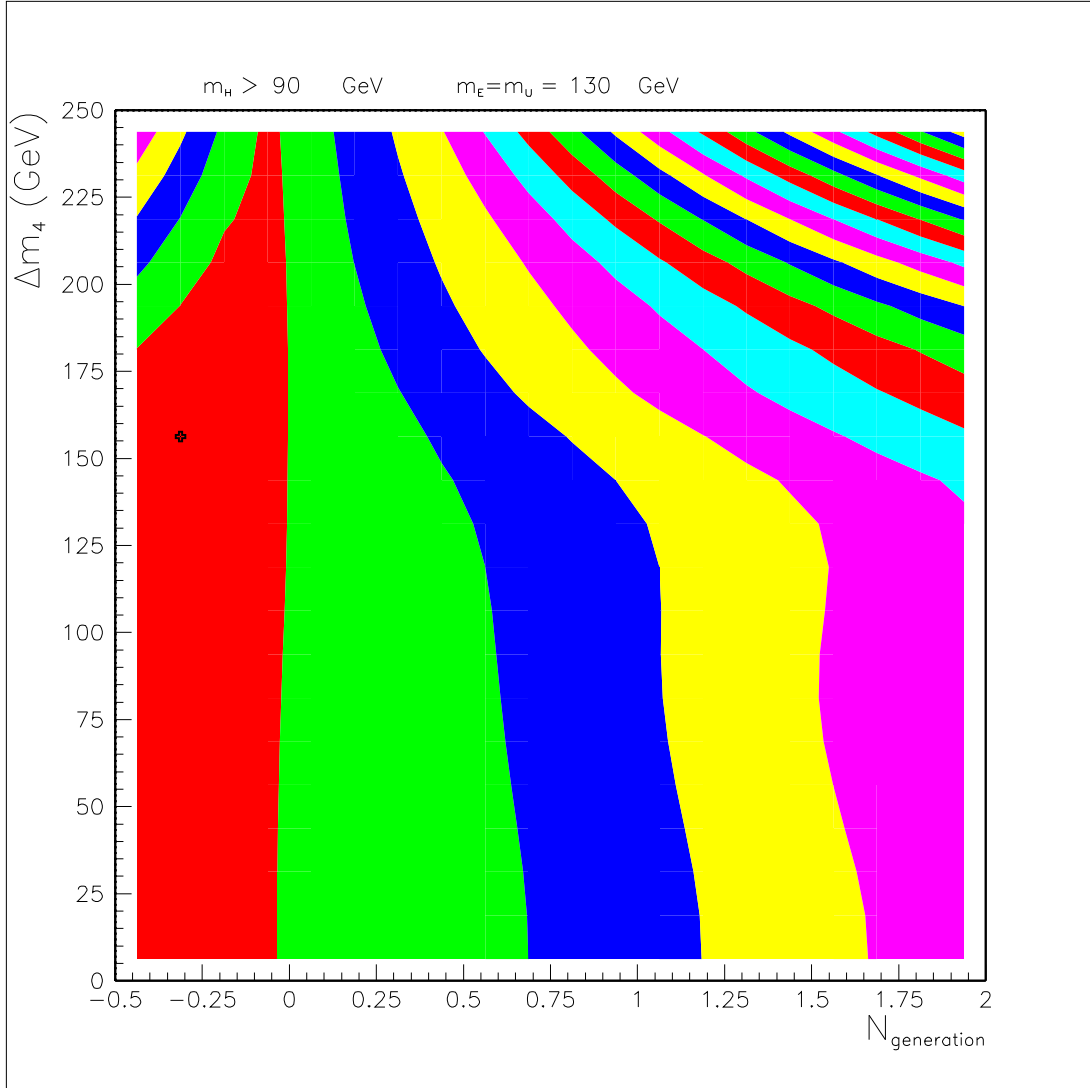


Figure 5.6: Constraints on the number of extra generations N_g and the mass difference Δm in the anti-cross degenerate case: $(m_N = m_D) > (m_E = m_U = 130 \text{ GeV})$. The lower bound $m_{U,D} > 130 \text{ GeV}$ comes from Tevatron search [52]. All electroweak precision data and $m_H > 90 \text{ GeV}$ at 95% C.L. [53] were used in the fit. The cross corresponds to χ^2 minimum; regions show $< 1\sigma$, $< 2\sigma$, etc. allowed domains.

4-dimensional parameter space. Although this is currently impossible with LEPTOP, it can be done easily if the χ^2 is evaluated by means of the approximate expression (4.35) introduced in the previous chapter (see Sec. 4.3). The results of this search are summarized in Fig. 5.7, which also includes effects of changing the top mass (but not the Higgs mass or other SM parameters). On the x -axis we have the number of new generations, as usual, while on the y -axis we report the lower bound m_{inf} imposed on the four extra fermion masses (for example: the point (1; 150) corresponds to the minimum value of χ^2 which can be obtained for the case of 1 extra generation when all fermion masses are heavier than 150 GeV). To compare this figure with the previous ones, we should look at the horizontal line $m_{\text{inf}} = 130 \text{ GeV}$ in Fig. 5.7 (since this is the constraint imposed on all m_f in Figs. 5.4-5.6) and extract a bound for the number of allowed extra generations. If we do this, we see that $N_g = 1$ is excluded almost at 2σ , just as

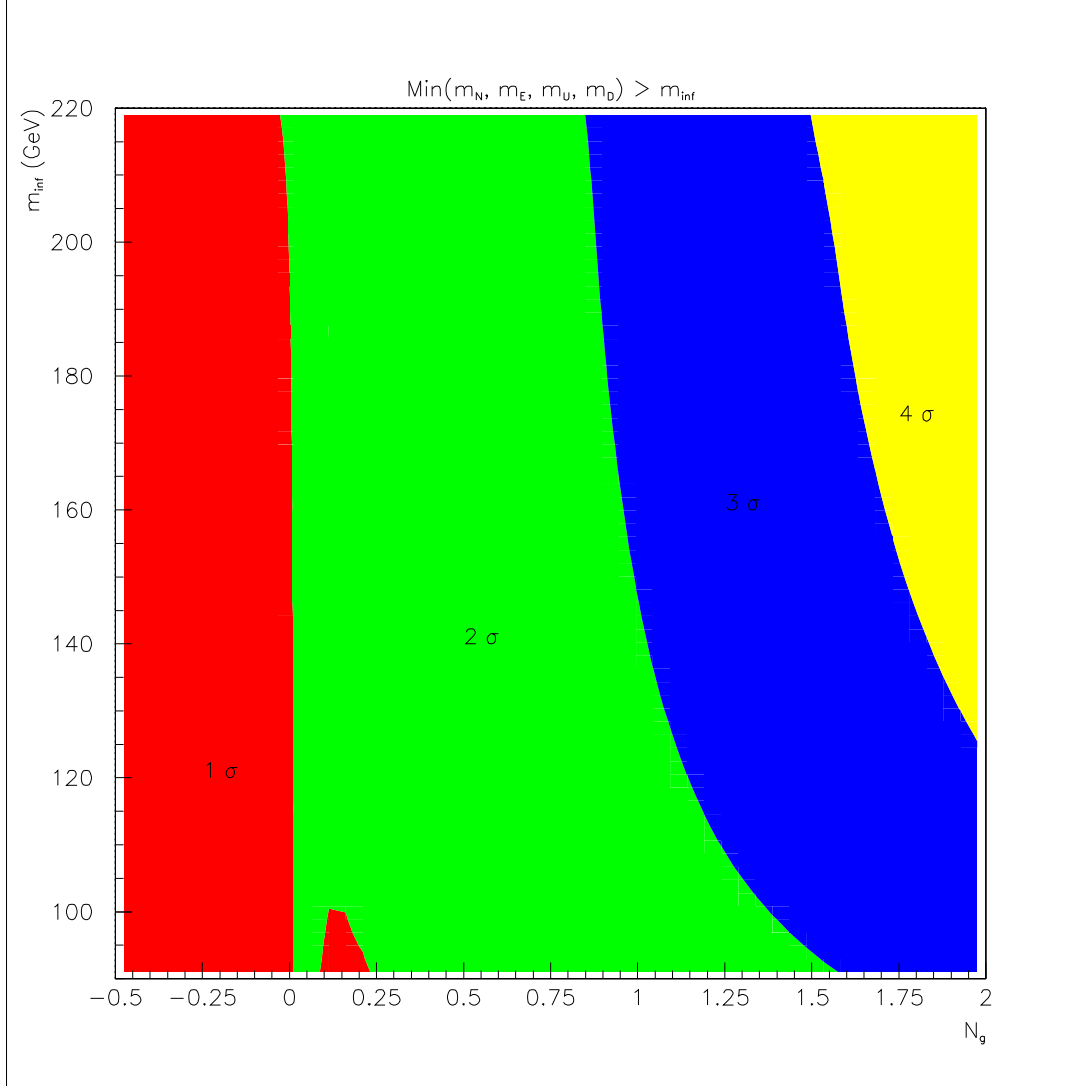


Figure 5.7: Constraints on the number of extra generations N_g (x -axis) as a function the lower bound on new fermion mass m_{inf} (y -axis). The χ^2 is evaluated using the approximate expression (4.35); the masses of the four extra fermions m_N , m_E , m_U , m_D and the top mass m_t are integrated out. For each point (N_g, m_{inf}) this plot shows the best value of the χ^2 which can be obtained having N_g extra generations and bounding all the new fermion masses to be heavier than m_{inf} .

it was in the cross degenerate case: this proves that leaving all the four fermion masses free to vary independently from one another does not help to improve the quality of the fit beyond the case of Fig. 5.5, and the general bound $m_f > 130$ GeV is enough to exclude the possibility of a fourth generation at 95% C.L.

Further considerations can be derived qualitatively by means of Eqs. (5.9-5.11). In the rest of this section we will use these equations to investigate the “best fit point” $(\bar{m}_N, \bar{m}_E, \bar{m}_U, \bar{m}_D)$, showing that many of its properties can be understood analytically. This is useful to get an idea of how much the results found in the special cases shown in Figs. 5.4-5.6 are representative of the general choice of extra fermion masses.

Using values from (5.1), Eqs. (5.9-5.11) can be rewritten in the following way:

$$\delta m_l = m_E - m_N, \quad (5.17)$$

$$\delta m_q = m_U - m_D, \quad (5.18)$$

$$x = \frac{1}{2} \left[\ln \left(1 + \frac{\delta m_l}{m_N} \right) + \ln \left(1 + \frac{\delta m_q}{m_D} \right) \right], \quad (5.19)$$

$$y = \frac{4}{9} \left[\left(\frac{\delta m_l}{m_Z} \right)^2 + 3 \left(\frac{\delta m_q}{m_Z} \right)^2 \right], \quad (5.20)$$

$$\left. \begin{aligned} \Delta'' V_m &= -\frac{16}{9} s^2 \\ \Delta'' V_A &= 0 \\ \Delta'' V_R &= -\frac{8}{9} \end{aligned} \right\} (1-x) + y. \quad (5.21)$$

We can now insert Eq. (5.21) into (4.35) and use Eq. (4.34) to find the “best values” \bar{x} and \bar{y} :

$$\bar{x} \approx 1 + \frac{0.344}{N_g}, \quad \bar{y} \approx -\frac{0.289}{N_g}. \quad (5.22)$$

Of course, we are interested only in the region $N_g > 0$. The first thing to note is that \bar{x} is always positive. This means (see Eq. (5.19)) that *positive* values for δm_l and δm_q are preferred, i.e. the overall χ^2 is better when the mass hierarchy within each extra doublet is $m_E > m_N$ and $m_U > m_D$. This is just what we have in the second and third SM generation, and is in perfect agreement with Figs. 5.4-5.6, where we already noted that the cross degenerate case gives the best fit while the anti-cross degenerate gives the worst.

Another relevant fact is that \bar{y} is always negative. Looking at Eq. (5.20), it is clear that this condition can never be realized: as a consequence, the best fit point (5.22) is physically unreachable, and we can expect in general a rather poor χ^2 . Also, since the quality of the fit is worsened by a large positive value of y , from Eq. (5.19) we learn that χ^2 is better when x is “less suppressed”, because in this way it is simpler to have x large keeping y small. So we conclude that the best fit point always has m_N and m_D as small as possible. This has a straightforward consequence: as soon as direct search from accelerator experiments will raise the lower bound on extra fermion masses, the case of a fourth generation will be even strongerly excluded by precision measurements. This is clearly visible in Fig. 5.7, where the contour lines strictly approach $N_g = 0$ when m_{inf} increases.

The last interesting property of the best fit point $(\delta \bar{m}_l, \delta \bar{m}_q)$ that we can extract from Eq. (5.21) is more quantitative. Clearly, for any given m_N and m_D the first derivative of χ^2 with respect to $\delta \bar{m}_l$ and $\delta \bar{m}_q$ must be zero - just by definition of “best fit”. On the other hand, δm_l and δm_q enter $\Delta'' V_i$ (and thus χ^2) *only* through x and y , and we know that the only point (5.22) where χ^2 is stable under *independent* variation of x and y is physically unreachable. Therefore, the condition $\delta \chi^2 = 0$ can only be realized *if* the Jacobian determinant of the transformation $(\delta m_l, \delta m_q) \rightarrow (x, y)$ is zero:

$$\left| \frac{\partial(x, y)}{\partial(\delta m_l, \delta m_q)} \right| = \left| \begin{array}{cc} \frac{1}{2m_E} & \frac{1}{2m_U} \\ \frac{8}{9} \frac{\delta m_l}{m_Z^2} & \frac{8}{3} \frac{\delta m_q}{m_Z^2} \end{array} \right| = 0. \quad (5.23)$$

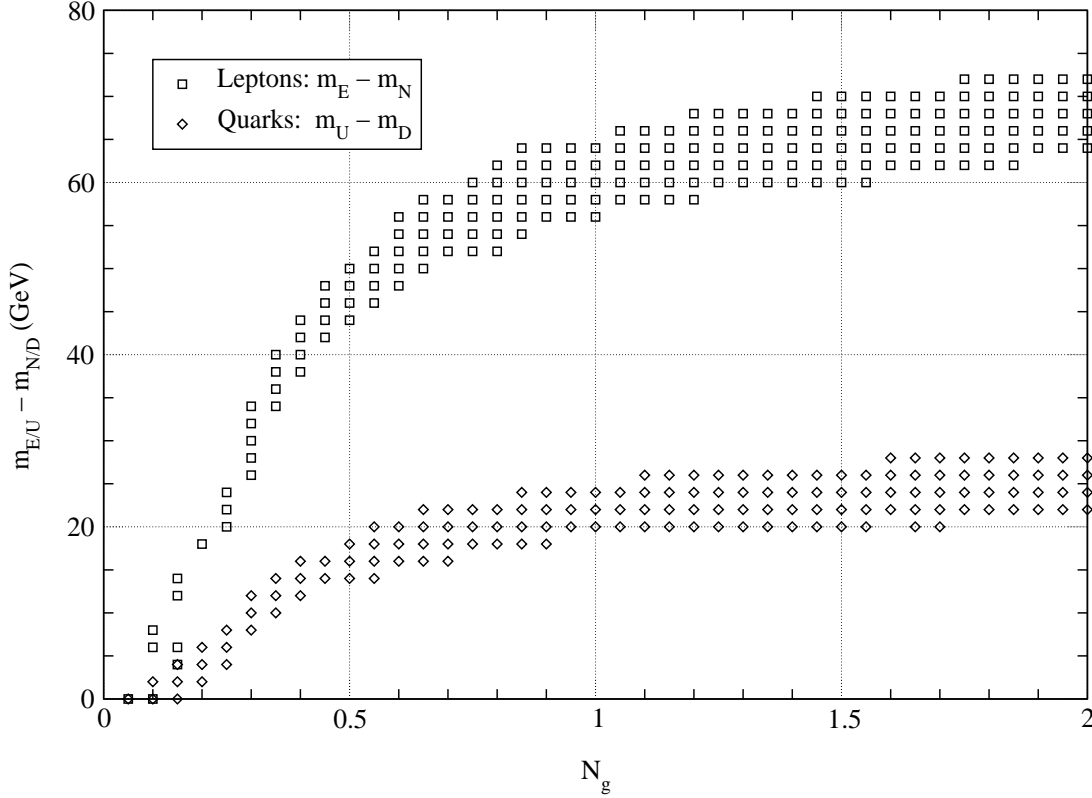


Figure 5.8: Lepton and quark mass splitting $\delta\bar{m}_l$ and $\delta\bar{m}_q$ for the best fit point, as a function of the number of extra generations N_g , for different values of the common mass $m_N = m_D = m_{\text{inf}}$. This figure is derived from the same data used to generate Fig. 5.7; in particular, the χ^2 is evaluated using the approximate expression (4.35).

After some simple calculation, this gives:

$$\delta\bar{m}_l = 3 \frac{\bar{m}_U}{\bar{m}_E} \delta\bar{m}_q. \quad (5.24)$$

If the masses of all the extra fermions are comparable in size, then the factor \bar{m}_U/\bar{m}_E can be neglected and from Eq. 5.24 we get that the lepton mass splitting is approximately three times larger than the quark one. This fact can be immediately verified by looking at Fig. 5.8, where we plot the mass differences δm_l and δm_q as a function of the number of extra generations N_g : it is straightforward to see that the relation $\delta\bar{m}_l \approx 3\delta\bar{m}_q$ is almost always satisfied, regardless of the number of new generations or of the different value of the common mass $m_N = m_D$.

Let us conclude this section summarizing the properties of the “best fit” $(\bar{m}_N, \bar{m}_E, \bar{m}_U, \bar{m}_D)$ that we found to hold in the heavy fermion limit:

- *electron* is always heavier than *neutrino*, and *up-quark* is always heavier than *down-quark*: $\bar{m}_E > \bar{m}_N$, $\bar{m}_U > \bar{m}_D$;
- *neutrino* and *down-quark* are as light as possible: $\bar{m}_N = m_N^{\text{min}}$, $\bar{m}_D = m_D^{\text{min}}$;
- the lepton mass splitting is approximately three times larger than the quark mass splitting: $(\bar{m}_E - \bar{m}_N) \approx 3(\bar{m}_U - \bar{m}_D)$.

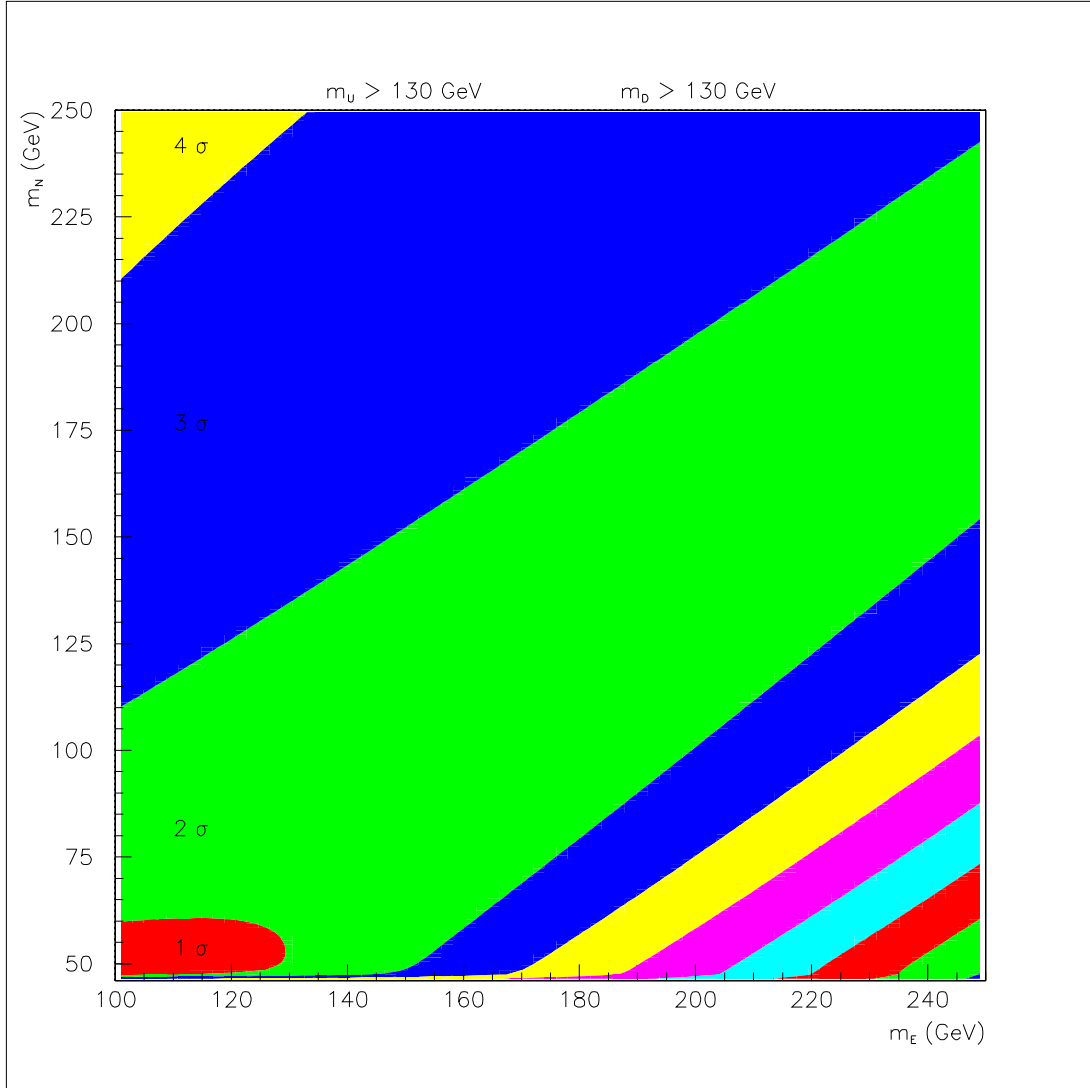


Figure 5.9: Constraints on the masses of the neutral heavy lepton m_N and the charged heavy lepton m_E . The χ^2 is evaluated using the approximate expression (4.35). The extra quark masses m_U and m_D and the top mass m_t are integrated out, and the Tevatron bound $m_q > 130$ GeV is assumed. Regions show $< 1\sigma$, $< 2\sigma$, etc. allowed domains.

5.3 Comparison with experimental data: $m_N < m_Z$

According to Ref. [52], the lower bound on m_E from LEP II is approximately 80 GeV. However, quasi-stable neutral lepton N can be considerably lighter. From LEP II searches of the decays $N \rightarrow lW^*$, where W^* is virtual while l is e , μ or τ , it follows that $m_N > 70 \div 80$ GeV if the mixing angle between N and the three known neutrinos is larger than 10^{-6} [54]. Thus let us take in this section this mixing to be less than 10^{-6} : in this case only DELPHI bound $m_N > 45$ GeV [45] from the measurement of the Z -boson width is applicable. If m_N is larger than $m_Z/2$, searches at LEP II of the reaction $e^+e^- \rightarrow N\bar{N}\gamma$ should bound m_N . The observation of a “lonely photon” was suggested long time ago as a method to study cross section of the e^+e^- annihilation into

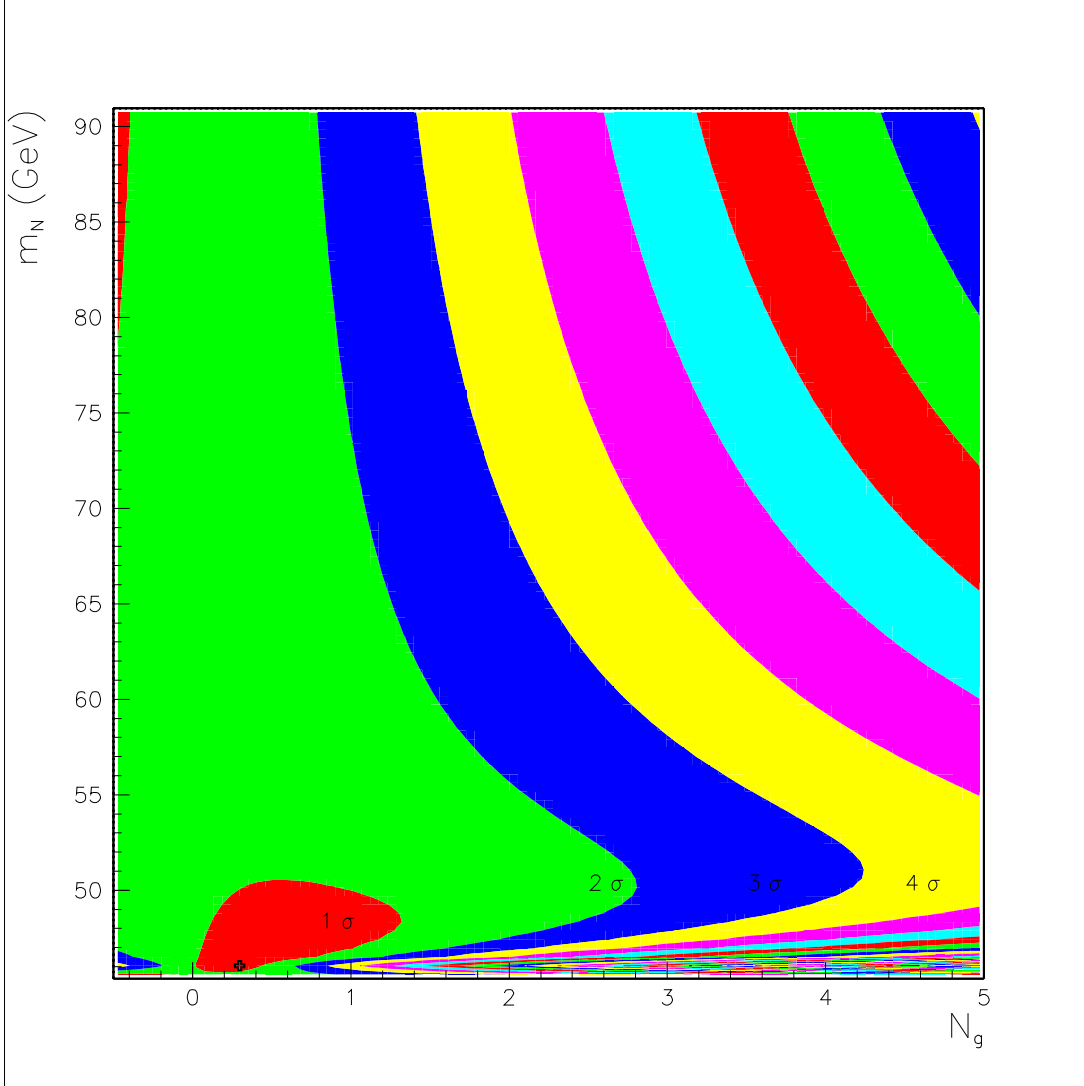


Figure 5.10: Constraints on the number of extra generations N_g and the mass of the neutral heavy lepton m_N . The values $m_E = 100$ GeV, $m_U = 220$ GeV, $m_D = 200$ GeV were used. All electroweak precision data and $m_H > 90$ GeV at 95% C.L. from LEP II [53] were used in the fit. The cross corresponds to χ^2 minimum; regions show $< 1\sigma$, $< 2\sigma$, etc. allowed domains.

neutrinos [55]. DELPHI collaboration performed such a search at $E \leq 183$ GeV and found that the total number of neutrinos is $N_\nu = 2.92 \pm 0.25(\text{stat}) \pm 0.14(\text{syst})$ [56]; however, most of the events correspond to the production of a *real* Z -boson in reaction $e^+e^- \rightarrow \gamma Z \rightarrow \gamma\nu\bar{\nu}$, so bounds of Ref. [56] are inapplicable to reaction $e^+e^- \rightarrow \gamma Z^* \rightarrow \gamma N\bar{N}$ for $m_N > m_Z/2$. Also, although the cross section for single photon production in e^+e^- annihilation at LEP II is big, it is saturated by t -channel diagrams, where ν_e are produced, so there is no chance to observe N production with reasonable statistics using the present data.

For particles with masses of the order of $m_Z/2$ oblique corrections drastically differ from what we have in the heavy fermion limit. In particular, renormalization of Z -boson wave function produces large negative contribution to V_A . From the analysis of the initial set of precision data

in Refs. [46, 47] (published in years 1994-1995) it was found that the existence of additional light fermions with masses around 50 GeV is allowed. Now analyzing all precision data and using bounds from direct searches we conclude that the *only* presently allowed light fermion is neutral lepton N . This is clearly visible in Fig. 5.9, where we show the 1σ , 2σ , etc. allowed domain as a function of m_N and m_E . This figure was generated using the approximate χ^2 given in Eq. (4.35), just as we did in the previous section, and m_U , m_D , m_t are correctly integrated out. It is immediate to see that the 1σ region include only a small area around $m_N = 45 \div 60$ GeV, $m_E = 100 \div 130$ GeV, and no other solutions are allowed by precision measurements.

As a further example, we take $m_U = 220$ GeV, $m_D = 200$ GeV, $m_E = 100$ GeV and draw the exclusion plot in coordinates (N_g, m_N) using the program LEPTOP. Results are shown in Fig. 5.10 and looking at it we can see that if the neutrino is light enough the description of the data is not worse than in the Standard Model: for $m_N \approx 50$ GeV even two new generations are allowed within 1.5σ .

5.4 The case of SUSY

In this section we investigate bounds on extra generations which occur in SUSY extensions. When SUSY particles are heavy they decouple (i.e. their contributions to electroweak observables become power suppressed) and the same Standard Model exclusion plots shown in Figs. 5.4-5.10 are valid. The present lower bounds on the sparticle masses from direct searches close most of the regions which may be interesting for radiative corrections, leaving available mainly only this decoupled domain. One possible exception is a contribution of the third generation squark doublet, enhanced by large stop-sbottom splitting: in this way we get noticeable positive contributions to functions V_i [37, 57], which may help to compensate negative contributions of degenerate extra generations.

We analyze the simplest case of the absence of $\tilde{t}_L - \tilde{t}_R$ mixing in Fig. 5.11. In this figure, extra fermions are assumed to be degenerate with common mass 130 GeV, and according to Ref. [37] the masses of the stop and sbottom are related by the MSSM formula:

$$\begin{aligned} m_{\tilde{t}_L}^2 - m_{\tilde{b}_L}^2 &= m_t^2 - m_b^2 + m_W^2 \cos 2\beta \\ &\approx m_t^2 \quad (\text{for } \tan \beta \approx 2). \end{aligned} \quad (5.25)$$

The exclusion plot presented in Fig. 5.11 is in coordinates $(N_g, m_{\tilde{b}})$: it is straightforward to see that also with inclusion of SUSY corrections new heavy generations are disfavored.

To understand why adding sfermions does not help to improve the quality of the fit, let us consider the case of horizontally degenerate heavy fermions. In this limit, the expressions for the ΔV_i corrections coming from an extra generation are well approximate by Eq. (5.13). Concerning sfermions contributions, according to Ref. [37] they are almost universal, and after some simple calculations we get the approximate relation:

$$\Delta'' V_i = \frac{4}{3} \left(\frac{m_{\tilde{t}} - m_{\tilde{b}}}{m_Z} \right)^2. \quad (5.26)$$

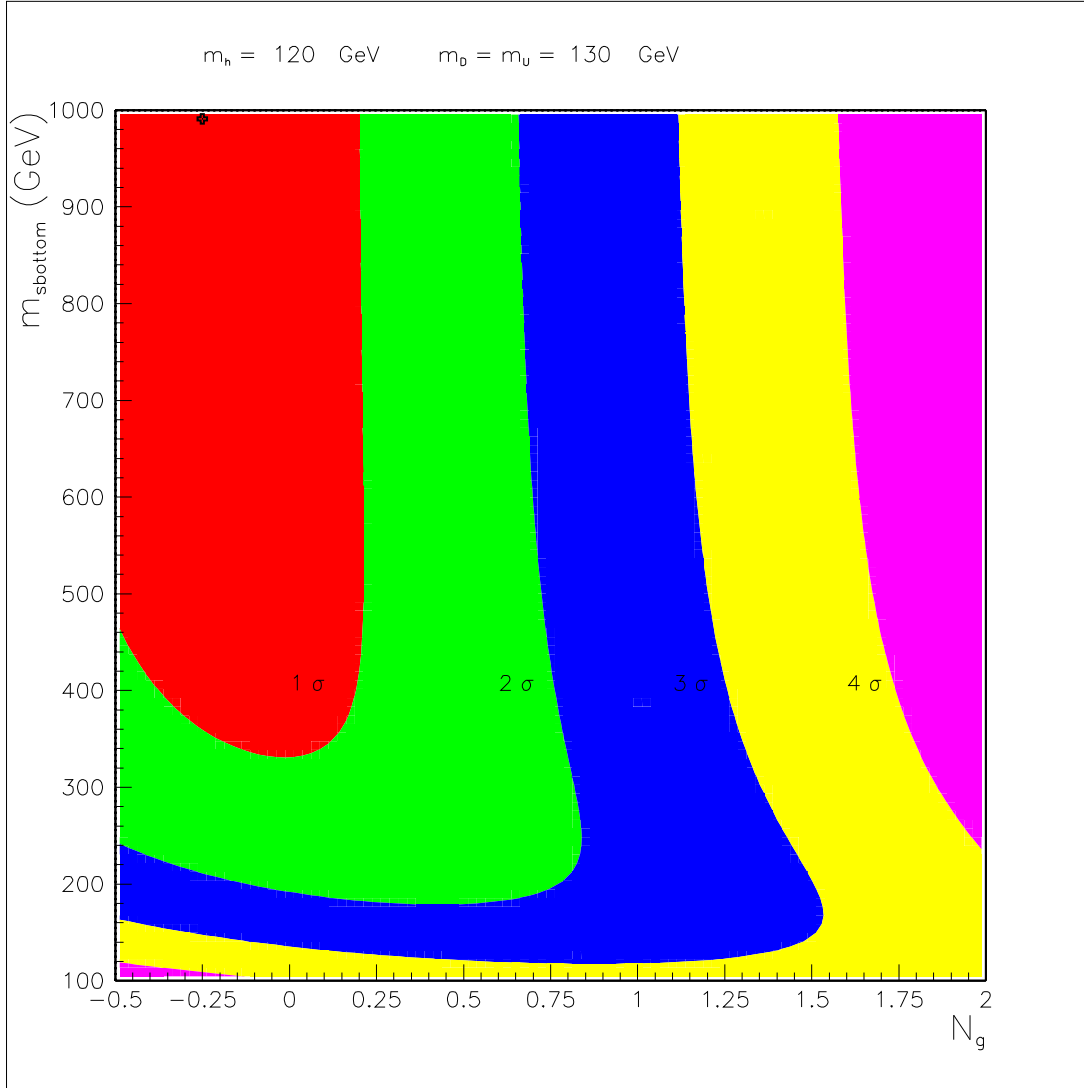


Figure 5.11: The 2-dimensional exclusion plot for the N_g degenerate extra generations and the mass of sbottom $m_{\tilde{b}}$ in SUSY models and for the choice $m_D = m_U = m_E = m_N = 130 \text{ GeV}$, using $m_H = 120 \text{ GeV}$, $m_{\tilde{g}} = 200 \text{ GeV}$ and assuming the absence of $\tilde{t}_L - \tilde{t}_R$ mixing. Little cross corresponds to χ^2 minimum; regions show $< 1\sigma$, $< 2\sigma$, etc. allowed domains.

Comparing this formula with Eq. (5.13), it is clear why the quality of the fit is unaffected: contributions of sfermions simply mimic those of non-degenerate extra fermions, and since the latter are excluded by precision measurements (as we discussed in detail in Sec. 5.2) also the former are.

The case of SUSY sfermions clearly proves that to change the fate of extra generations we must search for New Physics giving *non-universal* contributions. From Chapter 4, we know that a chargino almost degenerate with the lightest neutralino and close in mass to $m_Z/2$ induces a large negative correction into V_A , just as a 50 GeV neutrino does, so in this case we can expect a general improvement of the quality of the fit. To check whether this really happens, let us consider once more the case of horizontal degeneracy and make some numerical estimates.

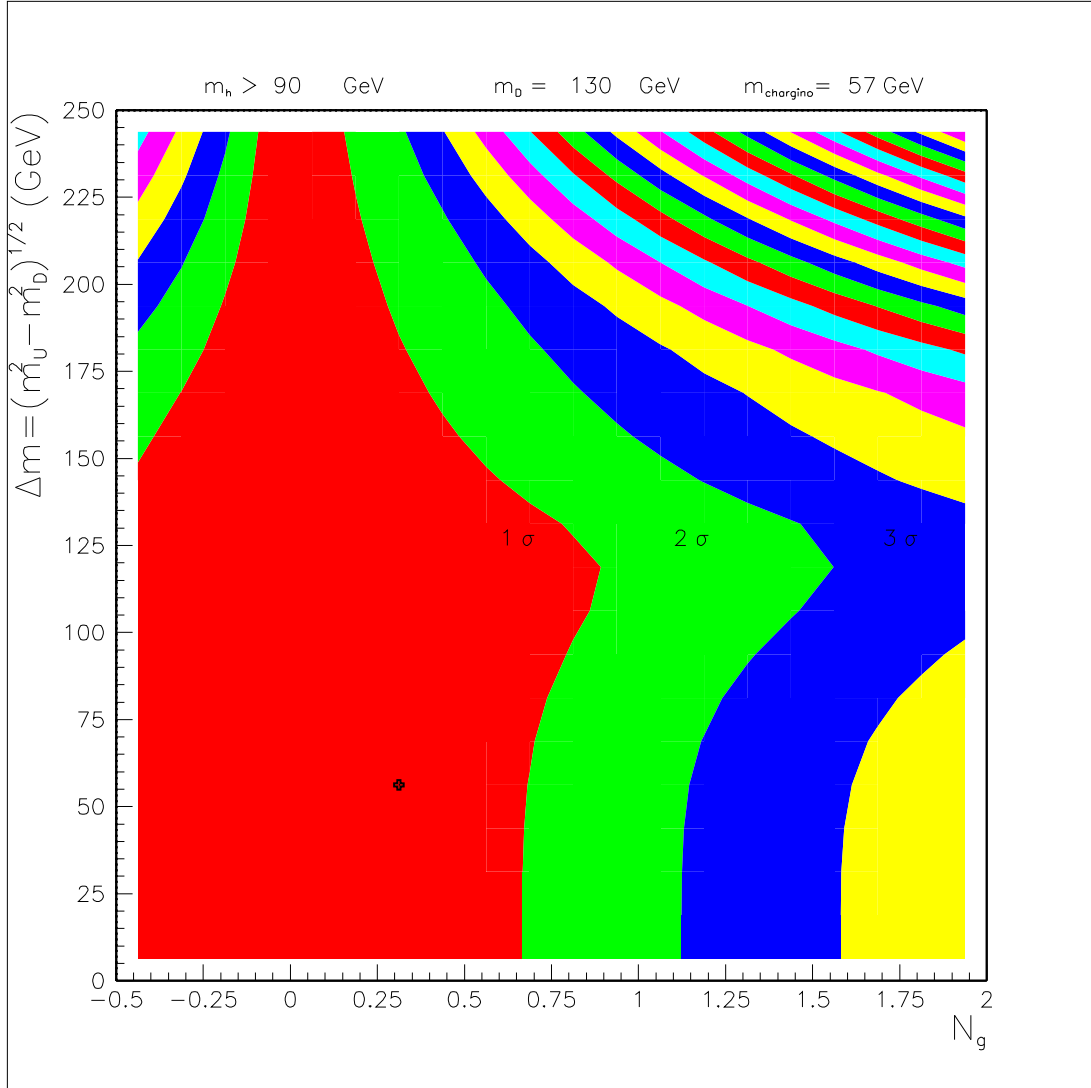


Figure 5.12: Constraints on the number of extra generations N_g and the mass difference in the extra generations Δm in case of 57 GeV higgsino-dominated quasi degenerate chargino and neutralino. The lowest allowed value $m_D = 130$ GeV from Tevatron search [52] was used and $m_E = m_D$, $m_N = m_U$ was assumed. All electroweak precision data and $m_H > 90$ GeV at 95% C.L. [53] were used in the fit. The cross corresponds to χ^2 minimum; regions show $< 1\sigma$, $< 2\sigma$, etc. allowed domains.

Subtracting the experimental values $\overline{\delta V_i}$ given in (4.34) from Eq. (5.13) we get:

$$\delta^{\text{th-exp}}[V_m, V_A, V_R] = [-0.340, +0.327, -0.894] + [y, y, y], \quad (5.27)$$

where y is defined in Eq. (5.20). Clearly, the overall χ^2 will be better when all the $\delta^{\text{th-exp}}V_i$ vanish. The main obstacle to this is the large splitting between negative $\delta^{\text{th-exp}}V_{m,R}$ and positive $\delta^{\text{th-exp}}V_A$: universal $SU(2)_V$ breaking contributions described by y cannot compensate it. Now let us include effects of almost degenerate chargino-neutralino and give some numerical example. In the higgsino-dominated case, for $m_{\tilde{\chi}} = 57$ GeV we have:

$$\delta^{\tilde{H}}[V_m, V_A, V_R] = [+0.185, -0.678, +0.237], \quad (5.28)$$

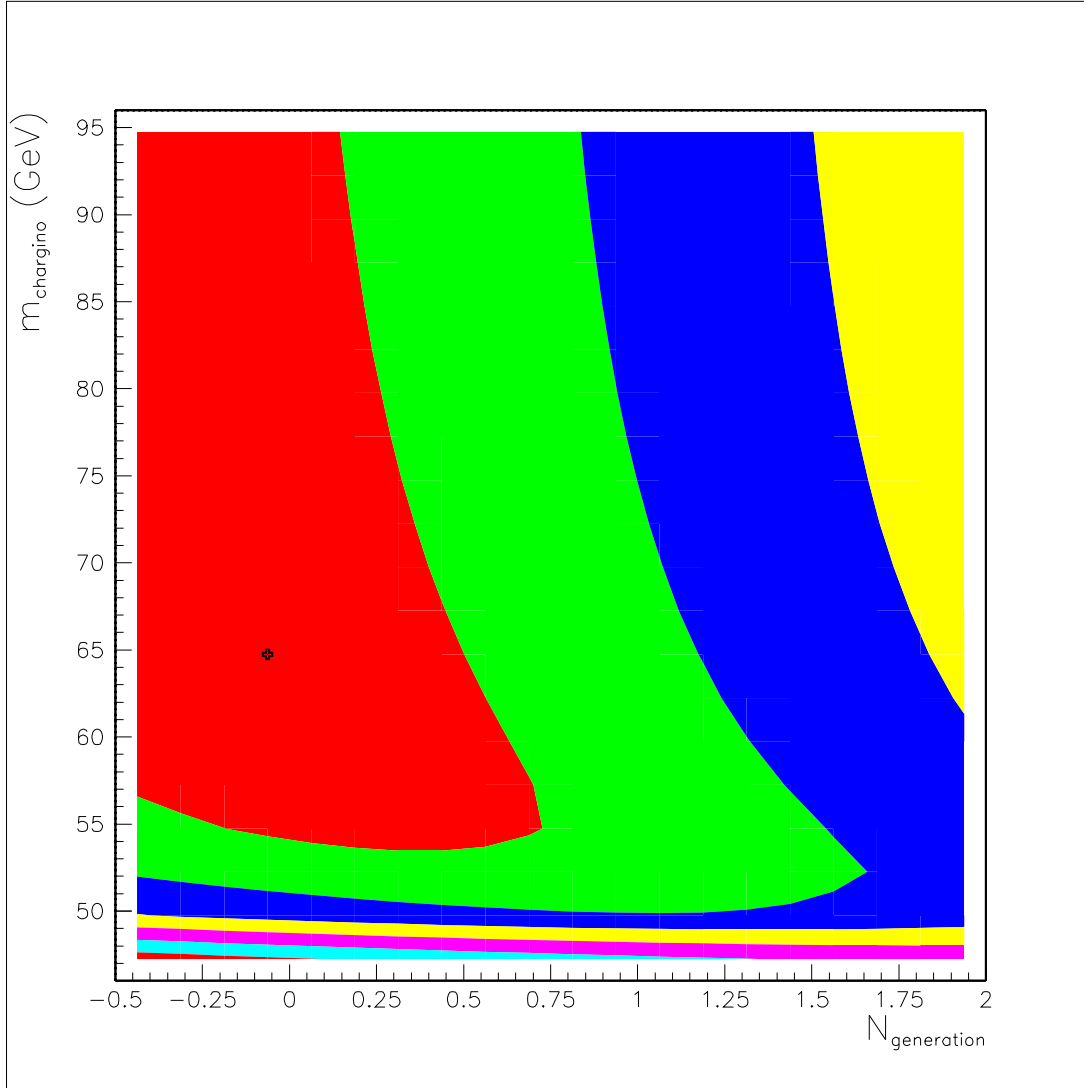


Figure 5.13: Constraints on the number of extra generations N_g and the gaugino mass $m_{\tilde{\chi}}$ in case of higgsino-dominated quasi degenerate chargino and neutralino. The lowest allowed value $m_D = 130$ GeV from Tevatron search [52] was used and $m_E = m_D$, $m_N = m_U \approx 180$ GeV ($\Delta m = 125$ GeV) was assumed. All electroweak precision data and $m_H > 90$ GeV at 95% C.L. [53] were used in the fit. The cross corresponds to χ^2 minimum; regions show $< 1\sigma$, $< 2\sigma$, etc. allowed domains.

while in the wino-dominated case with $m_{\tilde{\chi}} = 63$ GeV we find:

$$\delta^{\tilde{W}}[V_m, V_A, V_R] = [+0.209, -0.816, +0.177]. \quad (5.29)$$

Comparing these expressions with Eq. (5.27), we see that adding (5.28) or (5.29) to it partially compensates the large differences $\delta^{\text{th-exp}}(V_m - V_A)$ and $\delta^{\text{th-exp}}(V_R - V_A)$, so in both these cases the overall χ^2 will be smaller. Also, since we have $\delta^{\text{th-exp}}(V_m - V_R) > 0$, $\delta^{\tilde{H}}(V_m - V_R) < 0$ and $\delta^{\tilde{W}}(V_m - V_R) > 0$ (see also Figs. 4.2 and 4.3), we conclude that the quality of the fit will be slightly better in the higgsino-dominated case than in the wino-dominated case. This result is in agreement with Figs. 5.13 and 5.14.

Fig. 5.12 demonstrates how presence of chargino-neutralino pair (dominated by higgsino) with

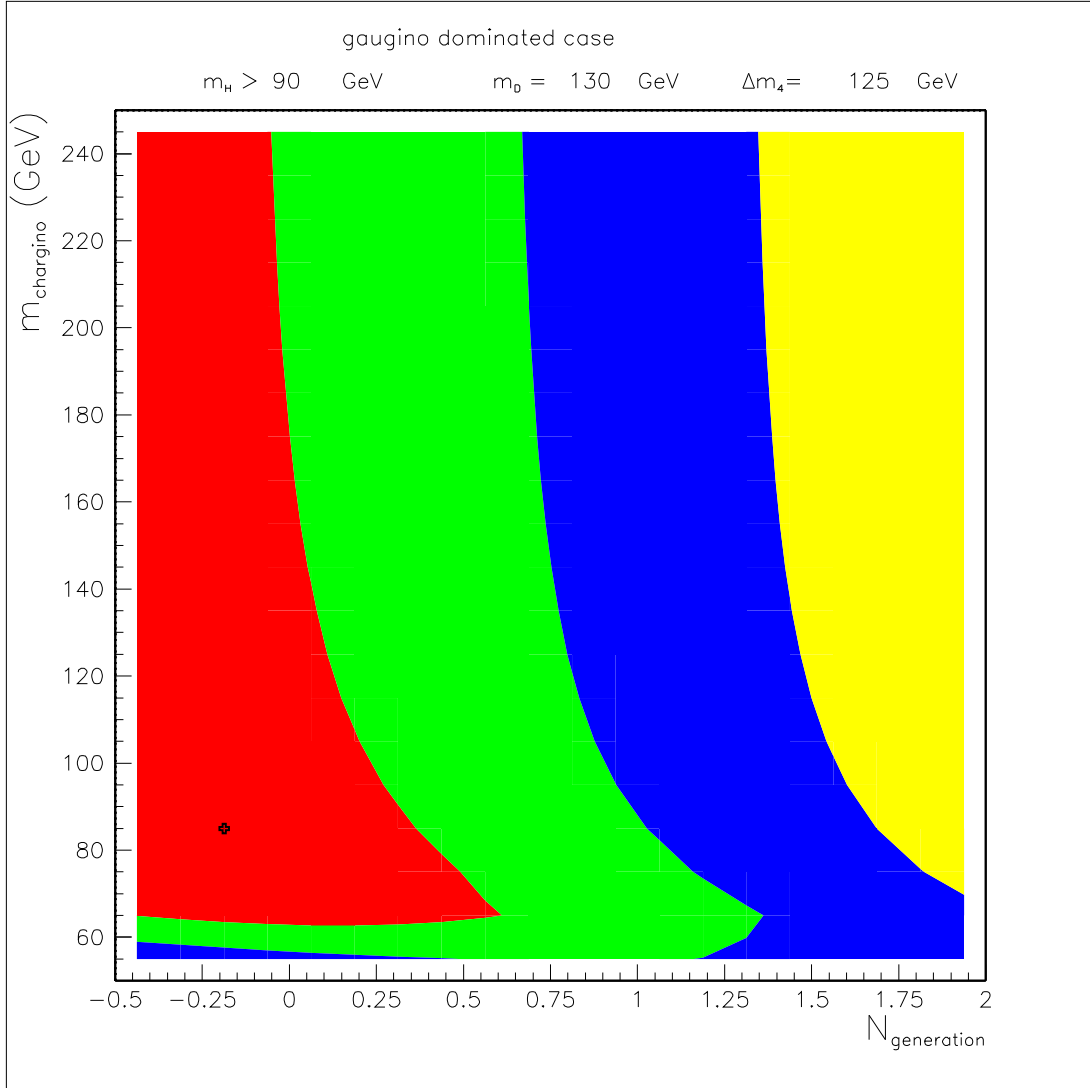


Figure 5.14: Constraints on the number of extra generations N_g and the gaugino mass $m_{\tilde{\chi}}$ in case of wino-dominated quasi degenerate chargino and neutralino. The lowest allowed value $m_D = 130$ GeV from Tevatron search [52] was used and $m_E = m_D$, $m_N = m_U \approx 180$ GeV ($\Delta m = 125$ GeV) was assumed. All electroweak precision data and $m_H > 90$ GeV at 95% C.L. [53] were used in the fit. The cross corresponds to χ^2 minimum; regions show $< 1\sigma$, $< 2\sigma$, etc. allowed domains.

mass 57 GeV relaxes the bounds shown on Fig. 5.4: we see that one extra generation of heavy fermions is now allowed within 1.5σ domain. Also, in Figs. 5.13 and 5.14 we draw the exclusion plots in coordinates $(N_g, m_{\tilde{\chi}})$ for both higgsino and wino domination, respectively: it is evident how precision measurements favor a light value of chargino-neutralino mass as soon as the number of extra generations increases.

5.5 Conclusions

As we saw in Sec. 5.3, inclusion of new generations in Standard Model is not excluded by precision data if new neutral leptons are rather light having mass of the order of 50 GeV (see Fig. 5.10). Mixing of new leptons with leptons from three known generations should be small, $\theta \lesssim 10^{-6}$, to avoid bounds from direct search at LEP II. We can not exclude stability of one of these new neutrinos; in this case it becomes interesting for cosmology. If the early universe was charge symmetric, annihilation of $N\bar{N}$ in primordial plasma bounds the present abundance Ω_N of these particles to be less than 10^{-3} (formula for heavy neutrino abundance in case $m_N \ll m_Z$ was obtained in [58]). If the early universe was charge asymmetric, the abundance of relic N 's is larger. However their contribution to mass density of the halo of our galaxy can not be larger than $0.01 \div 0.1$ - otherwise they would be already detected in laboratory searches for dark matter [59]. Even this small admixture of 50 GeV neutrino in the halo of our galaxy can help to explain gamma background through $N\bar{N}$ annihilation into e^+e^- with subsequent scattering of electrons and positrons on optical photons [60].

Concerning SUSY extensions: if masses of sparticles are of the order of several hundred GeV or larger their contribution to electroweak radiative corrections is negligible, hence the above statements remain valid. However in the case of quasi degenerate chargino and neutralino with masses about 60 GeV extra generations of heavy fermions appear to be less forbidden than without SUSY.

In order to experimentally investigate the case of $m_N < 50$ GeV a special post-LEP II run of LEP I' measuring the Z-line shape slightly above the Z-peak is needed. In this way the bound [45] will be improved. For $m_N > 50$ GeV search for the reaction $e^+e^- \rightarrow \gamma Z^* \rightarrow \gamma N\bar{N}$ with larger statistics than that of [56] and improved systematics is needed. Finally, further experimental search for light chargino and neutralino [61] is of interest. These searches could close the existing windows of "light" extra particles, or open a door into a realm of New Physics.

Conclusions

In this thesis, we considered effects of radiative corrections on electroweak precision measurements, using them to put bounds on New Physics parameters. Here we summarize the main results obtained:

- In Chapter 2 we investigated the origin of the numerical closeness among three different definitions of the electroweak mixing angle, finding that the degeneracy between \hat{s}^2 and s^2 , as well as that between s_l^2 and s^2 , occurs only for $m_t \sim 170$ GeV and therefore is merely accidental. Conversely, for the case of \hat{s}^2 and s_l^2 the dependence of their difference on the m_t is only logarithmic, so their closeness would have occurred even if the top quark mass would have been quite different from its actual value. Also, we provided an explicit and very simple relation between the phenomenological quantity s^2 and the $\overline{\text{MS}}$ parameter \hat{s}^2 .
- In Chapter 3 we discussed in detail how both the decoupling and the non-decoupling approach to the running of coupling constants in the $\overline{\text{MS}}$ scheme produce the same numerical value of m_{GUT} , despite of the different initial conditions. The concept of threshold was introduced and used, and the dependence of $\hat{\alpha}_s$ on the SM parameters $\hat{\alpha}$, \hat{s}^2 and \hat{m}_t and the MSSM quantities m_{SUSY} and $\tan\beta$ was studied. Combining the results obtained in this chapter with analysis of \hat{s}^2 carried out in the previous chapter it is straightforward to evaluate the impact of the numerical value of the physical observables $\bar{\alpha}$, s^2 and m_t on the prediction of $\hat{\alpha}_s$ from the demand of SUSY Grand Unification.
- In Chapter 4 we analyzed in detail the effects of radiative corrections for the case of a chargino almost degenerate with the lightest neutralino on electroweak precision measurements. Both the higgsino-dominated and the wino-dominated scenario were studied, and for these limits simple analytical formulae were derived. For the case of wino domination, our bound $m_{\tilde{\chi}} \gtrsim 56$ GeV is presently the strongest constraint which can be imposed without making any assumption on the mass spectrum of other superpartners.
- In Chapter 5 we investigated the effects of new fermion generations on precision measurements, showing that even 1 extra generation with all particles heavier than Z boson is strongly disfavored by present experimental data. However, for the specific case of the extra neutrino around 50 GeV in mass, the situation changes and the quality of the fit is not worse than the SM. Concerning SUSY extensions, contributions of sfermions do not affect bounds on extra generations, while for the case of almost degenerate chargino/neutralino these bounds are relaxed.

The results discussed in this thesis are presented in the published papers [1, 2, 3] and in Ref. [4], currently submitted for publication on PLB. Also, results quoted in Chapters 4 and 5 were presented at the conference PASCOS99, and will appear in the proceedings [5, 6].

Acknowledgments

It is a pleasure for me to express my gratitude to Mikhail Vysotsky for introducing me in the field of Particle Physics and Phenomenology, for his continuous support during my Ph.D. activity and for his friendship.

I am also grateful to Victor Novikov, Lev Okun and Alexander Rozanov, together with whom the work presented in Chapter 5 was developed, for their kindness and constant availability, and to Giovanni Fiorentini for always supporting me during the last three years.

A special thanks to all the researchers of the theoretical group of Ferrara University and of the 'Istituto TeSRE' of Bologna for their friendship and kindness, and to my family and friends for their constant patience and encouragement.

Finally, I am grateful to Lidia for leading me to look at things from a different point of view.

Appendix A

The V_i functions

In this appendix we give formulas for the V_i functions in terms of gauge boson self-energies, vertex and box diagrams. We only summarize the final results, addressing the reader to Ref. [22] for a more complete discussion.

The expression for V_m can be obtained comparing Eq. 1.56 with 2.28:

$$V_m = \frac{16\pi s^4}{3\bar{\alpha}} \left[\frac{c^2}{s^2} \Pi_Z(m_Z^2) + \left(1 - \frac{c^2}{s^2} \right) \Pi_W(m_W^2) - \Pi_W(0) - \Pi_\gamma(m_Z^2) - 2\frac{s}{c} \Pi_{\gamma Z}(0) - \delta\alpha_{t,W} - D \right]. \quad (\text{A.1})$$

The function V_A is given in Eq. (77) of Ref. [22]:

$$V_A = \frac{16\pi c^2 s^2}{3\bar{\alpha}} \left[\Pi_Z(m_Z^2) - \Pi_W(0) - \Sigma'_Z(m_Z^2) - D - 8cs F_A^{Ze} \right], \quad (\text{A.2})$$

where $\Sigma'_Z(m_Z^2)$ comes from Z -boson wave-function renormalization and F_A^{Ze} is the axial part of the Zll vertex (see Sec. 2.1.4).

The function V_R can be derived comparing Eqs. 1.58, 2.12 and 2.34:

$$V_R = \frac{16\pi c^2 s^2}{3\bar{\alpha}} \left[-\frac{c^2 - s^2}{cs} \left[F_V^{Ze} - (1 - 4s^2) F_A^{Ze} + \Pi_{\gamma Z}(m_Z^2) \right] - \Pi_\gamma(m_Z^2) + \Pi_Z(m_Z^2) - \Pi_W(0) - 2\frac{s}{c} \Pi_{\gamma Z}(0) - \delta\alpha_{t,W} - D \right], \quad (\text{A.3})$$

where F_V^{Ze} is the vector part of the Zll vertex (see Sec. 2.1.4).

These functions were introduced in Ref. [22] to study the dependence of precision measurements on the top and higgs masses, and the overall numerical coefficients were chosen in such a way that the leading top contribution into V_i is simply $(m_t/m_Z)^2$. However, since extra particles which occur in many extensions of the SM (like for example the MSSM) participate to V_i through radiative corrections, these functions can also be used as a convenient parameterization of New Physics. In this case, it is more practical to write $V_i = V_i^{\text{SM}} + \delta^{\text{NP}} V_i$ (see also Sec. 4.3), since in general the expressions for the $\delta^{\text{NP}} V_i$ are simpler than Eqs. (A.1-A.3). In particular:

- vertex and box contributions can usually be neglected;
- the combination $\Pi_\gamma(m_Z^2) + \delta\alpha_{t,W}$ simply reduces to $\Sigma'_\gamma(0)$;
- $\Pi_{\gamma Z}(0)$ gets contributions only from the gauge sector of the SM, so it vanishes when considering effects of New Physics (at least for what concerns the MSSM and extra generations, the two cases we are interested in).

Therefore, we have:

$$\delta^{\text{NP}}V_m = \frac{16\pi c^2 s^2}{3\bar{\alpha}} \left[\Pi_Z(m_Z^2) - \left(1 - \frac{s^2}{c^2}\right) \Pi_W(m_W^2) - \frac{s^2}{c^2} \Pi_W(0) - \frac{s^2}{c^2} \Sigma'_\gamma(0) \right]_{\text{NP}}, \quad (\text{A.4})$$

$$\delta^{\text{NP}}V_A = \frac{16\pi c^2 s^2}{3\bar{\alpha}} \left[\Pi_Z(m_Z^2) - \Pi_W(0) - \Sigma'_Z(m_Z^2) \right]_{\text{NP}}, \quad (\text{A.5})$$

$$\delta^{\text{NP}}V_R = \frac{16\pi c^2 s^2}{3\bar{\alpha}} \left[\Pi_Z(m_Z^2) - \Pi_W(0) - \Sigma'_\gamma(0) - \frac{c^2 - s^2}{c s} \Pi_{\gamma Z}(m_Z^2) \right]_{\text{NP}}. \quad (\text{A.6})$$

It is also useful to give here explicit formulas relating the $\delta^{\text{NP}}V_i$ functions to the S , T , U parameters introduced by Peskin and Takeuchi [51]:

$$S = \frac{3}{4\pi} (\delta^{\text{NP}}V_A - \delta^{\text{NP}}V_R), \quad (\text{A.7})$$

$$T = \frac{3}{16\pi c^2 s^2} \delta^{\text{NP}}V_A, \quad (\text{A.8})$$

$$U = -\frac{3}{4\pi(c_2 - s^2)} \left[(\delta^{\text{NP}}V_A - \delta^{\text{NP}}V_m) - 2s^2 (\delta^{\text{NP}}V_A - \delta^{\text{NP}}V_R) \right]. \quad (\text{A.9})$$

Let us conclude defining some functions which are widely used in Chapters 4 and 5:

$$F(m_W^2, m_U^2, m_D^2) = -1 + \frac{m_U^2 + m_D^2}{m_U^2 - m_D^2} \ln \left(\frac{m_U}{m_D} \right) - \int_0^1 \ln \frac{t^2 m_W^2 - t(m_W^2 + m_U^2 - m_D^2) + m_U^2}{m_U m_D} dt, \quad (\text{A.10})$$

$$F(x) \equiv F(m_Z^2, m_Z^2 x, m_Z^2 x) = \begin{cases} 2 \left[1 - \sqrt{4x-1} \arcsin \left(\frac{1}{\sqrt{4x}} \right) \right] & x > \frac{1}{4}, \\ 2 \left[1 - \sqrt{1-4x} \ln \left(\frac{1+\sqrt{1-4x}}{\sqrt{4x}} \right) \right] & x < \frac{1}{4}, \end{cases} \quad (\text{A.11})$$

$$F'(x) \equiv -x \frac{d}{dx} F(x) = \frac{1 - 2xF(x)}{4x - 1}. \quad (\text{A.12})$$

The following relation is useful in deriving Eqs. (5.3-5.5):

$$\int_0^1 (t^2 - t) \ln(t^2 - t + x) dt = \frac{1 + 2x}{6} F(x) - \frac{1}{18} - \frac{1}{6} \ln x. \quad (\text{A.13})$$

Bibliography

- [1] M. Maltoni, M.I. Vysotsky, *Mod. Phys. Lett.* **A13** (1998) 3099.
- [2] M. Maltoni, in *Proceedings of the XXVII ITEP Winter School of Physics*, in press.
- [3] M. Maltoni, M.I. Vysotsky, *Phys. Lett.* **B463** (1999) 230.
- [4] M. Maltoni, V.A. Novikov, L.B. Okun, A.N. Rozanov, M.I. Vysotsky, *hep-ph/9911535*, submitted to PLB.
- [5] M. Maltoni, Diminishing “charginos nearly degenerate with the lightest neutralino” slit using precision data, talk presented at the conference *PASCOS99* (Granlibakken, Lake Tahoe, California, 10-16 December 1999), to appear in the proceedings.
- [6] M. Maltoni, Extra quark-lepton generations and precision measurements, talk presented at the conference *PASCOS99* (Granlibakken, Lake Tahoe, California, 10-16 December 1999), to appear in the proceedings.
- [7] C. Burigana, M. Malaspina, N. Mandolesi, L. Danese, D. Maino, M. Bersanelli, M. Maltoni, Internal Report *ITeSRE 198/1997*, *astro-ph/9906360*.
- [8] D. Maino, C. Burigana, M. Maltoni, B. D. Wandelt, K. M. Görski, M. Malaspina, M. Bersanelli, N. Mandolesi, A. J. Banday, E. Hivon, *Astronomy and Astrophysics Supplement Series*, in press, *astro-ph/9906010*.
- [9] M. Maltoni, M. I. Vysotsky, *Yad. Fiz.* **62** (1999) 1278, *Phys. Atom. Nucl.* **62** (1999) 1203, *hep-ph/9804464*.
- [10] S.L. Glashow, *Nucl. Phys* **22** (1961) 579;
S. Weinberg, *Phys. Rev. Lett.* **19** (1967) 1264;
A. Salam, in *Proceedings of the 8th Nobel Symposium*, Ed. N. Svartholm (Almqvist and Wiksells, Stockholm, 1968), pag. 367.
- [11] N. Cabibbo, *Phys. Rev. Lett.* **10** (1963) 531;
S.L. Glashow, I. Iliopoulos, M. Maiani, *Phys. Rev.* **D2** (1970) 1285;
M. Kobayashi, K. Maskawa, *Prog. Theor. Phys.* **49** (1973) 652.
- [12] C.N. Yang, R.L. Mills, *Phys. Rev.* **96** (1954) 191.

- [13] W. Hollik, in *Precision tests of the Standard Electroweak Model*, Ed. P. Langacker (World Scientific, Singapore, 1995).
- [14] E. Guadagnini, Lectures given to 1st course Ph.D. students at University of Pisa (Pisa, Italy, 1997).
- [15] V.A. Novikov, L.B. Okun, M.I. Vysotsky, *Phys. Lett.* **B324** (1994) 89.
- [16] V.A. Novikov et al., *Rept. Prog. Phys.* **62** (1999) 1275.
- [17] H.E. Haber, G.L. Kane, *Phys. Rep.* **117** (1985) 75.
- [18] H. Georgi, S.L. Glashow, *Phys. Rev. Lett.* **32** (1974) 438.
- [19] D. Kazakov, Lectures presented at the *XXIV ITEP Winter School of Physics* (Moscow, Russia, 1996).
- [20] J. Bagger, J. Wess, *Supersymmetry and Supergravity*, Ed. A.S. Wightman, P.W. Anderson (Princeton University Press, Princeton, 1983).
- [21] J. Erler, P. Langacker, in *Review of Particle Physics*, *Eur. Phys. J.* **C3** (1998) 91, Chapter 10.
- [22] V.A. Novikov, L.B. Okun, M.I. Vysotsky, *Nucl. Phys.* **B397** (1993) 35.
- [23] A. Sirlin, *Phys. Lett.* **B232** (1989) 123.
- [24] P. Gambino, A. Sirlin, *Phys. Rev.* **D49** (1994) 1160.
- [25] V.A. Novikov, L.B. Okun, A. Rozanov, M.I. Vysotsky, *Uspekhi Fiz. Nauk* **166** (1996) 539 (Russian), *Physics-Uspekhi* **39** (1996) 503 (English).
- [26] B.A. Kniehl, *Nucl. Phys.* **B347** (1990) 86.
- [27] A. Djouadi, C. Verzegnassi, *Phys. Lett.* **B195** (1987) 265;
A. Djouadi, *Nuovo Cim.* **100A** (1988) 357;
A. Djouadi, P. Gambino, *Phys. Rev.* **D49** (1994) 3499.
- [28] N.A. Nekrasov, V.A. Novikov, L.B. Okun, M.I. Vysotsky, *Yad. Fiz.* **57** (1994) 883 (Russian), *Phys. Atom. Nucl.* **57** (1994) 827 (English).
- [29] P. Gambino, *Acta Phys. Pol.* **B27** (1996) 3671, *hep-ph/9611358*.
- [30] G. Degrassi, P. Gambino, A. Sirlin, *Phys. Lett.* **B394** (1997) 188.
- [31] V.A. Novikov, L.B. Okun, M.I. Vysotsky, in *Reports on the working groups on precision calculations for the Z resonance*, report *CERN 95-03* (1995) 7.
- [32] V. Novikov et al., preprints *ITEP-19-95*, *CPPM-1-95*;
http://cppm.in2p3.fr./leptop/intro_leptop.html.
- [33] W.J. Marciano, J.L. Rosner, *Phys. Rev. Lett.* **65** (1990) 2963.

- [34] V. Barger, M.S. Berger, P. Ohmann, *Phys. Rev.* **D47** (1993) 1093.
- [35] P. Langacker, N. Polonsky, *Phys. Rev.* **D47** (1993) 4028; *Phys. Rev.* **D49** (1994) 1454; *Phys. Rev.* **D52** (1995) 3081.
- [36] R. Barbieri, P. Ciafaloni, A. Strumia, *Nucl. Phys.* **B442** (1995) 461.
- [37] I.V. Gaidaenko et al., *JETP Lett.* **67** (1998) 761, *hep-ph/9812346*.
- [38] DELPHI Collab., P. Abreu et al., preprint *CERN-EP/99-037* (1999).
- [39] A. Perrotta, Search for SUSY particles in nearly mass degenerate scenarios with the DELPHI detector at LEP2, talk presented at the conference *PASCOS99* (Granlibakken, Lake Tahoe, California, 10-16 December 1999), to appear in the proceedings.
- [40] DELPHI Collab., P. Abreu et al., preprint *CERN-EP/98-176* (1998); ALEPH Collab., preprint *CERN-EP/99-014* (1999).
- [41] J.F. Gunion, S. Mrenna, preprint *UCD-99-01* (1999); C.H. Chen, M. Drees, J.F. Gunion, *Phys. Rev. Lett.* **76** (1996) 2002; J.L. Feng et al., preprint *IASSNS-HEP-99-19* (1999).
- [42] R. Barbieri et al., *Phys. Lett.* **B279** (1992) 169.
- [43] W. Hollik, C. Schappacher, *Nucl. Phys.* **B545** (1999) 98.
- [44] P.H. Chankowski et al., *Nucl. Phys.* **B417** (1994) 101.
- [45] DELPHI Collab., P. Abreu et al., *Phys. Lett.* **B274** (1992) 230.
- [46] N. Evans, *Phys. Lett.* **B340** (1994) 81.
- [47] P. Bamert, C.P. Burgess, *Z. Phys.* **C66** (1995) 495.
- [48] T. Inami et al., *Mod. Phys. Lett.* **A10** (1995) 1471.
- [49] A. Masiero et al., *Phys. Lett.* **B355** (1995) 329.
- [50] V.A. Novikov et al., *Mod. Phys. Lett.* **A10** (1995) 1915; erratum, *ibid.* **A11** (1996) 687.
- [51] M. Peskin, T. Takeuchi, *Phys. Rev. Lett.* **65** (1990) 964; *Phys. Rev.* **D46** (1992) 381.
- [52] Review of Particle Physics, *Eur. Phys. J.* **C3** (1998) No. 1-4.
- [53] Limits on Higgs boson masses from combining the data of the four LEP experiments at $\sqrt{s} < 183$ GeV, ALEPH, DELPHI, L3 and OPAL Collaborations, preprint *CERN-EP/99-060* (1999).
- [54] OPAL Collab., K. Ackerstaff et al., *Eur. Phys. J.* **C1** (1998) 45.
- [55] A.D. Dolgov, L.B. Okun, V. Zakharov, *Nucl. Phys.* **B41** (1972) 197.
- [56] P. Ferrari et al., preprint *DELPHI 98-55 PHYS 780*.

-
- [57] I.V. Gaidaenko et al., *Phys. Rep.* **320** (1999) 119.
- [58] M.I. Vysotsky, A.D. Dolgov, Ya.B. Zel'dovich, *JETP Lett.* **26** (1977) 188;
B.W. Lee, S. Weinberg, *Phys. Rev. Lett.* **39** (1977) 165;
K. Sato, H. Kobayashi, *Prog. Theor. Phys.* **58** (1977) 1775;
P. Hut, *Phys. Lett.* **B69** (1977) 85.
- [59] D. Caldwell, in *Proceedings of the XXVII ICHEP* (Glasgow, 1994), Ed. P.J. Bussey, I.G. Knowles, IOP, 1995;
P. Belli et al., *hep-ph/9903501*.
- [60] D. Fargion et al., *JETP Lett.* **69** (1999) 434, *Pisma Zh. Eksp. Teor. Fiz.* **69** (1999) 402, *astro-ph/9903086*.
- [61] DELPHI Collab., P. Abreu et al., preprint *CERN-EP/99-037* (1999).